Fabrication of self-organized quantum wires using multiatomic steps and their application to semiconductor lasers

多段原子ステップを用いた自己組織化量子細線の作製
およびその半導体レーザーへの応用

Shinjiroh Hara

A dissertation submitted in partial fulfillment
of the requirements for the degree of
Doctor of Philosophy (Engineering)
in Hokkaido University

January, 1998

Dedicated to my parents

Acknowledgments

This thesis describes a part of the research work carried out at Research Center for Interface Quantum Electronics and Faculty of Engineering, Hokkaido University, under the direction of Professor Takashi Fukui, while the author was a graduate student at Faculty of Engineering, Hokkaido University, from 1993 to 1998.

The author would like to express his sincere thanks to Professor Takashi Fukui, Research Center for Interface Quantum Electronics, Hokkaido University, for his constant support, guidance and encouragement. Without them, this work could not be accomplished.

The author also wishes to express his sincere thanks to Associate Professor Junichi Motohisa, Research Center for Interface Quantum Electronics, Hokkaido University, for his constant support, guidance and encouragement.

The author would like to express his especial appreciation to Professor Hideki Hasegawa, Graduate School of Electronics and Information Engineering, Hokkaido University, Professor Yoshihito Amemiya, Graduate School of Electronics and Information Engineering, Hokkaido University, Professor Shunichi Muto, Graduate School of Applied Physics, Hokkaido University, and Professor Kanji Yoh, Research Center for Interface Quantum Electronics, Hokkaido University, for their constant support, guidance and encouragement.

The author also wishes to express his thanks to Associate Professor Toshiya Saitoh, Research Center for Interface Quantum Electronics, Hokkaido University, Associate Professor Tamotsu Hashizume, Graduate School of Electronics and Information Engineering, Hokkaido University, and Research Associate Hajime

Fujikura, Graduate School of Electronics and Information Engineering, Hokkaido University, for their helpful discussions, suggestions and encouragement.

The author also wishes to express his special thanks to Dr. Hajime Shoji of Fujitsu Laboratories Ltd. for his useful and helpful discussions, suggestions and advice for the fabrication processes and the characterization techniques of semiconductor lasers with quantum confinement structures.

The author also is indebted to Dr. Hirotatsu Ishii, Dr. Bing-Xing Yang, Dr. Shu Goto, Dr. Satoshi Kodama, Dr. Richard Nötzel, Dr. Hidemasa Tomozawa, Associate Professor Masamichi Akazawa, Research Associate Nan-Jian Wu, Dr. Seiya Kasai, Dr. Satoshi Suzuki and Dr. Jun-ya Ishizaki, for their useful discussions, suggestions and encouragement.

The author also gives his special gratitude to Kazuhide Kumakura, Yasuhiko Ishikawa, Hiroshi Okada, Tsuyoshi Ozeki and Hayato Takeuchi, for their valuable discussions, suggestions and constant encouragement.

The author also wants to express his special thanks to Kazuaki Nakakoshi, Kazunobu Ohkuri, Megumi Usami, Masashi Akabori, Makoto Sakuma, Tetsuo Umeda and Yasuhiro Oda, for their technical assistance and constant encouragement.

The author acknowledges with gratitude for a financial support generously supplied by the Japan Society for the Promotion of Science through the research fellowships for young scientists from 1995 to 1998.

Finally, the author would like to thank his parents for their constant support and encouragement.

Contents

Chapter I

Introduction

1.1 Background

First proposal of one-dimensional periodic potential or superlattice structures was reported by L. Esaki and R. Tsu in 1970 [1]. Such superlattice structures are obtained by a periodic variation of alloy composition achieved during an epitaxial growth of compound semiconductors because of advances in techniques of an epitaxial growth with the precise controllability of a thin semiconductor layer growth. Particularly, so far, molecular beam epitaxy (MBE) and metalorganic vapor phase epitaxy (MOVPE) have been demonstrating the realization of semiconductor heterostructures with atomically smooth interfaces and have made it possible to realize new optical and electronic devices based on quantum mechanical effects. These epitaxial growth methods, for example, have realized low-dimensional quantum confinement structures, such as quantum well (QWL), quantum wires (QWRs) and quantum dots (QDTs), which have the size of "well" regions being comparable to de Broglie wavelength of electrons (~ 10nm).

In the last fifteen years, novel properties of the new devices based on quantum confinement structures have been theoretically predicted and reported, for example, in optical devices such as semiconductor lasers. To utilize quantum confinement structures as an active layer of the semiconductor laser is very promising for the improvement of its characteristics. The improvement in the temperature dependence of threshold current by multi-dimensional quantum confinement structures [2], the increase of gain in QWR lasers [3] and the increase of gain and the reduction of threshold current density in QDT lasers [4] have been theoretically investigated and predicted.

At the same time, many fabrication methods of low-dimensional quantum confinement structures have been intensively investigated and reported so far. There

have been two main streams of the research on them. One is on the modification by *ex situ* processes, such as an anisotropic reactive ion etching [5] and an ion beam implantation [6], after the epitaxial growth of GaAs/AlGaAs QWL structures. The other is on *in situ* formation of low-dimensional quantum confinement structures during the epitaxial growth. Because the former method has a possibility to introduce damages by etching or ion beam implantation processes to QWR and QDT regions, in order to avoid such problems originated from the disordering of surfaces or interfaces, the *in situ* formation methods have been more intensively investigated in the last fourteen years. To my knowledge, there are five main streams of the investigations as follows:

(1) Self-organization growth of QWR structures on vicinal [7-13] and high Miller indices substrates [14,15], which have no patterns fabricated with any lithography and etching techniques on the substrates.

(2) Growth on patterned non-planar substrates, which are patterned with lithography and etching techniques before the epitaxial growth, for example, QWR structures at the bottom of V-grooves [16,17] and on top of mesa structures [18,19] and QDT structures at the bottom of tetrahedral-shaped recesses [20].

(3) Selective area growth of QDT [21-24] and QWR [25-28] structures on the masked substrates, which have thin SiO_2 or Si_3N_4 layers patterned with lithography and etching techniques on semiconductor substrates, and QWR structures using native oxide masks on a cleaved plane of a superlattice [29].

(4) Self-assembling formation of QDT [30-33] based on Stranski-Krastanov growth mode or quantum disk [34] structures based on strain-driven spontaneous reorganization in lattice-mismatched materials system especially on high Miller indices substrates.

(5) T-shaped QWR [35,36] and QDT [37] structures formed by an overgrowth of QWL layer on a cleaved surface of multi-QWL layers, which are exposed by *in situ* cleavage.

These *in situ* formation methods, which are sometimes called "self-organization" or "self-assemble", are very promising for new optical and electronic device applications,

because it is possible to form high density nanometer-size quantum confinement structures without the introduction of damages in quantum confinement regions of electrons and holes by any artificial processes such as a lithography, an etching and an ion implantation. Furthermore, the size and the density of such quantum structures can be controlled only by adjusting the epitaxial growth conditions. Extremely small (~ 10 nm) and high density (10^9 ~ 10^{10} cm^{-2}) quantum structures and their narrow size distribution (± 10 %) can be realized with the *in situ* "self-organization" techniques. In particular, for the fabrication of semiconductor lasers with very low threshold current density and extremely narrow line width, three-dimensional island-like structures formed during the epitaxial growth of lattice-mismatched materials system have been intensively used to realize coherent zero-dimensional QDT structures [30-33], and, actually, semiconductor lasers with these kinds of QDTs in their active regions have been demonstrated [38-40]. However, for device applications, precise position-control of quantum structures seems to need a further optimization of their fabrication processes.

On vicinal substrates, the use of *monoatomic* and *multiatomic* steps has been proposed and partially demonstrated to realize two-dimensional quantum confinement structures such as QWRs. QWR structures using *monoatomic* steps on vicinal GaAs (001) substrates, which are well known as a "lateral superlattice", and are usually called a "tilted superlattice (TSL)" or a "fractional layer superlattice (FLS)", have been formed by both MBE [7,9] and MOVPE [8], and their applications to "quantum wire transistors" [41], "electron wave interference transistors" [42] and semiconductor lasers [43,44] have been proposed and partially demonstrated. On the other hand, QWR structures using *multiatomic* steps have also been demonstrated on vicinal GaAs (001) surfaces by MOVPE [10], on vicinal GaAs (110) surfaces by gas source MBE [11,12], on vicinal InP (001) surfaces by metalorganic molecular beam epitaxy (MOMBE) [13], on GaAs (113)A surfaces, which have macro steps comprised of two sets of high-index facets, by MBE [14] and on GaAs (775)B surfaces by MBE [15]. However, there have been only a few reports on the application of these kinds of QWR structures or *multiatomic* steps to electronic devices such as "electron wave

interference transistors" [45,46].

1.2 Objective of the Present Work

As described in the previous section, self-organization technologies in the epitaxial growth are very important and promising for the fabrication of nanometer-scale quantum confinement structures, because novel devices based on quantum mechanical effects can be realized with such technology. Application of QWR structures on vicinal substrates to semiconductor lasers has also been reported [43,44], as well as other self-organized quantum structures.

Objectives of the present work are to fabricate QWR structures using GaAs multiatomic steps grown on vicinal GaAs (001) substrates by MOVPE and to apply them to the active regions of semiconductor laser diodes. The following specific points are investigated in detail in the present work:

(1) Fabrication of GaAs/AlGaAs QWR structures on GaAs multiatomic steps and investigation of their photoluminescence properties, as the first trial.

(2) Investigation of the improvement methods for GaAs and InGaAs QWR structures using thin AlAs layers as lower barrier layers of QWRs on GaAs multiatomic steps and coherent GaAs multiatomic steps grown on patterned vicinal GaAs (001) substrates with a line and space pattern perpendicular to misorientation direction of substrates.

(3) Investigation of growth mode transition in thin InGaAs layers on GaAs multiatomic steps, their application to InGaAs/GaAs QWR structures and investigation of their optical properties.

(4) Fabrication of laser diodes with InGaAs QWRs in their active regions by separate confinement heterostructures and investigation of their characteristics.

1.3 Synopsis of Chapters

Following the introduction in this chapter, in chapter 2, preparation and characterization methods of samples, which are multiatomic steps on vicinal GaAs (001) substrates and QWR structures using such multiatomic steps, are described. First of all, the growth system of MOVPE, which is used for the formation of multiatomic steps and QWR structures in this works, is described. Secondly, step bunching phenomenon on vicinal substrates for the multiatomic step formation, which is very important phenomenon in the present works, is explained. Finally, characterization methods of multiatomic steps and QWR structures are introduced. Atomic force microscopy (AFM) for the surface observation and analysis of multiatomic steps grown by MOVPE and optical characterization methods based on photoluminescence (PL) measurement for quantum structures are explained.

In chapter 3, the formation of GaAs multiatomic steps on vicinal GaAs (001) substrates and the fabrication of GaAs/AlGaAs QWR structures are investigated. Using AFM, MOVPE grown surfaces on vicinal GaAs (001) substrates are observed. Then, GaAs/AlGaAs QWR structures are characterized by transmission electron microscopy and PL method. The results of PL measurements are also discussed by the comparison with a simple theoretical calculation.

In chapter 4, as the improvement methods for size uniformity of GaAs QWR structures, two specific attempts are introduced. GaAs QWR structures using thin AlAs layers as lower barrier layers and GaAs/AlGaAs wire-like structures using GaAs multiatomic steps on patterned vicinal GaAs (001) substrates are investigated. In the former half of this chapter, thin AlAs layer surfaces on GaAs multiatomic steps are characterized by AFM and optical characterization of AlGaAs/GaAs/AlAs QWR structures are also investigated. In the latter half, as a control method for the uniformity of step period, the straightness and the continuity of multiatomic steps, GaAs multiatomic steps grown on patterned vicinal GaAs (001) substrates with a line and space pattern perpendicular to misorientation direction of the substrates are characterized by AFM. GaAs/AlGaAs wire-like structures using these multiatomic

steps are also characterized by cathodoluminescence (CL) measurements.

In chapter 5, growth mode transition of thin InGaAs layers on GaAs multiatomic steps and fabrication of InGaAs/GaAs QWR structures are investigated. First of all, it is described that growth mode of a thin InGaAs layer on GaAs multiatomic steps changes from the step flow growth mode to the mixture of three-dimensional island formation mode and the step flow growth mode at the edge of GaAs multiatomic steps by controlling of epitaxial growth conditions. Secondly, optical properties of InGaAs/GaAs QWRs are also examined by PL, photoluminescence excitation (PLE) and photoluminescence in magnetic fields (MPL) measurements. Finally, the formation of coherent and straight InGaAs wire structures over more than thirty micrometer regions on patterned vicinal GaAs (001) substrates are briefly demonstrated.

In chapter 6, fabrication of laser diode using InGaAs QWRs, which are grown on GaAs multiatomic steps on vicinal GaAs (001) substrates by MOVPE, in its active region is investigated. After the introduction of sample preparation procedures for the laser diode, electroluminescence (EL) properties of InGaAs QWRs by pulsed current injections are examined and their pulsed laser operation are also demonstrated.

In chapter 7, the present works are summarized and the conclusions of the works are described.

References

[1] L. Esaki and R. Tsu: IBM J. Res. & Dev., **14**, 61 (1970).

[2] Y. Arakawa and H. Sakaki: Appl. Phys. Lett., **40**, 939 (1982).

[3] M. Asada, Y. Miyamoto and Y. Suematsu: Jpn. J. Appl. Phys., **24**, L95 (1985).

[4] M. Asada, Y. Miyamoto and Y. Suematsu: IEEE J. Quantum Electron., **QE-22**, 1915 (1986).

[5] K. Kash, A. Scherer, J. M. Worlock, H. G. Craighead and M. C. Tamargo: Appl. Phys. Lett., **49**, 1043 (1986).

[6] J. Cibert, P. M. Petroff, G. J. Dolan, S. J. Pearton, A. C. Gossard and J. H. English: Appl. Phys. Lett., **49**, 1275 (1986).

[7] P. M. Petroff, A. C. Gossard and W. Wiegmann: Appl. Phys. Lett., **45**, 620 (1984).

[8] T. Fukui and H. Saito: Appl. Phys. Lett., **50**, 824 (1987).

[9] J. M. Gaines, P. M. Petroff, H. Kroemer, R. J. Simes, R. S. Geels and H. English: J. Vac. Sci. Technol. B, **6**, 1378 (1988).

[10] T. Fukui and H. Saito: Jpn. J. Appl. Phys. **29**, L483 (1990).

[11] K. Inoue, K. Kimura, K. Maehashi, S. Hasegawa, H. Nakashima, M. Iwane, O. Matsuda and K. Murase: J. Cryst. Growth **127**, 1041 (1993).

[12] M. Takeuchi, K. Shiba, K. Sato, H. K. Huang, K. Inoue and H. Nakashima: Jpn. J. Appl. Phys. **34**, 4411 (1995).

[13] M. J. S. P. Brasil, A. A. Bernussi, M. A. Cotta, M. V. Marquezini, J. A. Brum, R. A. Hamm, S. N. G. Chu, L. R. Harriott and H. Temkin: Appl. Phys. Lett., **65**, 857 (1994).

[14] R. Nötzel, N. N. Ledentsov, L. Däweritz, K.Ploog and M. Hohenstein: Phys. Rev. B, **45**, 3507 (1992).

[15] M. Higashiwaki, M. Yamamoto, T. Higuchi, S. Shimomura, A. Adachi, Y. Okamoto, N. Sano and S. Hiyamizu: Jpn. J. Appl. Phys. **35**, L606 (1996).

[16] E. Kapon, D. M. Hwang and R. Bhat: Phys. Rev. Lett., **63**, 430 (1989).

[17] E. Colas, S. Simhony, E. Kapon, R. Bhat, D. M. Hwang and P. S. D. Lin: Appl. Phys. Lett., **57**, 914 (1990).

[18] Y. Nakamura, S. Koshiba, M. Tsuchiya, H. Kano and H. Sakaki: Appl. Phys. Lett., **59**, 700 (1991).

[19] S. Koshiba, H. Noge, H. Akiyama, T. Inoshita, Y. Nakamura, A. Shimizu, Y. Nagamune, M. Tsuchiya, H. Kano, H. Sakaki and K. Wada: Appl. Phys. Lett., **63**, 363 (1994).

[20] Y. Sugiyama, Y. Sakuma, S. Muto and N. Yokoyama: Appl. Phys. Lett., **67**, 256 (1995).

[21] T. Fukui, S. Ando, Y. Tokura and T. Toriyama: Appl. Phys. Lett., **58**, 2018 (1991).

[22] Y. D. Galeuchet, H. Rothuizen and P. Roentgen: Appl. Phys. Lett., **58**, 2423 (1991).

[23] M. Nishioka, S. Tsukamoto, Y. Nagamune, T. Tanaka and Y. Arakawa: J. Cryst. Growth, **124**, 502 (1992).

[24] K. Kumakura, K. Nakakoshi, J. Motohisa, T. Fukui and H. Hasegawa: Jpn. J. Appl. Phys., **34**, 4387 (1995).

[25] T. Fukui and S. Ando: Electron. Lett., **25**, 410 (1989).

[26] T. Fukui, S. Ando and Y. K. Fukai: Appl. Phys. Lett., **57**, 1209 (1990).

[27] S. Tsukamoto, Y. Nagamune, M. Nishioka and Y. Arakawa: J. Appl. Phys., **71**, 533 (1992).

[28] S. Tsukamoto, Y. Nagamune, M. Nishioka and Y. Arakawa: Appl. Phys. Lett., **62**, 49 (1993).

[29] M. Notomi, Y. Kadota and T. Tamamura: Jpn. J. Appl. Phys., **34**, 1451 (1995).

[30] D. Leonard, M. Krishnamurthy, C. M. Reaves, S. P. DenBaars and P. M. Petroff: Appl. Phys. Lett., 63 (1993) 3203.

[31] J. M. Moison, F. Houzay, F. Barthe, L. Leprince, E. André and O. Vatel: Appl. Phys. Lett., **64**, 196 (1994).

[32] J. Ahopelto, A. A. Yamaguchi, K. Nishi, A Usui and H. Sakaki: Jpn. J. Appl. Phys., **32**, L32 (1993).

[33] J. Oshinowo, M. Nishioka, S. Ishida and Y. Arakawa: Appl. Phys. Lett., **65**, 1421 (1994).

[34] R. Nötzel, J. Temmyo and T. Tamamura: Nature, **369**, 131 (1994).

[35] A. R. Goñi, L. N. Pfeiffer, K. W. West, A. Pinczuk, H. U. Baranger and H. L. Stormer: Appl. Phys. Lett., **61**, 1956 (1992).

[36] T. Someya, H. Akiyama and H. Sakaki: Phys. Rev. Lett., **74**, 3664 (1995).

[37] W. Wegscheider, G. Schedelbeck, G. Abstreiter, M. Rother and M. Bichler: Phys. Rev. Lett., **79**, 1917 (1997).

[38] N. Kirstaedter, N. N. Lecentsov, M.Grundmann, D. Bimberg, V. M. Ustinov, S. S. Ruvimov, M. V. Maximov, P. S. Kop'ev, Zh. I. Alferov, U. Richter, P. Werner, U. Gösele and J. Heydenreich: Electron. Lett., **30**, 1416 (1994).

[39] H. Shoji, K. Mukai, N. Ohtsuka, M. Sugawara, T. Uchida and H. Ishikawa: IEEE Photon. Technol. Lett., **12**, 1385 (1995).

[40] J. Temmyo, E. Kuramochi, M. Sugo, T. Nishiya, R. Nötzel and T. Tamamura: Electron. Lett., **31**, 209 (1995).

[41] K. Tsubaki, T. Fukui, Y. Tokura, H. Saito and N. Susa: Electron. Lett., **24**, 1267 (1988).

[42] K. Tsubaki, Y. Tokura, T. Fukui, H. Saito and N. Susa: Electron. Lett., **25**, 728 (1989).

[43] H. Saito, K. Uwai and N. Kobayashi: Jpn. J. Appl. Phys., **32**, 4440 (1993).

[44] J. Yoshida, A. Kikuchi, I. Nomura and K. Kishino: Proc. 7th Int. Conf. IPRM (IEEE Catalog #95CH35720), 29 (1995).

[45] J. Motohisa, M. Akabori, S. Hara, J. Ishizaki, K. Ohkuri and T. Fukui: Physica B, **227**, 295 (1996).

[46] M. Akabori, J. Motohisa, T. Irisawa, S. Hara, J. Ishizaki and T. Fukui: Jpn. J. Appl. Phys., **36**, 1966 (1997).

Chapter II

Metalorganic Vapor Phase Epitaxial Growth and Characterization Methods of Samples

2.1 Introduction

In this chapter, preparation and characterization methods of samples in the present work are described. First, as an epitaxial growth method, metalorganic vapor phase epitaxy (MOVPE), which is one of the most useful methods for the formation of semiconductor heterostructures with atomically smooth interfaces, is used here. In the latter half of this chapter, atomic force microscopy (AFM), which is used as a surface characterization method of GaAs multiatomic steps grown by MOVPE, and photoluminescence (PL) and other related methods, which are used as optical characterization methods of QWRs, are briefly introduced.

2.2 Metalorganic Vapor Phase Epitaxy

As mentioned in the previous chapter, metalorganic vapor phase epitaxy (MOVPE) is one of the most important and useful methods for the formation of semiconductor heterostructures with atomically smooth interfaces. In MOVPE, in other words, there is the advantage in the capability to control the uniformity of epitaxially grown layer thickness over much larger area than MBE. In MBE, because the epitaxial growth proceeds in ultra high vacuum, its growth mechanism and surface reconstruction on semiconductor surfaces has been intensively investigated by *in situ* growth monitoring with reflection high energy electron diffraction (RHEED) method using electron beam. On the other hand, in MOVPE, there have never been useful methods for *in situ* growth monitoring, because the epitaxial growth proceeds in vapor phase. Recently, however, such *in situ* growth monitoring techniques in MOVPE, for

example, reflectance-difference spectroscopy (RDS) [1] and surface photo-absorption (SPA) [2], have been developed, and the surface reconstruction has been intensively examined [3,4].

In MOVPE, organometallic compound source materials are introduced into a reactor in vapor phase using a carrier gas. These organometallic compound materials with alkyl radicals are usually used as source materials for III column elements, because they have high vapor pressure, for example, trimethylaluminum (TMAl), trimethylgallium (TMGa), triethylaluminum (TEAl), triethylgallium (TEGa) and trimethylindium (TMIn). These are generally in liquid or solid phase at working temperatures. Source materials for V column elements are usually hydride compounds in gas phase, for example, arsine (AsH_3), and AsH_3 (20 %) diluted with hydrogen (H_2) is used in the present work. As the alternative of AsH_3 in the future, the use of tertiary-butylarsine (TBA) as source materials for V column elements has been intensively investigated, because AsH_3 is too toxic. Mono-silane (SiH_4) in gas phase is a source material conventionally used for a n-type doping. In MOVPE, epitaxial growth on semiconductor substrates proceeds with thermal decomposition of these organometallic and hydride compound materials, and is dominated by the diffusion of III column elements in a boundary layer over the semiconductor substrates. In conventional MOVPE growth conditions, arsenic molecules (or atoms) in vapor phase and the semiconductor surfaces in solid phase are in the equilibrium state.

In the present work, a horizontal low-pressure MOVPE system with the "reactor" made of quartz glass was used. GaAs substrates used in the present work were set on a "susceptor" made of carbon graphite, which was heated by radio frequency (RF) during the epitaxial growth. H_2 was used as a carrier gas for source materials and the total gas flow rate was maintained at 3.0 *l*/min. The working pressure was 76 Torr (0.1 atm), and was automatically controlled to within ± 0.1 Torr during the epitaxial growth. Before the MOVPE growth, all vicinal and singular GaAs (001) substrates were cleaned and etched by chemical solution to remove the contamination and oxides of the crystal surfaces. In these processes, it is very important to etch the surfaces slowly with an alkaline etchant, SemicoClean 23 of Furu-uchi Chemical Co., Ltd., so

as the vicinal surfaces may not be disordered by etching.

2.3 Epitaxial Growth on Vicinal Surfaces

Vicinal substrates used in the present work are usually tilted from a crystallographic direction of the semiconductor crystal surfaces with low Miller indices to a certain direction. Figure 2.1 shows the crystal orientation around (001) plane and the definition of vicinal (001) substrates. As shown in a side view of Fig. 2.1, "(001) misoriented by 5.0° toward the [-110] direction" means "(001) tilted by 5.0° toward (111)B plane".

The surfaces of vicinal substrates are usually the set of steps with atomic height. Such atomic steps are generally called as "monoatomic steps", and the steps assembling more than two monoatomic steps are called as "multiatomic steps". During the epitaxial growth on the vicinal substrates, these surface steps gather each other, resulting in the formation of multiatomic steps with atomically flat terraces. This phenomenon is well known as "step bunching". Therefore, the relationship between average step height, h, and average inter-step separation, λ, is described by the following equation; $\lambda = h \cdot \tan\theta$, where θ is the misorientation angle of vicinal substrates. Epitaxial growth on vicinal substrates is based on the assumption that crystal surfaces have terraces, steps and kinks during a crystal growth. Three processes can be distinguished: (1) atoms or molecules diffusing in vapor phase attach on the crystal surfaces (adsorption), (2) ad-atoms or ad-molecules migrate on the surfaces (surface migration), and (3) they are incorporated into the crystal (incorporation). There are some ad-atoms or ad-molecules re-evaporated from the surfaces (desorption), which do not contribute to the crystal growth.

There have been some reports on the formation of multiatomic steps on MOVPE grown vicinal surfaces [5-12]. Step bunching phenomenon has been observed, for example, on as-grown GaAs surfaces [5-7, 10], as-grown InGaP surfaces [11], as-

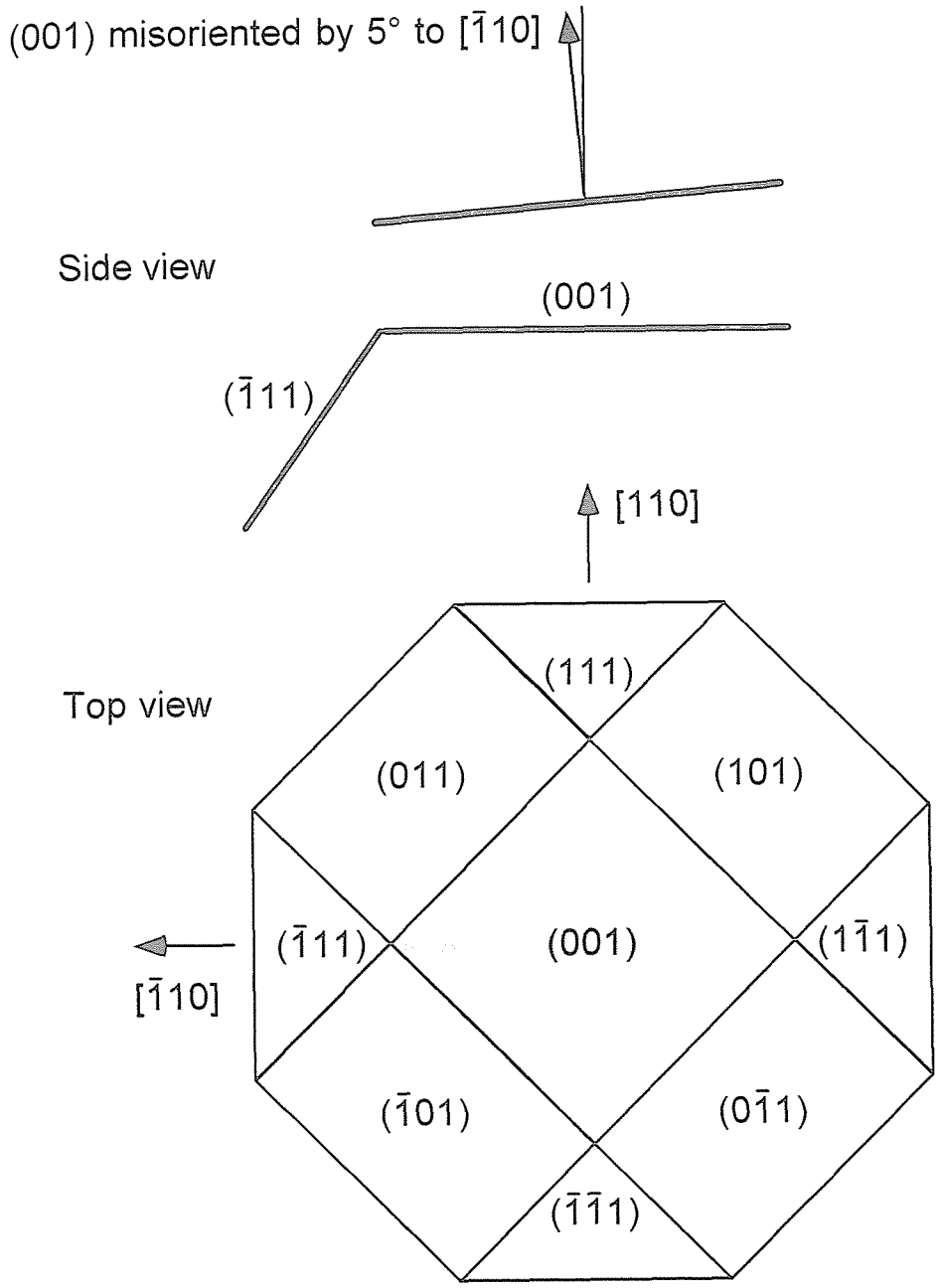

Fig. 2.1 Crystal orientation around (001) plane and definition of vicinal (001) substrate.

grown strained InGaAs surfaces [12] and GaAs surfaces annealed in AsH_3/H_2 ambience [8,9]. In some reports, the mechanism of step bunching was also discussed. Although its universal mechanism has not been demonstrated yet, the migration of ad-atoms during the epitaxial growth, that is, the kinetic motion of ad-atoms on the surfaces seems to lead the monoatomic steps to the formation of multiatomic steps [10,13]. Figure 2.2 shows a step bunching mechanism of the surface steps based on Schwoebel's model [14,15]. Schwoebel proposed a simple model that the step bunching phenomenon was driven by the anisotropy of the incorporation rates between at the up-side and the down-side step sites for surface migrating ad-atoms. When the incorporation rate at the up-side step sites is larger than that at the down-side ones, the ordering of the inter-step separations occurs, and vice versa, the formation of multiatomic steps, that is, the step bunching, occurs. These results have been discussed by comparing theoretical results using a simple simulation with experimental ones in MOVPE grown GaAs surfaces [13,16]. Recently, on the MOVPE grown vicinal GaAs (001) surfaces, it has also been pointed out by the investigations using an ultra high vacuum scanning electron microscopy (UHV-STM) that the anisotropy in the incorporation rates of the surface migrating ad-atoms at the step edges may be due to the partial disordering of the surface reconstruction near the multiatomic step edges [17].

2.4 Characterization Methods

2.4.1 Atomic Force Microscopy

Atomic force microscopy (AFM), which is developed by G. Binning *et al.* in 1986 [18], has atomic scale resolution both horizontally and vertically, and is useful for surface observation and analysis of nanometer-scale structures. It has an advantage to characterize surfaces of non-conductive materials being different from the fact that

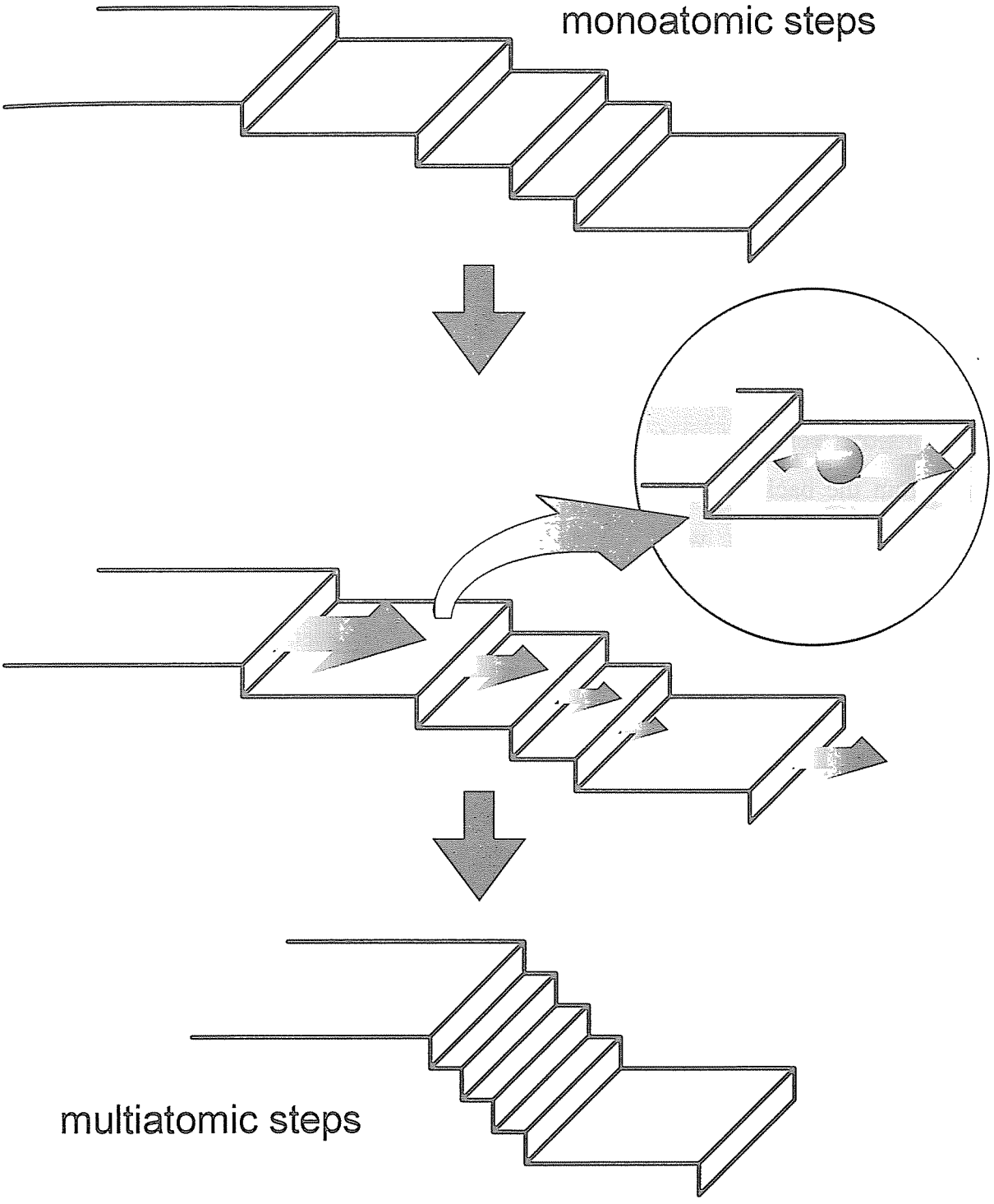

Fig. 2.2 Schematic of step bunching mechanism.

scanning tunneling microscopy (STM) can be used only for the characterization of conductive materials. Sample surfaces can be observed without any destruction of surface structures, because AFM based on "van der Waals' force" between two atoms can be used without physical contact with sample surfaces. It means that, when scanning tips are engaged and sample surfaces are scanned, there is the repulsion between two atoms, that is, an atom on the scanning tip and on the sample surface, and the distance between two atoms is maintained.

In the present work, NanoScope II or IIIa system of Digital Instruments Inc. are used with pyramid-shaped Si_3N_4 scanning tips. The initial calibration of the relative positions between the sample surfaces and the tips is done by the reflection of laser light from the back of scanning tips. The position of sample stage is controlled by piezoelectric materials, while scanning the sample surfaces. In the scanning mode used here, which is a constant force mode, the sample height is varied by the piezoelectric stage so as to keep the repulsive force between the scanning tip and the sample surface. All sample surfaces were scanned in air.

2.4.2 Optical Characterization

In this section, optical characterization methods for QWR structures are briefly summarized. All measurement methods are related to luminescence produced by radiative recombination of electrons and holes excited by light, electron beam or current injection.

photoluminescence

Photoluminescence (PL) measurement is one of the most useful characterization methods for optical properties of quantum structures without any physical contact with samples and destruction of sample structures. PL is the optical radiation emitted by a physical system resulting from excitation to a non-equilibrium state irradiation by light. Three processes can be distinguished: (1) creation of electron-hole pairs by

absorption of the exciting light, (2) radiative recombination of electron-hole pairs and (3) escape of the recombination radiation from the samples.

In the present work, argon ion (Ar^+) laser and titanium sapphire (Ti:S) laser, which is pumped by Ar^+ laser, are used as excitation sources in PL measurements. Excitation wavelength is 514.5 nm for an Ar^+ laser and around 840 nm for a Ti:S laser. All samples are usually set in the cryostats to keep the measurement temperatures. Polarization anisotropy of PL is measured through a polarization filter in front of a grating monochromator. To avoid the polarization sensitivity of the monochromator, the direction of QWRs was tilted by 45° relative to the gating direction of the monochromator. PL measurement set-up is a standard system with a lock-in amplifier and a light chopper.

photoluminescence excitation

In photoluminescence excitation (PLE) spectroscopy, by varying wavelengths of the excitation source, emissions by radiative recombination of electron-hole pairs, which are strongly depended on the absorption efficiency in a physical system for a wavelength, can be measured. Therefore, PLE spectroscopy is useful to examine the information of the energy band structures in materials. PLE spectroscopy has been used in the investigation of lattice mismatched material systems and low-dimensional quantum confinement structures, because PLE spectra, in particular, reflect the valence band profile of such materials and structures.

Figure 2.3 shows the experimental set-up used for the characterization of polarization anisotropy in QWRs. Ti:S laser, which can be varied from about 830 nm to 990 nm in the wavelength range, is used as an excitation source for PLE measurements of InGaAs/GaAs QWR structures. The double monochromator, whose focal length is 100 mm, of JOBIN-YVON is used in order to reduce the incidence of stray light to the detectors. Luminescence is detected by photo-multiplier tubes, R316 (S-1) of HAMAMATSU Photonics. The polarization state of the output of Ti:S laser is realized with a depolarizer and a Glan-Thomson prism. To avoid the polarization sensitivity of the monochromator, the direction of QWRs was tilted by 45° relative to

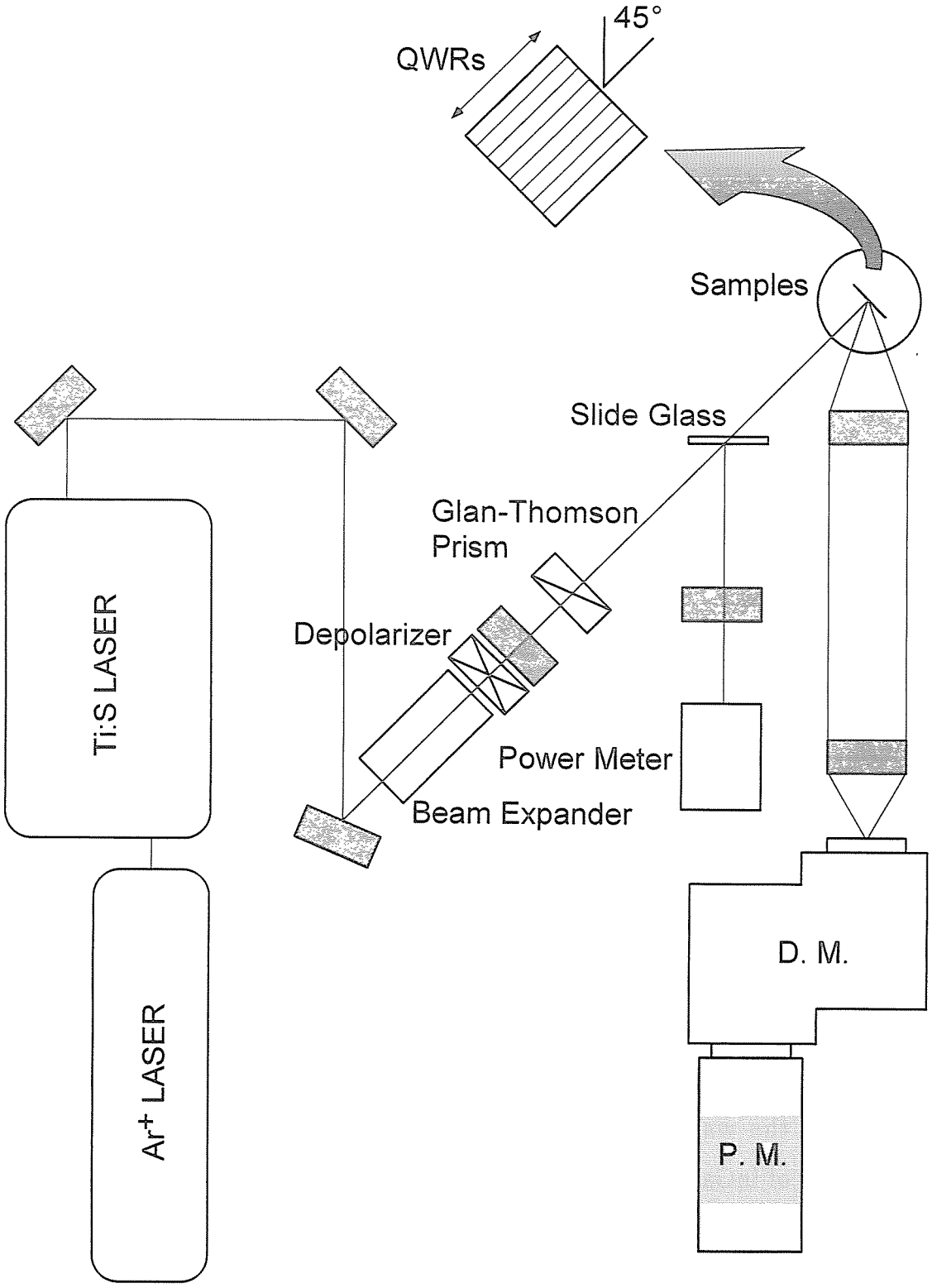

Fig. 2.3 Optical set-up for PLE measurements.

the gating direction of the monochromator. Excitation power in each wavelength was monitored by a power meter, while measuring PLE.

photoluminescence in magnetic fields

Luminescence measurements in magnetic fields have been carried out for QWR structures fabricated by etching of GaAs/AlGaAs QWL [19,20]. PL peak energy positions generally shift to the higher energy side depending on the increase of magnetic fields, B, because of the formation of Landau levels in magnetic fields. Such energy shift, ΔE, is usually called as a diamagnetic energy shift. ΔE is well fitted by the parabolic relation to B of diamagnetic shift of excitons, that is, $\Delta E = \beta B^2$, where β is the diamagnetic coefficient. However, when the direction of biased magnetic fields is parallel to the normal direction of QWL plane, and the in-plane lateral potential barrier exists in QWL, the in-plane cyclotron oscillation of electrons is restrained by the lateral potential. Therefore, PL characterization of QWR structures in magnetic fields is useful to evaluate the lateral confinement effect of QWRs.

Figure 2.4 shows the experimental set-up used for the characterization of PL properties of QWR structures in magnetic fields. Excitation light is introduced through an optical fiber to the sample surface set in a superconducting magnet, and luminescence also comes out through the same optical fiber. Biased magnetic fields was up to 10 T. Samples are maintained by liquid helium (LHe) at 4.2 K, while measuring.

cathodoluminescence

In cathodoluminescence (CL), excitation source of electrons and holes is electron beam. Therefore, quantum structures are measured by using facilities combined optical systems such as mirrors and monochromator with a conventional scanning electron microscope (SEM) in high vacuum. Sample holders are made of copper and are cooled down by liquid helium. In the present work, a grating monochromator, whose focal length is 300 mm, of OXFORD Instruments and other optical systems are combined with JSM-5410 of JEOL Ltd. CL was measured at 4.2 K for taking their

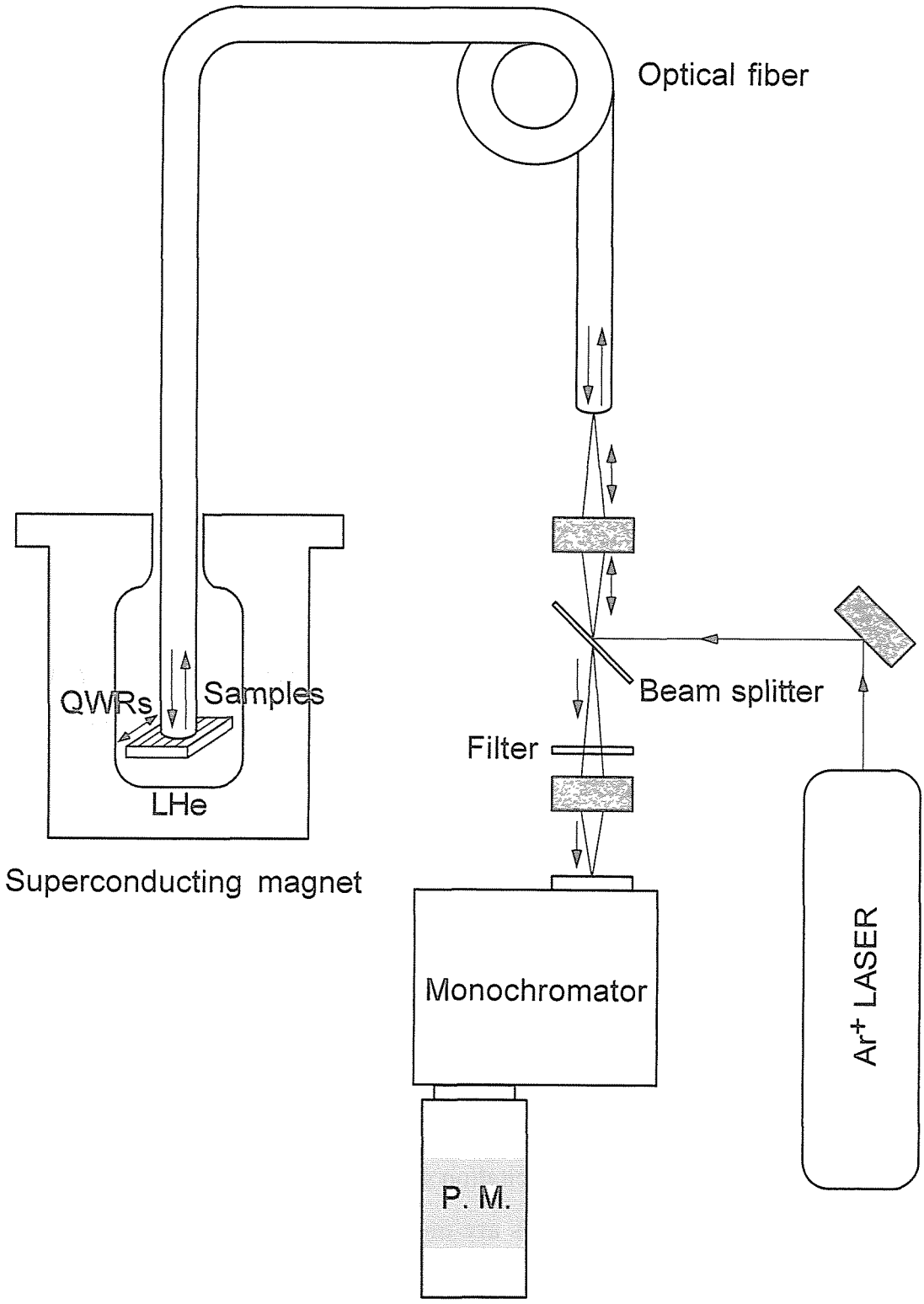

Fig. 2.4 Optical set-up for PL measurements in magnetic fields.

spectra and spatial resolved luminescent images. Excitation electron beam energy and current were 10 keV and 250 pA, respectively.

electroluminescence

In electroluminescence (EL), electrons and holes are excited by current injections. When light-emitting diode (LED) structures with a p-n junction are positively biased, spontaneous emission resulting from recombination of electrons and holes occurs. In the present work, because the fabrication of laser diodes with InGaAs QWRs in their active layers is a main purpose, a conventional separate confinement heterostructure (SCH) is formed as p-n junction diode structures. It is well known that, in laser structures with quantum confinement structures in active layers, optical confinement factors decrease as the thickness of well layers in QWL getting thinner, and that, as a result, threshold current densities increase. To increase optical distribution in active layers, optical confinement layers, which have lower refractive indices than those of carrier confinement layers, are formed outside carrier confinement layers in SCH.

EL measurement set-up is the same as a conventional set-up for PL measurements other than the carrier excitation by current injection with a pulse/function generator.

References

[1] D. E. Aspnes, J. P. Harbison, A. A. Studna and L. T. Florez: Phys. Rev. Lett., **59**, 1687 (1987).

[2] N. Kobayashi and Y. Horikoshi: Jpn. J. Appl. Phys., **28**, L1880 (1989).

[3] I. Kamiya, D. E. Aspnes, H. Tanaka, L. T. Florez, J. P. Harbison and R. Bhat: Phys. Rev. Lett., **68**, 627 (1992).

[4] Y. Yamauchi, K. Uwai and N. Kobayashi: Jpn. J. Appl. Phys., **32**, 3363 (1993).

[5] T. Fukui and H. Saito: Jpn. J. Appl. Phys., **29**, L483 (1990).

[6] M. Kasu and T. Fukui: Jpn. J. Appl. Phys., **31**, L864 (1992).

[7] M. Kasu and N. Kobayashi: Appl. Phys. Lett., **62**, 1262 (1993).

[8] K. Hata, A. Kawazu, T. Okano, T. Ueda and M. Akiyama: Appl. Phys. Lett., **63**, 1625 (1993).

[9] S. L. Skala, S. T. Chou, K. –Y. Cheng, J. R. Tucker and J. W. Lyding: Appl. Phys. Lett., **65**, 722 (1994).

[10] J. Ishizaki, S. Goto, M. Kishida, T. Fukui and H. Hasegawa: Jpn. J. Appl. Phys., **33**, 721 (1994).

[11] A. Gomyo, H. Hotta, F. Miyasaka, K. Tada, H. Fujii, K. Fukagai, K. Kobayashi and I. Hino: J. Cryst. Growth, **145**, 126 (1994).

[12] T. Kikkawa, K. Makiyama, H. Ochimizu, K. Kasai and J. Komeno: J. Cryst. Growth, **145**, 799 (1994).

[13] J. Ishizaki, K. Ohkuri and T. Fukui: Jpn. J. Appl. Phys., **35**, 1280 (1996).

[14] R. L. Schwoebel and E. J. Shipsey: J. Appl. Phys., **37**, 3682 (1966).

[15] R. L. Schwoebel: J. Appl. Phys., **40**, 614 (1969).

[16] H. Saito, K. Uwai, Y. Tokura and T. Fukui: Appl. Phys. Lett., **63**, 72 (1993).

[17] J. Ishizaki, Y. Ishikawa and T. Fukui: Mat. Res. Soc. Symp. Proc., **448**, 95 (1997).

[18] G. Binning, C. F. Quate and Ch. Gerber: Phys. Rev. Lett., **56**, 930 (1986).

[19] M. Kohl, D. Heitmann, P. Grambow and K. Ploog: Phys. Rev. Lett., **63**, 2124 (1989).

[20] A. S. Plaut, H. Lage, P. Grambow, D. Heitmann, K. von Klitzing and K. Ploog: Phys. Rev. Lett., 67, 1642 (1991).

Chapter III

Formation of GaAs Multiatomic Steps and GaAs Quantum Wires

3.1 Introduction

The application of monoatomic and multiatomic steps formed on vicinal GaAs substrates to the realization of two-dimensional quantum confinement structures has been proposed and demonstrated. GaAs multiatomic steps were formed during AlAs/GaAs multi-layer growth by MOVPE on vicinal GaAs (001) substrates misoriented by 2.0°, as demonstrated by T. Fukui and H. Saito [1]. Such step bunching phenomenon occurred not in AlAs layers but during GaAs layer growth under the low AsH_3 partial pressures. These results was explained by the difference of surface migration length between Ga and Al ad-atoms, that is, the migration length of Ga atoms is much larger than that of Al ones and the width of enlarged terraces. Step bunching in the GaAs layers leads to their lateral in-plane thickness variations, although the thickness of AlAs layers is always the same anywhere. These locally thick areas might show strong one-dimensional characteristics if their lateral dimension become comparable to de Broglie wavelength of electrons (~ 10 nm).

In this chapter, the formation of GaAs/AlGaAs QWR structures utilizing *multiatomic* steps self-organized by MOVPE on vicinal GaAs (001) substrates. Cross-sectional transmission electron microscope (TEM) images show the formation of locally thick QWR structures at the edge of multiatomic steps. The observed PL peak energy of QWRs shifts to the lower energy side, and the amount of the energy shift is in good agreement with a simple numerical calculation.

3.2 Experimental Procedure

A horizontal low-pressure MOVPE system was used with triethylaluminum (TEAl), triethylgallium (TEGa) and AsH_3 as the source materials. Vicinal GaAs (001) substrates misoriented by 3.0° and 5.0° towards [-110] direction and a singular GaAs (001) substrate were used. These three types of substrates were used in the same growth run. AsH_3 partial pressures were 1.7×10^{-4} atm for the GaAs buffer layer and 6.7×10^{-5} atm for the formation of GaAs QWR structures. The growth rate of GaAs was fixed at 0.048 nm/s in order to enhance the migration of Ga atoms on the surfaces. Vapor pressure ratio of (group V) / (group III) row materials, that is, V / III ratio was 62 for the GaAs QWR growth. The growth temperature was 600°C.

Figure 3.1 shows a schematic of GaAs QWR structures. First, a 68 nm-thick, which corresponds to 40-period, a $(AlAs)_3$ / $(GaAs)_3$ superlattice buffer layer was grown on the vicinal substrate in order to form *monoatomic* steps with nearly equal spacing on the surface [2]. Next, a 300 nm-thick GaAs buffer layer was grown to form equally spaced *multiatomic* steps. Details of *multiatomic* step formation processes and mechanism were discussed elsewhere [3-6]. Thermal treatment in AsH_3 / H_2 ambience was carried out for 30 min at 600 °C after the GaAs multiatomic steps formation in order to make the edge of multiatomic steps straighter. These thermal treatment effects have been observed on vicinal GaAs (001) surfaces grown by MOVPE [7]. Furthermore, in the thermal treatment, evaporation of Ga atoms might be rare, and step bunching phenomenon on vicinal GaAs (001) surfaces during the thermal treatment seems to be mainly caused by the migration of Ga atoms detached from the step edges and their re-incorporation to the step edges [8]. Next, a single GaAs/AlGaAs QWR structure was grown on the GaAs multiatomic steps. Average thickness of QWL and AlGaAs lower and upper barrier layers grown on the vicinal GaAs substrate were 4, 20 and 120nm, respectively, followed by a 10 nm-thick GaAs cap layer growth. Aluminum contents of AlGaAs layers was about 0.32. A similar GaAs/AlGaAs QWL structure was also grown on the singular (001) substrate as a reference.

AFM was used for the characterization of surface morphologies in air. Cross-sectional images of the QWR and QWL structures were characterized by a

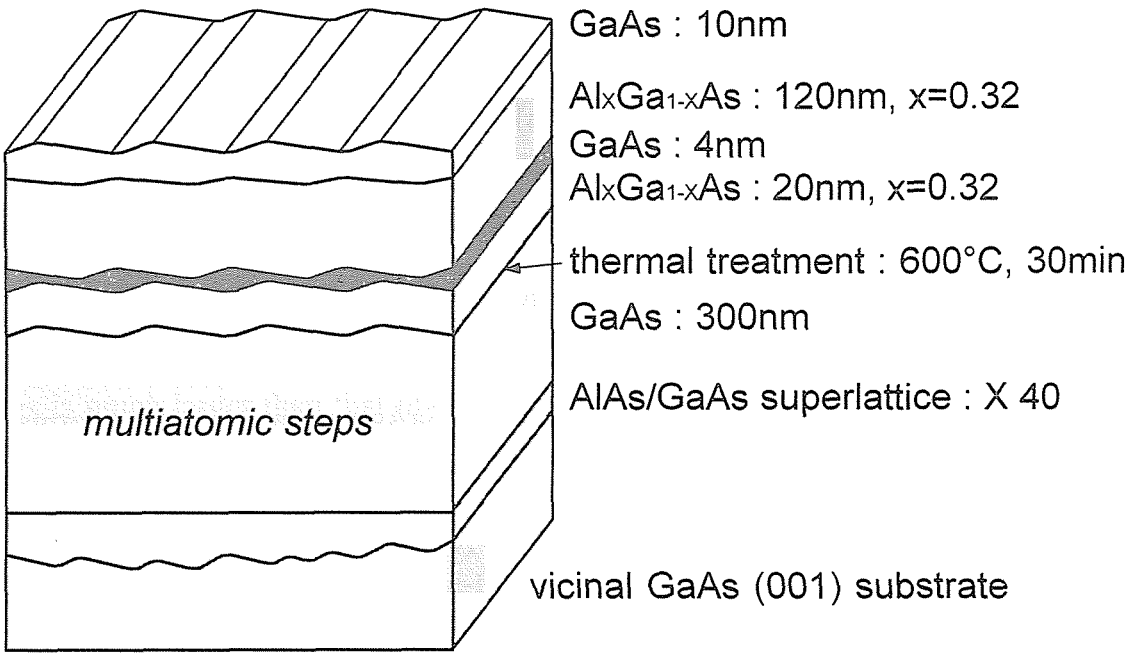

Fig. 3.1 Schematic of GaAs/AlGaAs quantum wire structures on GaAs multiatomic steps.

transmission electron microscopy (TEM). These cross-sectional TEM images were taken with JEM-3010 at 300kV. The optical properties of QWR structures on the multiatomic steps were measured by PL at 20K, using an Ar^+ laser.

3.3 Formation of GaAs Multiatomic Steps on Vicinal GaAs (001) Surfaces

In order to obtain the optimum growth condition for the uniform QWR structures, surface morphologies of the GaAs buffer layers were characterized by AFM. Figure 3.2 shows AFM images and the schematic of GaAs buffer layer surface after the thermal treatment on the vicinal substrates with various misorientation angle. The observed area was 1.7 μm × 1.7 μm. The presence of coherent multiatomic steps with extremely straight edges was observed over a wide observation area, although the continuity of several steps was disordered in some places. It was found that most of these steps were straight over 1.5 μm. On the average inter-step spacing, that is, the average step period, of the multiatomic steps, any significant differences among all misoriented surfaces could not be observed, and it was about 80 nm. This means that the average inter-step spacing of the multiatomic steps on the GaAs surfaces is mainly determined by the migration length of Ga ad-atoms and almost independent of the misorientation angle [3]. On the other hand, the average step height of the multiatomic steps increased as the misorientation angle of the vicinal substrates increases, as described in Fig. 3.2. Therefore, the vertical thickness of GaAs QWRs formed at the edge of the multiatomic steps can be controlled by changing the misorientation angle of the vicinal substrates. On the vicinal surfaces misoriented by more than 5.0°, in particular, the step edges can be straighter than on the surface misoriented by 2.0° and 3.0°. However, it was also found that the formation of GaAs multiatomic steps on the 6.0°- misoriented surfaces tended to be "unstable", that is, straight and coherent multiatomic steps were not always formed even under the same growth conditions, although their reasons could not be clarified. Since M. Kasu and N. Kobayashi have pointed out that step bunching phenomenon could be occurred when the

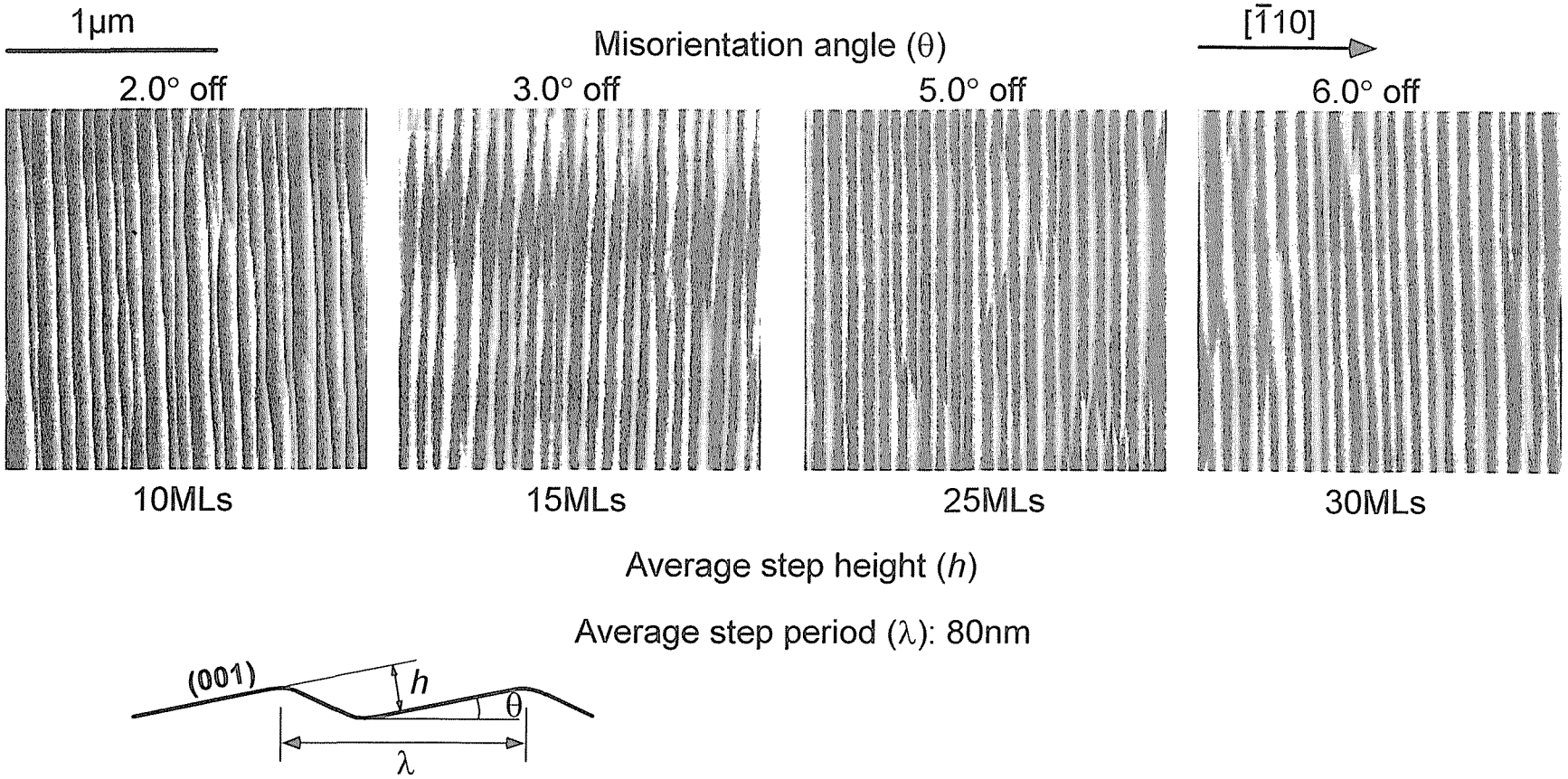

Fig. 3.2 Atomic force microscopy images of GaAs surfaces grown by MOVPE on vicinal GaAs (001) substrates. Misorientation direction was in the [-110] direction.

misorientation angle of the GaAs (001) substrates was equal to or less than 7.0° at the growth temperature between 575 °C and 650 °C, the phenomenon observed here may be attributed to the stability of the 6.0°- misoriented surfaces [9]. Figure 3.3 shows the histogram of the inter-step spacing obtained by the cross-sectional line profiles of the AFM images. The distribution of inter-step spacing on the 5.0°-misoriented surfaces was estimated to be within ± 13 %. These results indicate that QWR structures can be uniformly fabricated over a large area by controlling the epitaxial growth conditions.

3.4 Fabrication of GaAs Quantum Wire Structures Using Multiatomic Steps

Figure 3.4 shows cross-sectional TEM images and schematic views of (a) the QWL on the singular GaAs (001) substrate, and (b) the QWR structures on the 3.0°- and (c) on the 5.0°- misoriented substrate. As shown in Fig. 3.4 (c) for the 5.0°-misoriented wafer, the GaAs layer was thicker at the edge of multiatomic steps than on the terraces. It was estimated from this TEM image that the lateral GaAs width and the QWL thickness on the terraces were 10.7 and 3.1 nm, respectively. These facts imply that GaAs QWR structures can be formed at the edge of multiatomic steps. On the other hand, on the 3.0°- misoriented wafer, the thickness of GaAs QWLs at the edge of multiatomic steps was almost the same as on the terraces, and the GaAs QWL layer looked wavy, because the average step height was low. For the QWL on the singular (001) GaAs substrate, very abrupt GaAs/AlGaAs interfaces were obtained, as shown in Fig. 3.4 (a).

Figure 3.4 (c) also shows that the thickness of AlGaAs layers was almost constant even at the edge of multiatomic steps. These results can be explained by the difference of surface migration length between Ga and Al ad-atoms [1]. The surface migration length of Ga atoms is much larger than that of Al ones and the width of enlarged terraces. On the other hand, that of Al ones is shorter than the enlarged terrace width. These suggest that Al ad-atoms can be incorporated either on the

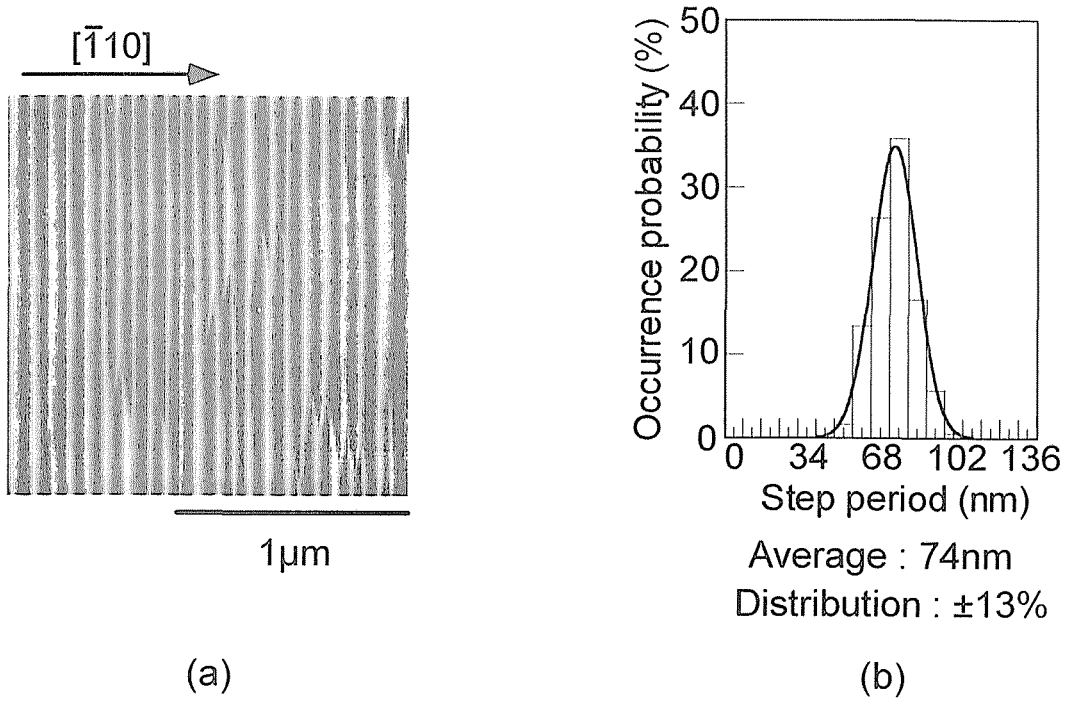

Fig. 3.3 (a) Atomic force microscopy image of GaAs multiatomic steps and (b) the histogram of step spacing. Misorientation angle and direction of vicinal substrates were 5.0° and in the [-110] direction.

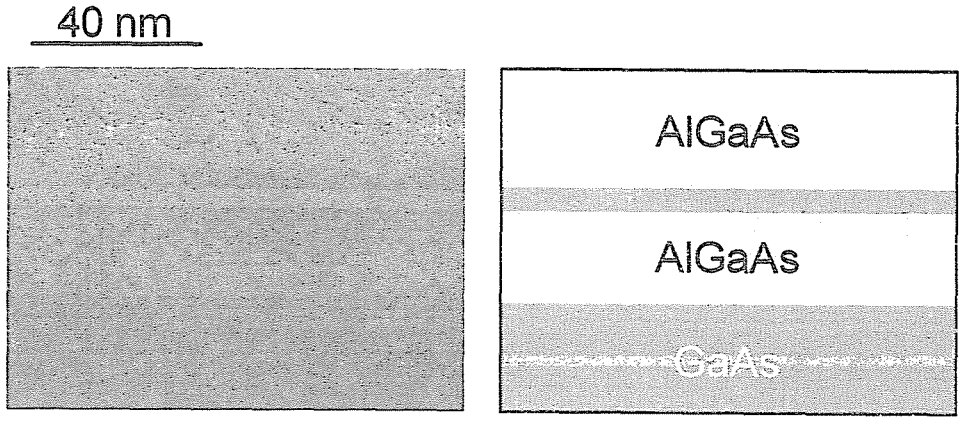

(a) on singular GaAs (001) substrate

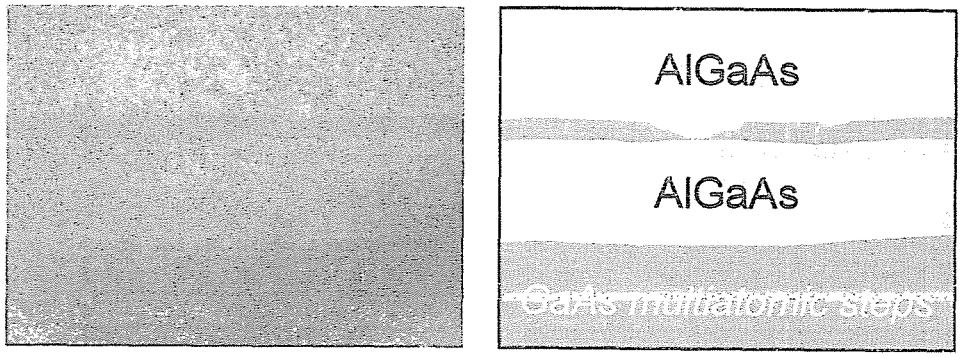

(b) on 3.0° misoriented (001) substrate

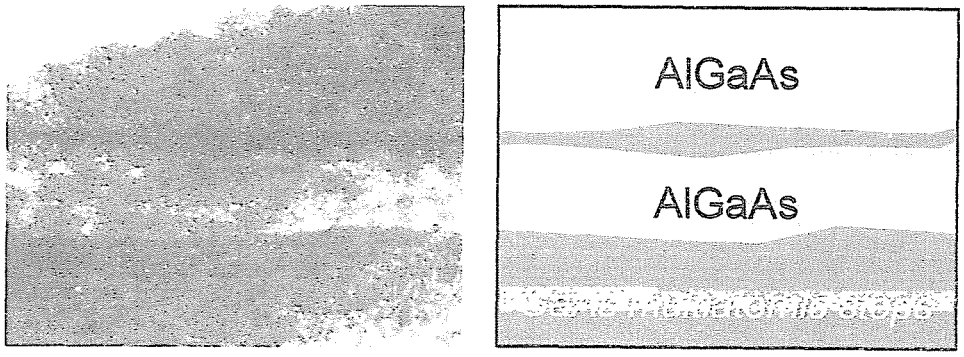

(c) on 5.0° misoriented (001) substrate

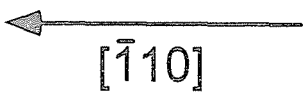

Fig. 3.4 Transmission electron microscopy images of quantum structures on (a) singular (001), (b) 3.0° misoriented and (c) 5.0° misoriented (001) GaAs substrates. Average well layer thickness was 4 nm.

terraces or at the step sites, although Ga ad-atoms easily can go down and up across monolayer steps. Therefore, these features can be expected more likely for AlAs layers on multiatomic steps than for AlGaAs layers that are ternary alloy.

3.5 Characterization of GaAs Quantum Wires

Photoluminescence Characterization

Figure 3.5 shows the PL spectra of the QWR structures on the misoriented substrates at 20 K compared with that of the QWL formed on the singular (001) substrate. PL peak energy corresponding to the QWL on the singular (001), 3.0°- and 5.0°- misoriented substrates, was 1.654, 1.652 and 1.631 eV, respectively. The full width at half maximum (FWHM) of these PL spectra was 30, 42 and 41 meV, respectively. Because of the fluctuation of QWL thickness, the FWHM of PL spectra for the QWR structures on the misoriented substrates was larger than the QWL on the singular (001) substrate. The PL peak energy of the QWR structures grown on the 3.0°- misoriented substrate was found to be almost the same as that of the QWL. On the other hand, that of the QWR structures grown on the 5.0°- misoriented substrate was 23 meV smaller than that of the QWL on the singular (001) substrate. In MOVPE growth, the total amount of the grown materials is basically the same for these structures, being independent of the substrate misorientation angle [10]. Furthermore, it was verified that the growth thickness was almost the same between wafer to wafer within the area of the carbon susceptor in the present MOVPE systems, and the growth thickness difference from run to run was within 1 %. Therefore, this peak energy shift indicates that locally thick areas are formed in GaAs QWL on the 5.0°-misoriented substrate, that is, QWR structures are formed at the edge of multiatomic steps as schematically shown in Fig. 3.4 (c).

Numerical Calculation of Photoluminescence Peak Energy

PL peak energy of the QWRs was calculated assuming the structure as shown in

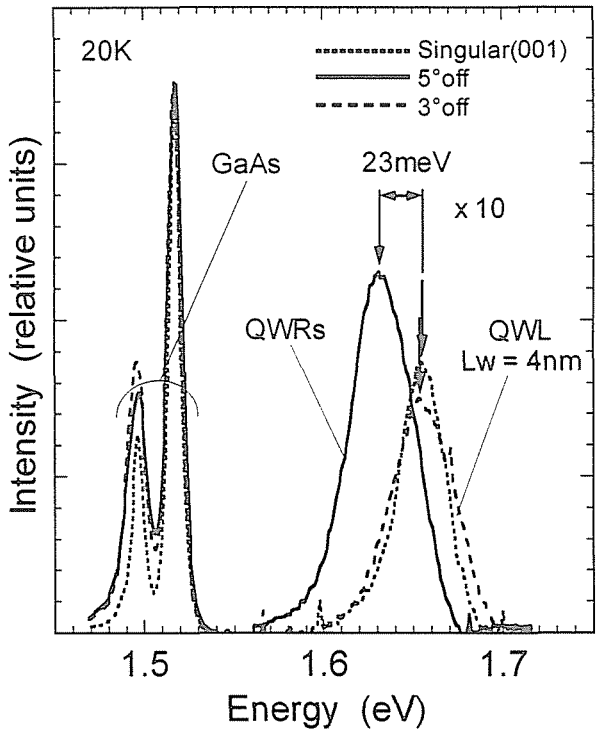

Fig. 3.5 Photoluminescence spectra of QWR structures on 5.0°- misoriented substrate (solid line) and 3.0°-misoriented substrate (dashed line), and QWL on the singular (001) substrate (doted line).

Fig. 3.1, and compared with the result of the experiments. Two-dimensional Schrödinger equation (3.1) was numerically solved by a finite difference method.

$$-\nabla\cdot\{p(x,y)\nabla\phi(x,y)\}+V(x,y)\phi(x,y)=\mathrm{E}\phi(x,y) \tag{3.1}$$

$$p(x,y)=\frac{\hbar^2}{2m(x,y)\mathrm{m}_0} \tag{3.2}$$

where *m(x,y)* is the position dependent effective mass. Electron and heavy hole energy levels in the QWRs formed on the multiatomic steps were estimated by the numerical calculations.

Main assumptions in this calculation are given as follows: First, it was assumed that the average height and spacing of the multiatomic steps on the 5.0°- misoriented substrate were 7.0 and 80 nm, respectively, and that the width of the *step bunching* area was 35.5 nm. These values were estimated from the AFM images in Fig. 3.2. It was also assumed the QWL thickness (t_{planar}) on the singular (001) substrates to be constant, 4nm. If the thickness of the GaAs QWL layers on the AlGaAs lower barrier layer are uniform, the GaAs thickness on the vicinal substrate is also equal to that on the singular (001) substrates, t_{planar}. This means that the GaAs growth thickness at the step bunching area, t_{step}, equals to that on the terrace, $t_{terrace}$ and t_{planar} ($t_{step} = t_{terrace} = t_{planar}$). On the other hand, if the GaAs growth rate at the edge of the multiatomic steps, t_{step}, is much larger than on the (001) terraces, $t_{terrace}$, the relation between such three kinds of the grown thickness is as follows; $t_{step} > t_{planar} > t_{terrace}$, because the total amount of the grown material is basically the same between on the singular GaAs (001) surface and the vicinal surface. Thicker GaAs at the edge of multiatomic steps corresponds to thinner GaAs layer on the terrace. Therefore, the cross-sectional shape of the QWRs at the edge of multiatomic steps is uniquely determined by the growth thickness ratio, $t_{terrace}/t_{planar}$. Since this parameter is a measure of the growth rates on the terraces or that at the edge of the multiatomic steps in the lateral direction, it is thought to be determined by the growth conditions such as AsH_3 partial pressures and GaAs growth rates. Therefore, according to the facts as mentioned above, the energy shifts were calculated as a function of the growth thickness ratio, $t_{terrace}/t_{planar}$ (< 1).

In this calculation, the values of $0.067\mathrm{m}_0$ and $0.0914\mathrm{m}_0$ were used as an electron

effective mass in the GaAs QWL and in the AlGaAs barrier layer, respectively, and $0.34m_0$ and $0.433m_0$ as heavy hole effective mass, respectively, where m_0 is electron rest mass. According to the Miller's rule [11], the band offset between AlGaAs and GaAs layers was 224 meV for the conduction band, ΔEc, and 150 meV for the valence band, ΔEv.

PL peak energy of the QWRs at the edge of multiatomic steps and the peak energy of the QWL on the singular GaAs (001) substrates were calculated as shown in Fig. 3.6. In this figure, the solid line shows the quantization energy shift of QWRs on the 5.0°- misoriented GaAs substrates, and the dashed line shows that of the QWLs on the singular GaAs (001) substrates at 20K. The quantization energy shift for the QWRs is always smaller than that for the QWL. The growth thickness ratio estimated from the cross-sectional TEM images in Fig. 3.4 (c) is about 0.75. The closed circle shows the experimental data from the result of PL characterizations at 20K. The calculated energy shift with respect to the peak energy of the QWL on the singular (001) substrates is 25.4 meV toward the lower energy side at $t_{terrace}/t_{planar} = 0.75$. Therefore, the experimental data, the energy shift of 23 meV to the lower energy side, that is, the red shift, is in good agreement with the numerical calculation.

3.6 Summary

In this chapter, the self-organized fabrication of QWR structures utilizing coherent GaAs multiatomic steps were demonstrated. The main results are summarized as follows.

(1) To clarify the optimum conditions for the fabrication of QWR structures, GaAs multiatomic steps on the vicinal substrates were investigated by AFM. For the 5.0°-misoriented wafers, in particular, more coherent and straighter GaAs multiatomic steps could be formed on the surfaces than the other wafers. Average height and spacing of the multiatomic steps were 7.0 nm (25 MLs) and 80 nm, and the distribution of inter-step spacing was estimated to be within ± 13 %.

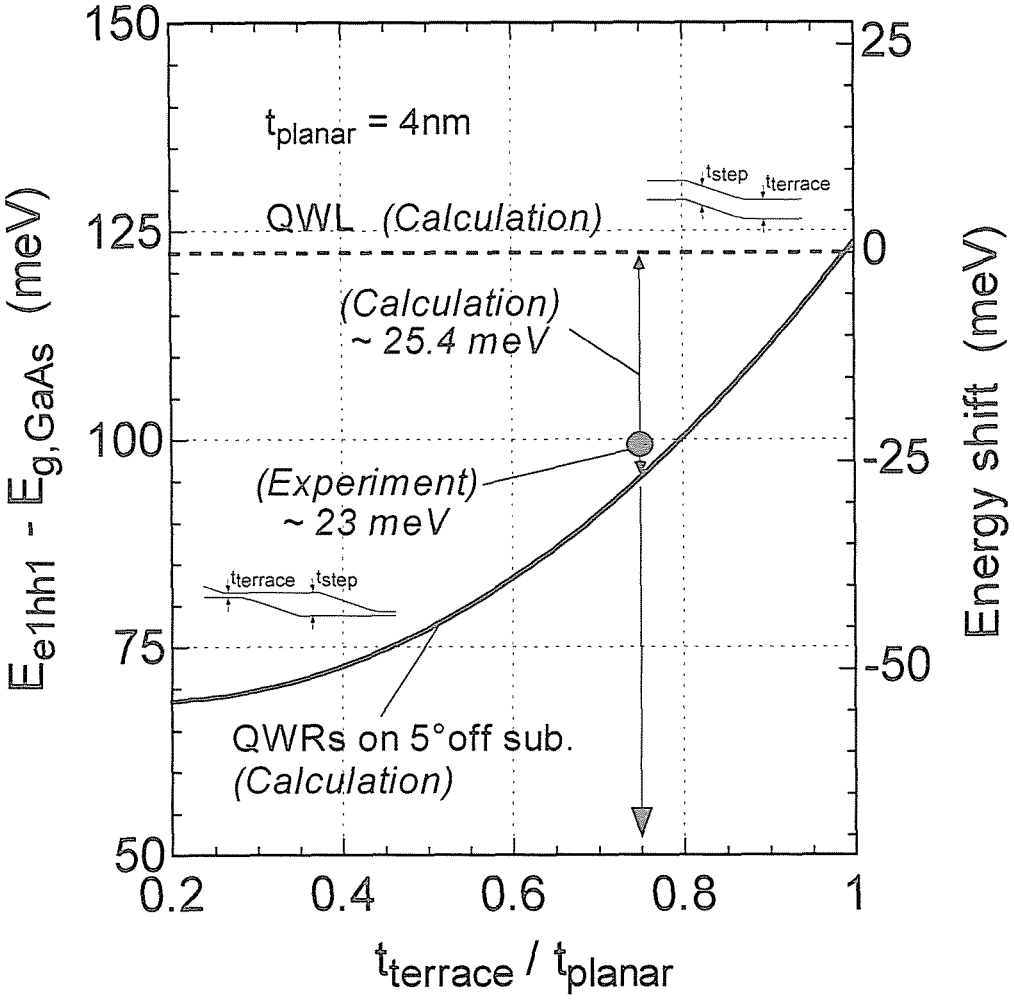

Fig. 3.6 Photoluminescence peak energy as a function of thickness variation of GaAs layer, $t_{terrace}/t_{planar}$: (solid line) QWR structures on 5.0°- misoriented substrate; (dashed line) QWL on the singular (001) substrate. Well thickness on the singular (001) substrate(t_{planar}) is fixed at 4 nm in this calculation.

(2) As results of the cross-sectional TEM observations, it was verified that GaAs layers at the edge of multiatomic steps on the 5.0°- misoriented substrate was thicker than that on the (001) terraces, on the other hand, the GaAs/AlGaAs interfaces on a singular (001) substrates was abrupt.

(3) Such GaAs QWR structures were also investigated by PL at 20 K. PL peak energy of the QWRs grown on the 5.0°- misoriented substrate was 23 meV smaller than that of the QWL on a singular GaAs (001) substrate.

(4) The result of PL energy shift in GaAs QWRs was also compared with a simple numerical calculation. It was shown that the PL peak energy shift of QWRs on the 5.0°- misoriented substrate was well fitted with the calculation results. This means that electrons and holes should be confined in the QWR regions at the edge of multiatomic steps, not in the QWL regions on the (001) terraces.

References

[1] T. Fukui and H. Saito: Jpn. J. Appl. Phys., 29, L483 (1990).

[2] H. Saito, K. Uwai and N. Kobayashi: Jpn. J. Appl. Phys., 32, 4440 (1993).

[3] J. Ishizaki, S. Goto, M. Kishida, T. Fukui and H. Hasegawa: Jpn. J. Appl. Phys., 33, 721 (1994).

[4] J. Ishizaki, K. Ohkuri and T. Fukui: Jpn. J. Appl. Phys., 35, 1280 (1996).

[5] J. Ishizaki, Y. Ishikawa, K. Ohkuri, M. Kawase and T. Fukui: Appl. Surf. Sci., 113/114, 343 (1997).

[6] J. Ishizaki, Y. Ishikawa and T. Fukui: Mat. Res. Soc. Symp. Proc., 448, 95 (1997).

[7] M. Kasu and N. Kobayashi: Appl. Phys. Lett., 62, 1262 (1993).

[8] K. Ohkuri, J. Ishizaki, S. Hara and T. Fukui: J. Cryst. Growth, 160, 235 (1996).

[9] M. Kasu and N. Kobayashi: Jpn. J. Appl. Phys., 33, 712 (1994).

[10] M. Kasu, H. Saito and T. Fukui: J. Cryst. Growth, 115, 406 (1991).

[11] R. C. Miller, D. A. Kleinman and A. C. Gossard: Phys. Rev. B, 29, 7085 (1984).

Chapter IV

Improvement Methods for Size Uniformity of GaAs Quantum Wires

4.1 Introduction

In previous chapter, the fabrication of GaAs/AlGaAs QWR structures was demonstrated. In device applications of quantum nano-structures, their size fluctuation can be a serious problem, especially in their application to semiconductor lasers. GaAs/AlGaAs QWR structures fabricated in chapter 3 have the size distribution of QWRs, as shown in the broadened line width of PL spectra, although the inter-step spacing fluctuation of GaAs multiatomic steps was within ± 13 %.

Patterned substrates with V-grooves formed by chemical etching have been intensively utilized in the fabrication of quantum structures such as QWRs and QDTs [1]. E. Colas *et al.* formed such V-grooves on the vicinal substrates, and utilized the (111)A facets formed during AlGaAs layer growth on such patterned vicinal substrates as the fabrication method for periodic quantum structures [2,3]. Since such periodic AlGaAs facet structures were formed with the same period of the underlying V-grooves on the vicinal substrates, by combining step bunching on the MOVPE-grown vicinal GaAs surfaces investigated the present work with this phenomenon, the formation of GaAs multiatomic steps can be controlled.

In this chapter, as the improvement methods for size uniformity of GaAs QWR structures, two specific attempts are introduced. GaAs QWR structures using thin AlAs layers as lower barrier layers and GaAs/AlGaAs wire-like structures using GaAs multiatomic steps on patterned vicinal GaAs (001) substrates are investigated. In the former half of this chapter, thin AlAs layer surfaces on GaAs multiatomic steps are characterized by AFM and optical characterization of AlGaAs/GaAs/AlAs QWR structures are also investigated. In the latter half, as a control method for the uniformity of step period, the straightness and the continuity of multiatomic steps,

GaAs multiatomic steps grown on patterned vicinal GaAs (001) substrates with a line and space pattern perpendicular to the misorientation direction of the substrates are characterized by AFM. GaAs/AlGaAs wire-like structures using lateral growth of GaAs from the edge of these multiatomic steps are also characterized by CL measurements.

4.2 Fabrication of GaAs Quantum Wires Using AlAs on GaAs Multiatomic Steps

In this section, the fabrication and characterization of QWR structures with thin AlAs layers as lower barrier are introduced in the first place. Surface morphologies of thin AlAs layers grown on coherent GaAs multiatomic steps are characterized by AFM through thin GaAs cap layers, and QWR structures fabricated on the AlAs multiatomic steps are also optically characterized.

4.2.1 Experimental Procedure

Samples were grown on both vicinal GaAs (001) substrates misoriented by 5.0° towards the [-110] direction and singular (001) substrates. A horizontal low-pressure MOVPE system with triethylaluminum (TEAl), triethylgallium (TEGa) and AsH_3 was used. AsH_3 partial pressures were 4.2×10^{-4} atm for GaAs buffer layer and 6.7×10^{-5} atm for GaAs QWR structures. Growth rates for GaAs buffer, AlAs lower barrier and GaAs single QWL layer were 1.1, 0.067 and 0.046 nm/s, respectively.

A schematic of GaAs QWR structures is shown in Fig. 4.1, and the details of fabrication processes are as follows: First, a 40-period $(AlAs)_3$ / $(GaAs)_3$ superlattice buffer layer was grown on the vicinal substrate in order to form the initial surface with monoatomic steps. Then, a thick GaAs buffer layer was grown at 650 °C to form multiatomic steps with a step height of about 22 monolayers (MLs) and the mean spacing of about 70 nm on the surfaces. Details of the multiatomic step formation

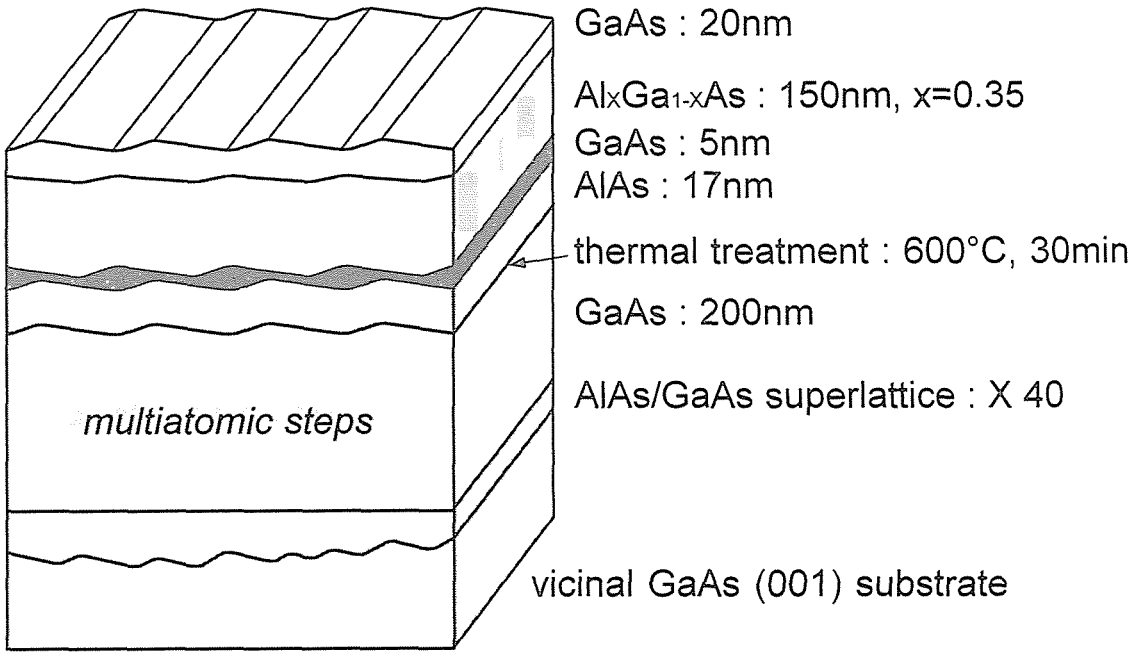

Fig. 4.1 Schematic of AlGaAs/GaAs/AlAs quantum wire structures on GaAs multiatomic steps.

processes and mechanism were described in chapter 2, and have been investigated and reported elsewhere [4-7]. Thermal treatment in AsH_3 / H_2 atmosphere was carried out for 30 min at 600 °C after the GaAs multiatomic step formation in order to make the steps edges straighter. The temperature was 600 °C, and the AsH_3 partial pressure was about 6.7×10^{-5} atm during the thermal treatment. Next, using AlAs as the lower barrier layer, single QWL structures were grown on GaAs multiatomic steps at 650 °C. For the QWL growth using AlGaAs as the lower barrier layer, locally thick GaAs layers at the edge of AlGaAs multiatomic steps, that is, the formation of QWR structures, was already confirmed with a cross-sectional transmission electron microscopy (TEM), as described in the previous chapter. Single QWL structures were simultaneously grown on a singular GaAs (001) substrate as a reference for QWRs. Average thickness of AlAs lower barrier layer, GaAs QWL layer (Lw), and AlGaAs upper barrier layer were 17, 5 and 150 nm, respectively. Aluminum content of AlGaAs layers was about 0.35.

Surface morphologies were analyzed by AFM in air. PL spectra were taken at 20K using an Ar^+ laser. Cross-sectional TEM images were taken with JEM-2010 at 200 keV.

4.2.2 Surface Observation of Multiatomic Steps

First, in order to obtain the optimum step structures prior to QWR fabrication, GaAs buffer layer surfaces were observed by AFM. Figure 4.2 (a) shows the surface morphology of GaAs buffer layer on the 5.0°-misoriented substrate after 30 min-thermal treatment in AsH_3 / H_2 atmosphere. The observation area was 1.7 μm × 1.7 μm. The presence of coherent multiatomic steps with extremely straight edges was observed on the GaAs buffer layer surfaces over a wide area. Figure 4.2 (b) shows the histogram of the step period obtained by the cross-sectional line profiles of the AFM image in Fig. 4.2 (a). The average height and spacing of the multiatomic steps were about 5.5 nm, which equals to 19 MLs, and 63 nm, respectively, as schematically

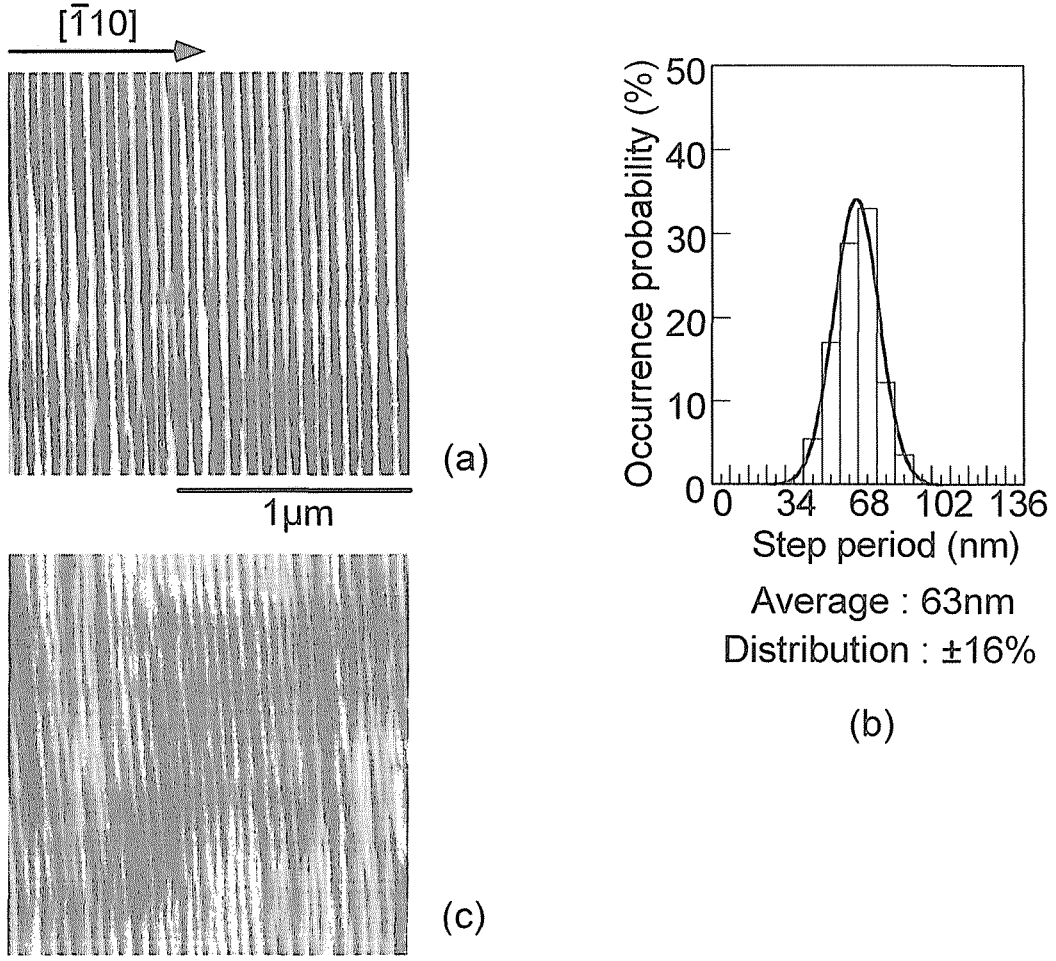

Fig. 4.2 (a) Atomic force microscopy image of GaAs multiatomic steps and (b) the histogram of step spacing. (c) AlGaAs surface morphology on GaAs multiatomic steps. Thickness of AlGaAs layers were about 20 nm. Misorientation angle and direction of vicinal substrates were 5.0° and in the [-110] direction. Growth temperatures were 650 °C.

shown in the figure. The fluctuation of step spacing was within ± 16 %.

In the previous chapter, the line width of PL spectra from the GaAs QWRs was rather broad, nevertheless the distribution of the step period on the GaAs multiatomic steps was within ± 13 %. In Fig. 4.2 (c), it can be seen that the step edges of AlGaAs multiatomic steps tend to be disordered during the growth, and the step spacing of the multiatomic steps was smaller than that on the underlying GaAs buffer layer surfaces. In the current QWR structures, it is important to keep such coherent GaAs multiatomic steps even after the growth of the lower barrier layers. Figures 4.3 shows the AFM images of AlAs surface morphologies on the GaAs multiatomic steps shown in Fig. 4.2 (a). The misorientation angle and direction of the vicinal GaAs (001) substrates were 5.0° and the [-110] direction, respectively. For the surface observations of these samples by AFM in air, 3 nm-thick GaAs cap layers were grown after the AlAs layer growth because AlAs can be easily oxidized in air. Although the step edges of AlAs multiatomic steps began to be slightly disordered as the growth thickness of AlAs layers increases, it was found that the inter-step separation and the straightness of the step edges can be kept after the growth of AlAs layers. As shown in Fig. 4.4 (a), average height and spacing of the multiatomic steps were about 5.7 nm, which corresponds to 20 MLs, and 66 nm, respectively, and the distribution of the step spacing was within ± 14 %. Even after the AlAs layer growth at 600 °C, the underlying GaAs multiatomic steps can be kept, and it can be seen that the step period was almost the same as that of the GaAs multiatomic steps. The straightness of the step edges was better than that on the AlAs layers grown at 650 °C, although the crystal quality of AlAs layers may be much higher at 650 °C than at 600 °C. Therefore, these results indicate that QWR structures can be uniformly fabricated by using AlAs at the lower barrier layer rather than using AlGaAs.

4.2.3 Optical Characterization

Figure 4.5 shows a cross-sectional TEM image and its schematic of GaAs QWR

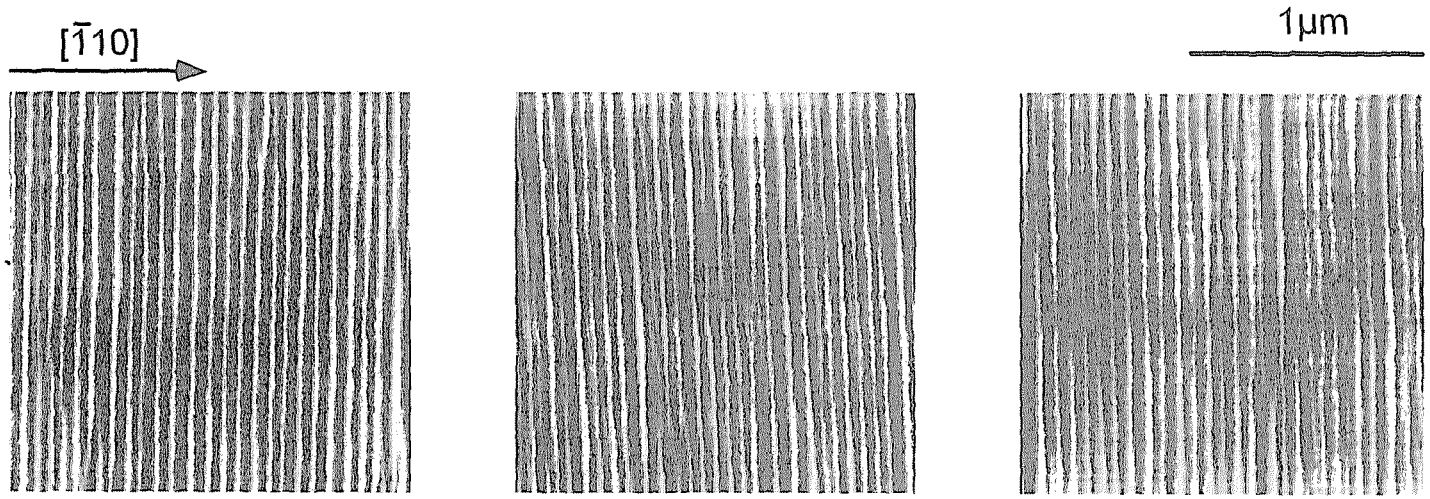

Fig. 4.3 Atomic force microscopy images of AlAs surfaces on GaAs multiatomic steps. Misorientation angle and direction of vicinal substrates were 5.0° and in the [-110] direction. All observations were done through the 3 nm-thick GaAs cap layers on the AlAs layers.

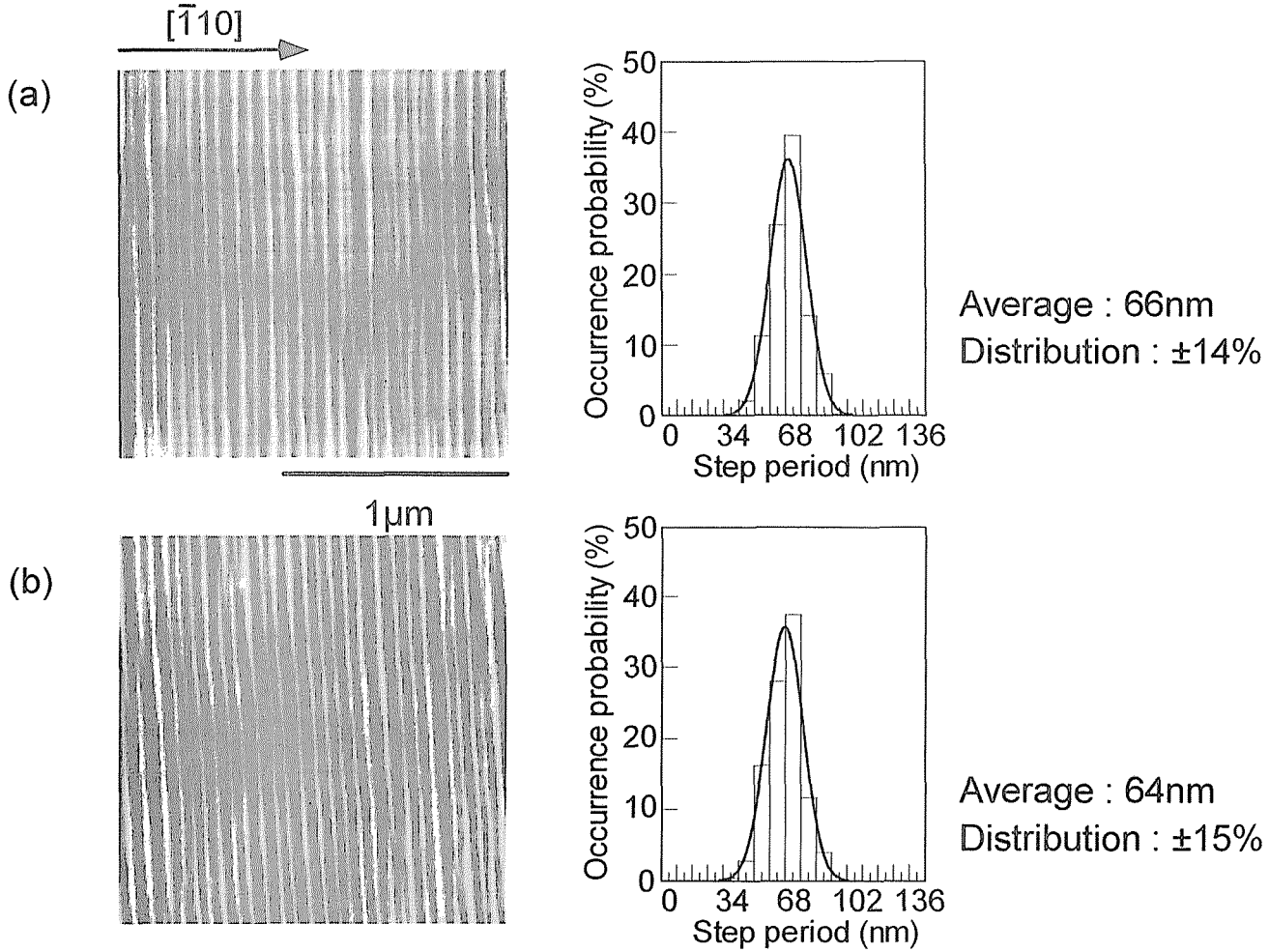

Fig. 4.4 Atomic force microscopy images of AlAs surfaces on GaAs multiatomic steps. The thickness of AlAs layers were about 17 nm. Growth temperatures of AlAs layers were (a) 650°C and (b) 600°C. Misorientation angle and direction were 5.0° and in the [-110] direction. Surface observations were done through the 3 nm-thick GaAs cap layers.

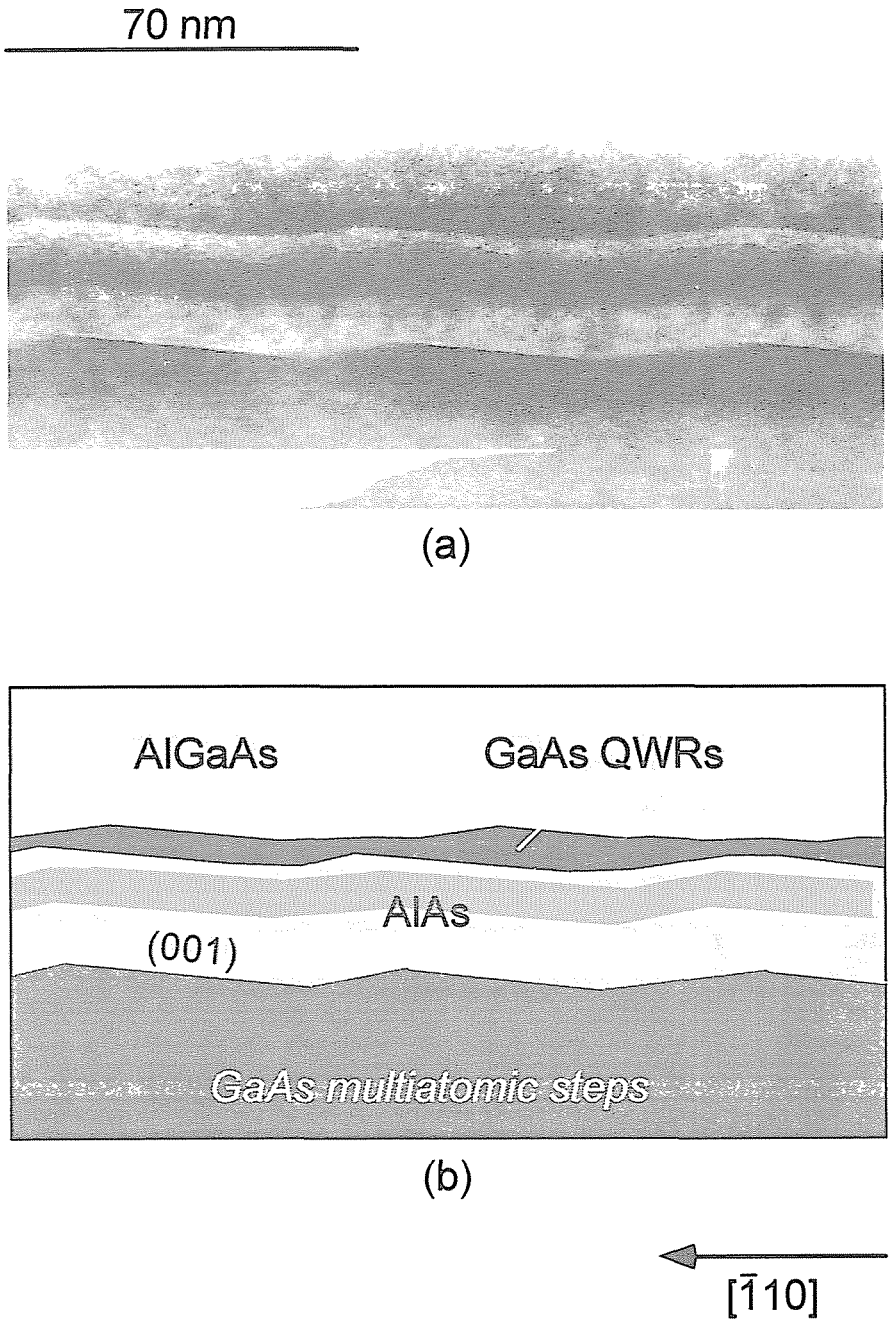

Fig. 4.5 Transmission electron microscope image of GaAs QWR sructurtes on 5.0° misoriented GaAs (001) substrate.

structures fabricated at the edge of AlAs multiatomic steps grown at 650 °C. This cross-sectional TEM image also supports that AlAs layers had the uniform thickness both at the edges and on the (001) terraces of GaAs multiatomic steps, and that the step period of AlAs multiatomic steps was the same as that of GaAs ones. The vertical thickness and the lateral width of GaAs QWR structures can be roughly estimated to be 10 nm and several 10 nm, respectively.

In order to examine the effect of using AlAs lower barrier layer instead of AlGaAs on the improvement of size uniformity of QWRs, PL properties of QWR structures were characterized. PL spectra of QWRs were also compared with those of QWL on the singular GaAs (001) substrates. In the first place, Figure 4.6 shows PL spectra at 20 K. The upper spectra are from the QWR structures with AlAs lower barrier layers, and the lower ones are from those with AlGaAs lower barrier layers. The average QWL thickness (Lw) was about 5 nm (1.617 eV) for the sample with AlAs and about 4 nm (1.654 eV) for the sample with AlGaAs. PL peak positions of QWRs structures were 1.593 eV for the sample using AlAs as lower barrier layers and 1.631 eV for that using AlGaAs. It was found that, in both cases, PL peak energies of QWRs were smaller than those of QWL formed on the singular GaAs (001) substrates. Although the peak energy should shift toward higher energy side because of two-dimensional quantum confinement effects, these spectra show the energy shifts to lower energy side. This means that locally thick QWR structures are formed at the edge of multiatomic steps, as discussed in chapter 3. In these PL spectra, the full width at half-maximum (FWHM) of QWRs with AlAs as lower barrier layer was estimated to be 25 meV, which is about 16 meV smaller than that with AlGaAs. This means that the size uniformity of QWRs with AlAs lower barrier layer was much improved. Fine-area PL spectrum of QWRs with AlAs by using Au-Ge patterned mask, whose open area is 2 μm-wide and 800 μm-long, was also taken. Through this kind of patterned mask, PL spectrum originating from about thirty QWRs can be measured. It was found that the FWHM of PL spectrum from about thirty QWRs was 17 meV, which was 8 meV smaller than that from the whole area, as shown in Fig. 4.7. This result implies that the size fluctuation of QWRs still remain for a wide area.

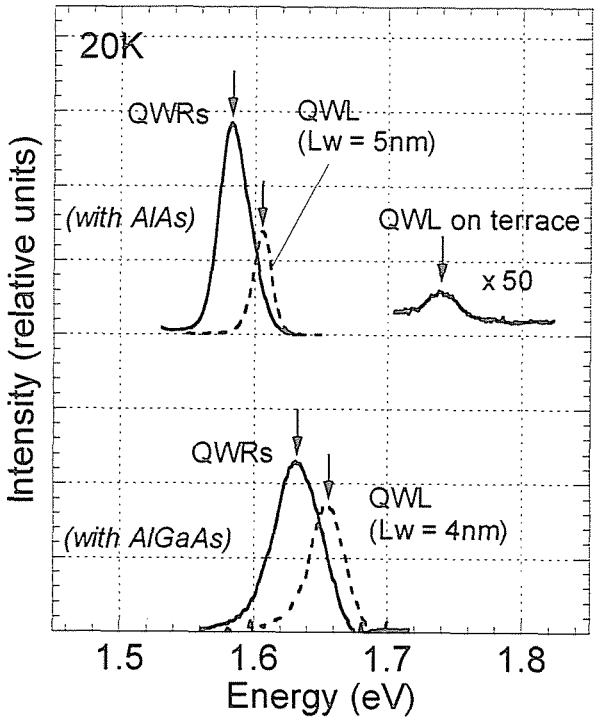

Fig. 4.6 Photoluminescence spectra of QWRs on 5.0°-misoriented substrate (solid line) and QWL on the singular (001) substrate (dashed line). Upper spectra are for quantum structures with AlAs layers as lower barrier layer, and lower ones are for those with AlGaAs layers.

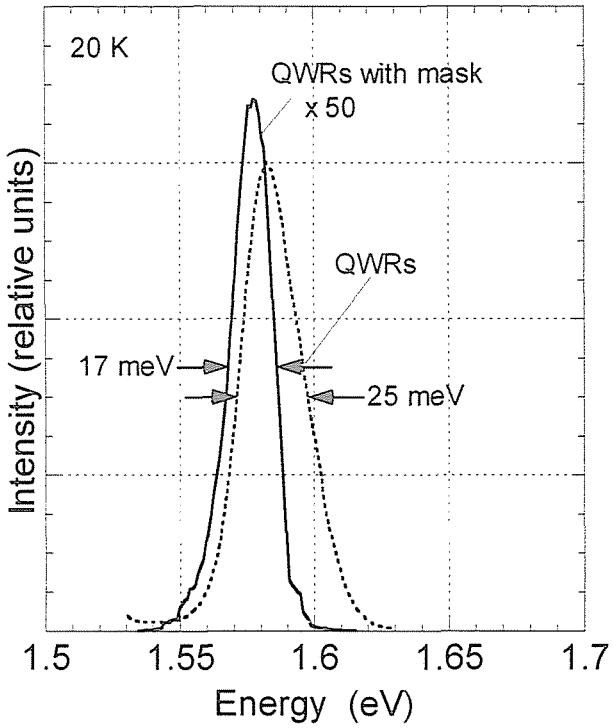

Fig. 4.7 Photoluminescence spectra of QWRs on 5.0°-misoriented substrate at 20K. Solid line is PL spectrum through the 2μm-width and 800 μm-long line patterned mask, which corresponds to the luminescence of about thirty QWRs, and doted line is that without the mask.

From the AFM observations of AlAs multiatomic steps, the distribution of their step spacing was estimated to be within ± 14 %. If the size fluctuation of QWR structures is almost the same as the distribution of the step spacing, ± 14 %, the fluctuation of the quantization energy in QWRs can be roughly estimated by the simple numerical calculation used in chapter 3. Strictly speaking, the uniformity of the step period does not completely equal to that of the QWRs' size because the cross-sectional shape of the QWRs can be changed by the fluctuation of the step period if the total amount of grown materials is independent of the substrate misorientation angle. In the current case, however, since the lateral width of the QWRs was about several times larger than the vertical thickness, the fluctuation of the vertical thickness of the QWRs, that is, the step height of the multiatomic steps, can be mainly affect the uniformity of the cross-sectional shape of the QWRs. Therefore, the assumption mentioned above can be appropriate to the calculation for the quantization energy fluctuation in the QWRs. This energy distribution was estimated to be about 16 meV, and was in good agreement with the FWHM of PL spectrum from about thirty QWRs. This implies that the size uniformity of QWRs depends on the spacing uniformity of AlAs multiatomic steps. Furthermore, in PL spectrum of the sample with AlAs as lower barrier layers, an additional weak spectrum at about 1.748 eV can be observed, as shown in Fig. 4.6. This spectrum probably corresponds to QWLs formed on the (001) terraces connecting with QWR areas. The result also supports that most of the photo-excited electrons and holes diffuses to the areas being lower energy states, that is, the QWR areas.

Polarization dependence of the QWRs using AlAs as lower barrier layers was also measured at 20K, and the results are shown in Fig. 4.8. Since the misorientation direction is [-110] and the direction along the QWRs is [110], the degree of polarization was defined as (I[110] - I[-110]) / (I[110] + I[-110]), where "I" is PL intensity. The degree of polarization for the QWRs was found to be 0.12. For the QWL on the singular GaAs (001) substrate, it was estimated to be about 0.04, and no large effect due to the internal stress is expected in this material systems. Therefore, the observed polarization anisotropy supports the successful formation of QWRs at

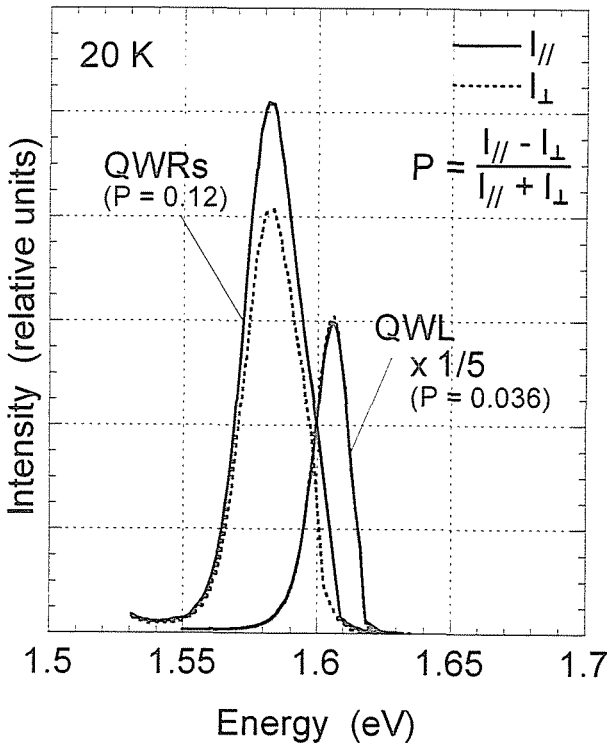

Fig. 4.8 Polarization dependence of photoluminescence spectra of QWRs on 5.0°- misoriented substrate and QWL on the singular (001) substrate at 20K. Solid line is PL intensity parallel to the QWRs ([110] direction) and doted line is that perpendicular to the QWRs ([-110] direction).

the edge of the multiatomic steps.

4.3 Fabrication of GaAs Multiatomic Steps on Patterned Vicinal Substrates

4.3.1 Sample Preparation Procedure

A horizontal low pressure MOVPE system was used with triethylgallium (TEGa), triethylaluminum (TEAl) and arsine (AsH_3) as group III and V sources. Partial pressure of AsH_3 was varied between 6.7×10^{-5} and 3.3×10^{-4} atm. Growth rate for GaAs and $Al_{0.27}Ga_{0.73}As$ multiatomic steps were 0.10 and 0.17 nm/s, respectively, and that for GaAs well layers was 0.050 nm/s.

Two types of vicinal GaAs (001) substrates with the line and space pattern in the [110] direction, which is perpendicular to the misorientation direction. One is a 4 μm-period pattern formed on the surfaces by using a conventional photolithography and wet chemical etching, and the other is a 1 μm-period one prepared by using an electron beam lithography and wet chemical etching. In the case of the 4 μm-period patterns, etching depth was 0.10 ~ 0.12 μm, and its width was about 2 μm. In the substrates with the 1 μm-period ones, etching depth and width were 0.10 ~ 0.12 μm and about 0.23 μm, respectively. All patterned vicinal substrates were etched by using the $HCl : H_2O_2 : H_2O$ (= 160 1 1) chemical etching solution at room temperature. Misorientation angle of the vicinal substrates was 2.0°.

Figure 4.9 shows a schematic illustration of the GaAs wire structures on patterned vicinal GaAs (001) substrates. First, GaAs/$Al_{0.27}Ga_{0.73}As$ multi-layer structures were grown on 4 μm-period line and space patterned substrates at 650 °C, in order to form multiatomic steps with the exactly oriented (001) terraces. Next, GaAs/$Al_{0.27}Ga_{0.73}As$ single QWL structure and GaAs cap layer were grown on these structures. Average thickness of GaAs and AlGaAs layers were about 5 and 60 nm, respectively. On the other hand, in the 1 μm-period patterned wafers, a thin GaAs buffer layer was initially grown on the substrate at 550 °C, because the shape of mesa

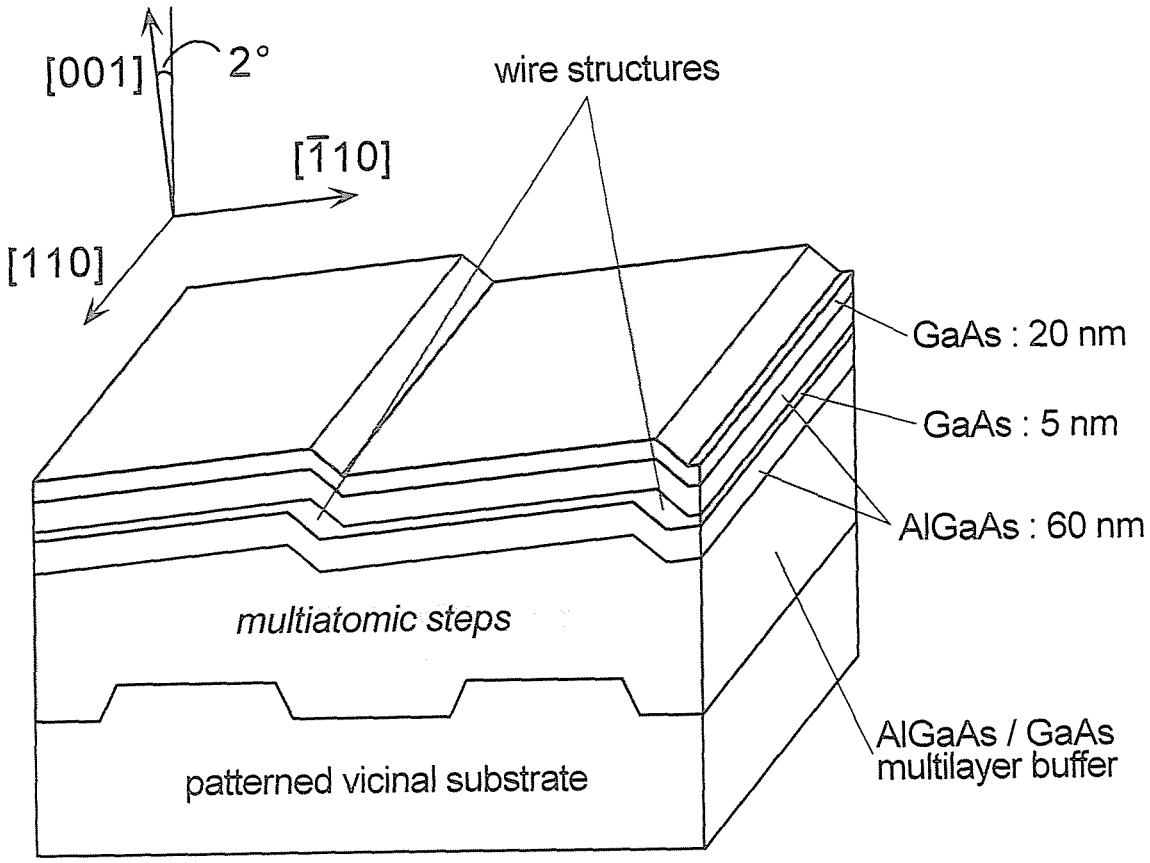

Fig. 4.9 Schematic of GaAs wire structures grown on patterned vicinal GaAs (001) substrates.

structures of line and space patterns tends to be disordered by the thermal etching effect before the growth at 650 °C. After that, GaAs and a 80-period $(AlAs)_3$ / $(GaAs)_3$ superlattice were grown as buffer layers at 650 °C. Next, in order to form multiatomic steps, GaAs/$Al_{0.27}Ga_{0.73}As$ multi-layer structures, followed by a single QWL structure growth at 650 °C. Average thickness of GaAs and AlGaAs of layers were 4 and 60 nm, respectively. QWL structures were simultaneously grown on *unpatterned* singular (001) substrates in the same growth run as a reference.

A scanning electron microscope (SEM) was used for observations of multiatomic steps and GaAs QWR structures. Cathodoluminescence (CL) was measured at 4.2 K for spectrum and spatial resolved luminescence image observations. The excitation electron beam energy and current were 10 keV and 250 pA, respectively.

4.3.2 Formation of Multiatomic Steps on Patterned Vicinal Substrates

First, in order to clarify the formation process of multiatomic steps on line and space patterned substrates, the cleaved cross-sections of multi-layer structures were observed by SEM. Figure 4.10 (a) shows cross-sectional SEM image of a typical GaAs/AlGaAs multi-layer structure on the 4 μm-period line and space patterned substrate. GaAs growth rate around the edges was faster than on the flat areas of mesa stripes at the initial stage of GaAs/AlGaAs multi-layer growth. On the other hand, AlGaAs growth rate was always the same, both around the edges and on the flat areas. As the growth proceeded, etched trenches were buried, and the periodic multiatomic step structures were formed because of the lateral growth of GaAs layers. It was also confirmed that, even though only thick GaAs layers were grown, it was possible to form periodic multiatomic steps on the patterned vicinal surfaces, although E. Colas *et al.* reported that the formation of multiatomic steps had occurred only in thick AlGaAs growth [2,3]. The step period was estimated to be 4 μm, which corresponds to the period of the initial line and space pattern on the substrate. This result indicates the uniformity of multiatomic step period can be much improved by the patterning on

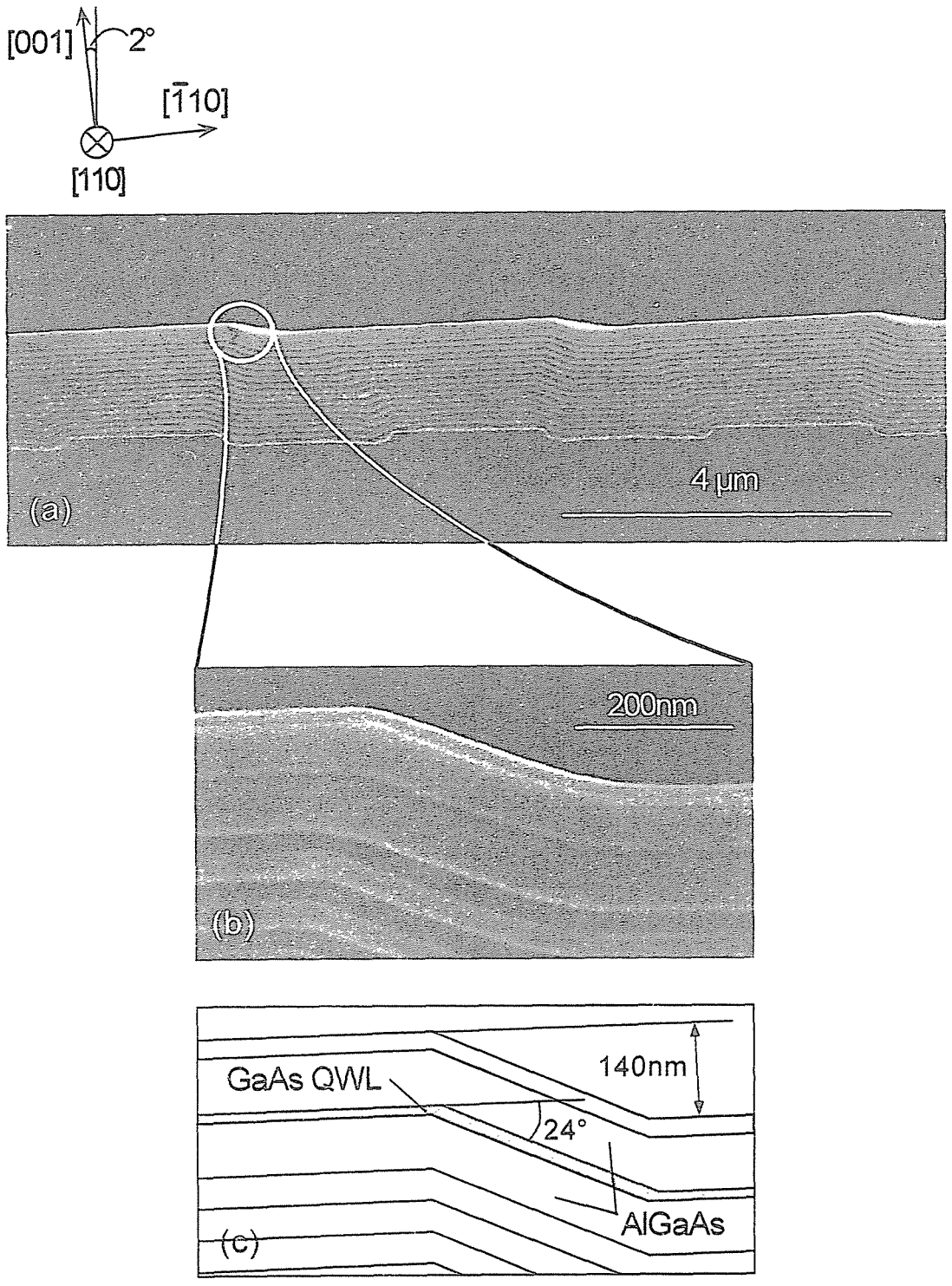

Fig. 4.10 (a) Cross-sectional scanning electron microscopy image of multiatomic steps on 4 μm-period line and space patterned vicinal GaAs (001) substrates, and (b) its high magnification image and (c) schematic near the step edge.

the vicinal substrate. Figures 4.10 (b) and (c) show a high magnification image and its schematic near the multiatomic step area, which indicate local thickness variation of the QWL layers. QWL at the edge of multiatomic steps is about 1.3 times thicker than that on the terraces. Furthermore, the angle between the multiatomic step areas and (001) terraces was about 24°, which indicates the surface of multiatomic step areas is closely to the (113)B facet. Such multiatomic steps were formed at the early stage of GaAs / AlGaAs multi-layer growth, and were maintained during the following growth. After the multiatomic step structures were formed, the terrace region between step edges was oriented to exactly [001] direction. This means that the height of multiatomic steps can be controlled by varying the misorientation angle and the period of line and space pattern on the vicinal substrates because no multiatomic steps existed on the (001) terrace regions.

Figures 4.11 (a) and (b) show cross-sectional SEM image and its schematic of a typical GaAs/AlGaAs multi-layer structure on the 1 μm-period line and space patterned substrate. Both AlGaAs and GaAs growth rates around the step edges were faster than on the flat areas of mesa stripes at the initial stage of GaAs/AlGaAs multi-layer growth. Thickness of AlGaAs and GaAs around the edges was about 1.2 and 2.2 times thicker than that on the terraces, respectively. Especially in the GaAs growth, the difference of growth rate between around the step edges and on the terraces was much larger than that on the 4 μm-period patterned substrates. For the GaAs/AlGaAs multi-layer growth on 1 μm-period patterned substrates, AsH_3 partial pressure was about 3.3×10^{-4} atm, which was 5 times higher than that on the 4 μm-period patterned substrate, because their etched trenches were buried immediately, and no multiatomic steps were formed under the low AsH_3 partial pressure conditions. This result implies that the surface migration of Ga and Al atoms is enhanced under the low AsH_3 partial pressure conditions.

4.3.3 Optical Characterization

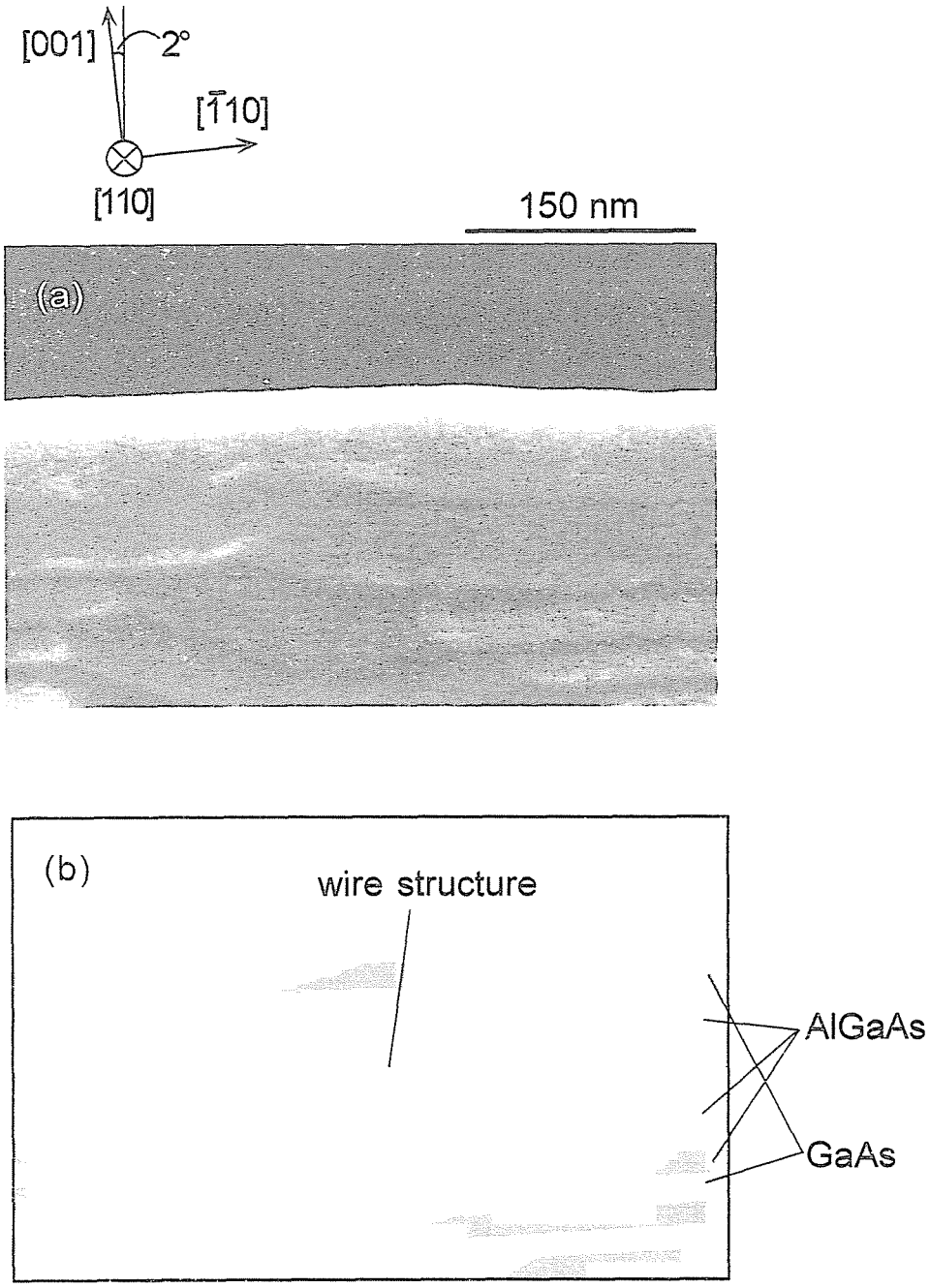

Fig. 4.11 (a) Cross-sectional scanning electron microscopy image near the step edge of multiatomic steps on 1 μm-period line and space patterned vicinal GaAs (001) substrates and (b) its schematic.

In order to optically characterize the formation of the locally thick wire-like structures at the edge of multiatomic steps, CL was measured at 4.2 K. Figure 4.12 shows CL spectrum of GaAs/AlGaAs QWL on 4 μm-period patterned vicinal substrate. Two features of the CL spectrum can be seen, that is, a main peak at 1.634 eV and a weak side peak at 1.611 eV. In order to identify the origin of the peaks, cross-sectional and top view of spatial resolved CL images for these emission peak energies. Figures 4.13 (a) and (b) show CL images detected at the energy of weak side peak (1.611 eV) and main peak (1.634 eV), respectively. From these CL images, it was found that the weak side peak and the main peak of CL spectrum were from the QWLs at the edge of multiatomic steps and on the (001) terrace areas, respectively. The thickness of QWLs was estimated from the CL emission peak energies. The peak energies of 1.611 and 1.634 eV correspond to the emission from 5.2 and 4.2 nm-thick QWLs. This also means that the thickness of QWL at the edge of multiatomic steps was about 1.2 times thicker than that of QWL on the (001) terraces, which was consistent with the results of cross-sectional SEM observations.

Figure 4.14 shows CL spectra of GaAs/AlGaAs QWLs on the 1 μm-period patterned vicinal and *unpatterned* singular (001) substrates at 4.2 K. CL spectrum from the QWL on patterned vicinal substrates had two peaks at 1.586 and 1.666 eV. On the other hand, that on *unpatterned* singular (001) substrates had a single peak at 1.643 eV. Figures 4.15 (a) and (b) show CL images detected at the energy of these two peaks for the QWL on patterned vicinal substrates. From these CL observations, it was verified that lower and higher energy peaks of the CL spectrum were from the QWL at the edge of multiatomic steps (a) and on the (001) terrace areas (b), respectively. The thickness of the QWLs was estimated from the CL emission peak energy. The peak energy of 1.586 eV corresponds to the emission from 6.6 nm-thick QWL, and that of 1.666 eV corresponds to that from 3.3 nm-thick one. Similarly, on the singular (001) substrate, that of 1.643 eV corresponds to that from 3.9 nm-thick QWL. The thickness of the QWL at the edge of multiatomic steps was about 2 times thicker than that of QWL on the (001) terraces. This result was also in good agreement with the results of cross-sectional SEM observations.

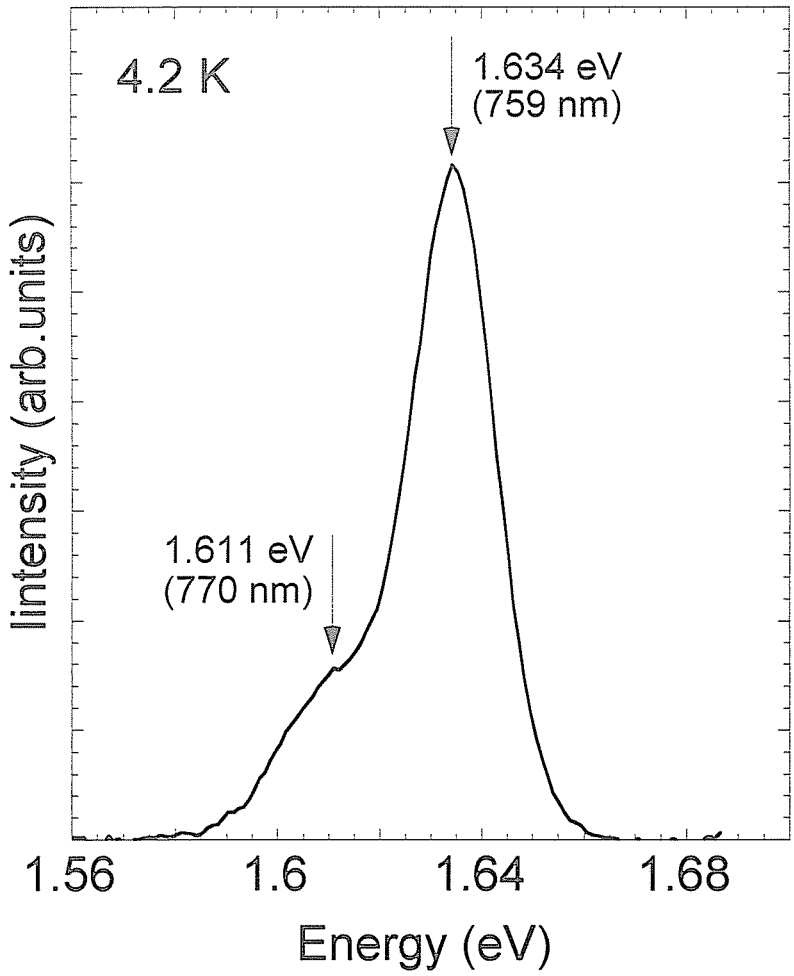

Fig. 4.12 Cathodoluminescence spactrum of QWL on 4 μm-period line and space patterned vicinal GaAs (001) substrates.

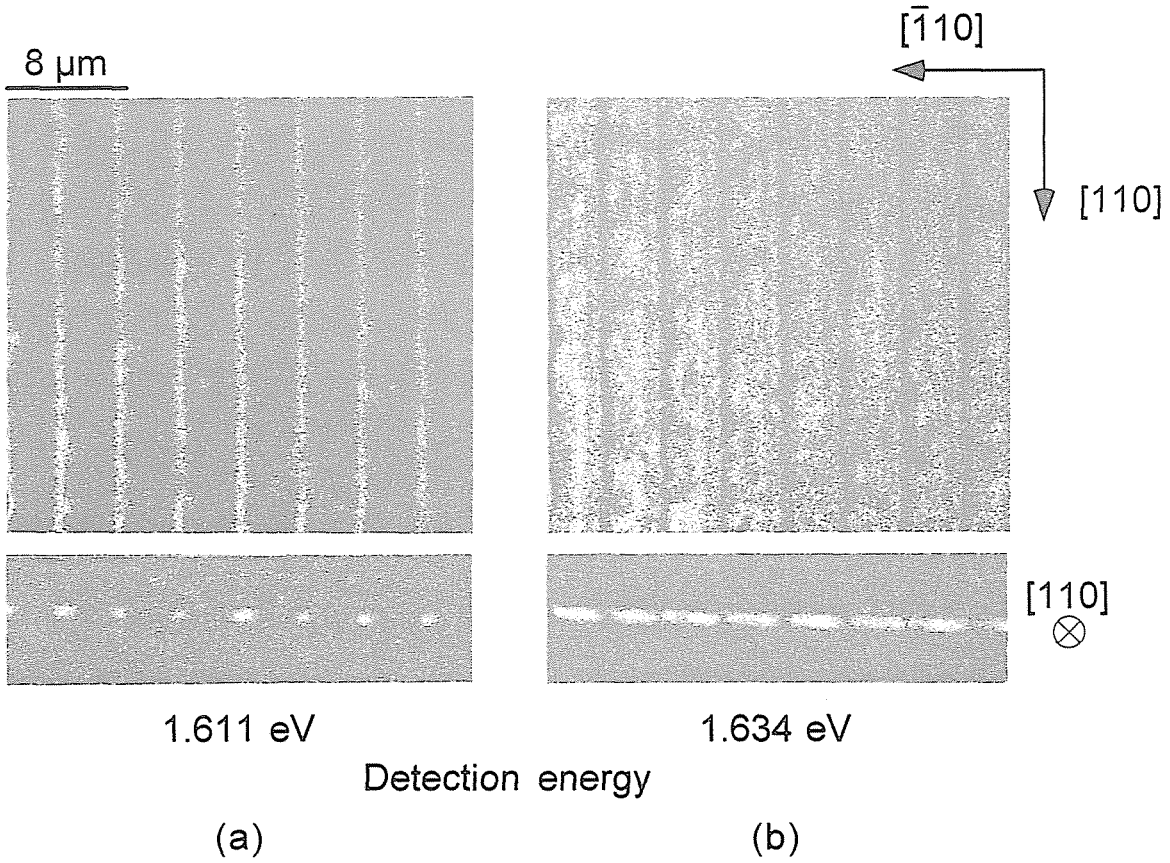

Fig. 4.13 Top (upper) and cross-sectional (lower) views of spatial resolved cathodoluminescence of QWL on 4 μm-period line and space patterned vicinal GaAs (001) substrates.

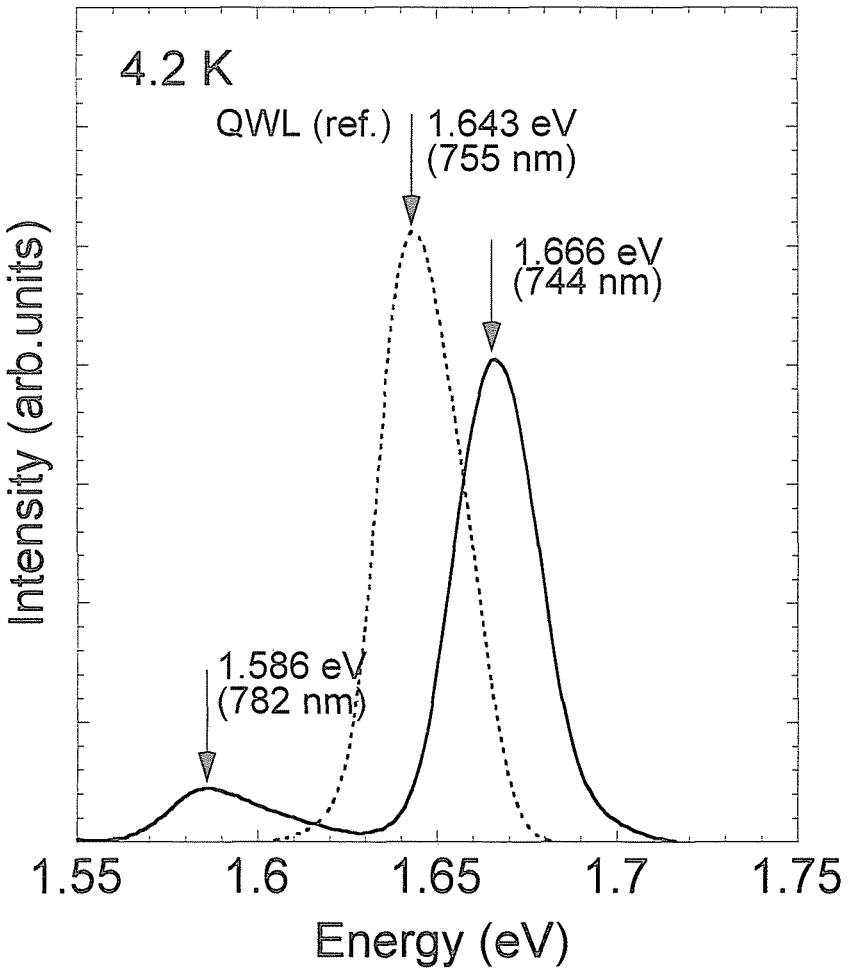

Fig. 4.14 Cathodoluminescence spactrum (solid line) of QWL on 1 μm-period line and space patterned vicinal GaAs (001) substrates. Doted line is spectrum of QWL on singular (001) substrate.

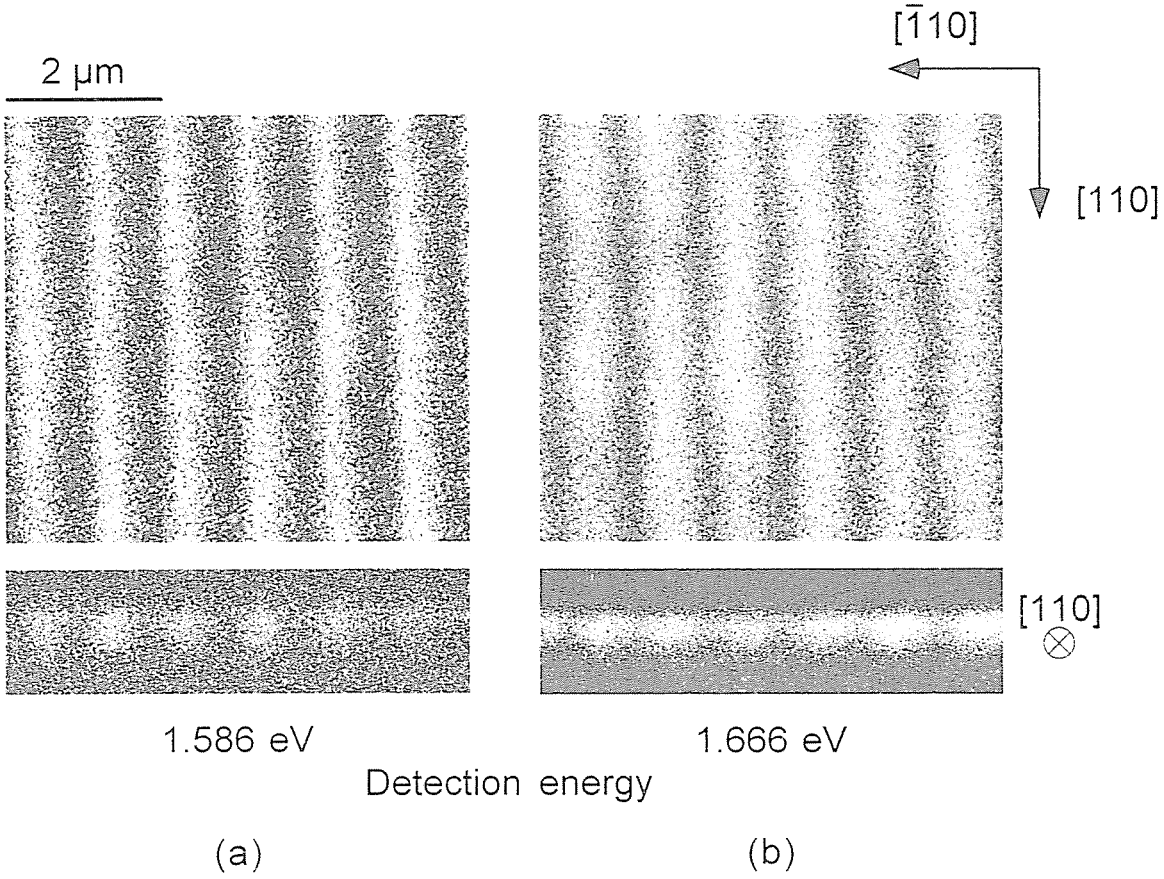

Fig. 4.15 Top (upper) and cross-sectional (lower) views of spatial resolved cathodoluminescence of QWL on 1 μm-period line and space patterned vicinal GaAs (001) substrates.

In the previous chapter, it was confirmed that PL peak energy shifts to lower energy side were due to the effects of both the two-dimensional quantum confinement in QWRs and the locally thick QWR formation at the edge of multiatomic steps. In the current investigations, however, although a direct evidence of the two-dimensional quantum confinement effects in QWRs could not be obtained, the results imply that the straightness, the continuity and the uniformity of multiatomic steps can be perfectly controlled by adjusting the growth conditions, the misorientation angle and the period of the line and space patterns. It should also be noted that larger in-plane thickness modulation of the QWL can be obtained by using these patterned vicinal substrates. Furthermore, uniform CL emissions both from the edge of multiatomic steps and the (001) terrace areas were clearly observed over a wide area more than thirty micrometers. This result suggests that the thickness of QWL layers at the edge of multiatomic steps was uniform, and that straight QWR structures with high continuity and uniformity along the multiatomic steps can be fabricated.

4.4 Summary

In this chapter, as the improvement methods for size uniformity of GaAs QWR structures, two specific attempts were introduced. GaAs QWR structures using thin AlAs layers as the lower barrier layers and GaAs/AlGaAs wire-like structures using GaAs multiatomic steps on patterned vicinal GaAs (001) substrates were investigated. Main results are summarized below.

(1) Surface morphologies of AlAs and AlGaAs layers, which were used as lower barrier layers of the QWR structures, on GaAs multiatomic steps were investigated by AFM. Coherent GaAs multiatomic steps with extremely straight edges over a wide area had the tendency to be disordered during the growth of AlGaAs layers on them. It was found that the underlying coherent GaAs multiatomic steps were well traced by AlAs rather than AlGaAs.

(2) QWR structures using AlAs as lower barrier layers were fabricated and

characterized by PL at 20K. FWHM of PL spectrum from the QWRs using AlAs layers was about 16 meV smaller than that using AlGaAs, which originates from the much improvement of the size uniformity in QWR structures by using AlAs as lower barrier layers.

(3) It was also observed that PL peak energies of the QWRs were smaller than those from the QWL formed on the singular (001) GaAs substrates, and that polarization anisotropy in PL spectra of the QWRs with AlAs was about 0.12.

(4) GaAs layers grown on patterned vicinal GaAs (001) substrates by MOVPE formed extremely straight and coherent multiatomic steps. SEM observations revealed that such multiatomic steps can be formed in the same period with the underlying vicinal substrates' one.

(5) Cross-sectional SEM images showed that coherent GaAs multiatomic steps were formed with the (001) terraces during GaAs/AlGaAs multi-layer growth on patterned vicinal substrates, and that GaAs well layer thickness at the edges of multiatomic steps was about 2 times thicker than that on the terraces for the wafers with the 1 μm-period line and space pattern.

(6) From cross-sectional CL image observations, two emission peaks in CL spectrum at 4.2 K were from QWL at the edges and on the (001) terraces of multiatomic steps. The thickness of GaAs well layers estimated from CL emission peak energy was consistent with that from SEM images. In the top view of CL images, uniform emissions both from the edge and the (001) terrace areas of multiatomic steps were also observed clearly over a wide area more than thirty micrometers.

References

[1] E. Kapon, D. M. Hwang and R. Bhat: Phys. Rev. Lett., **63**, 430 (1989).

[2] E. Colas, E. Kapon, S. Simhony, H. M. Cox, R. Bhat, K. Kash and P. S. D. Lin: Appl. Phys. Lett., **55**, 867 (1989).

[3] E. Colas, S. Simhony, E. Kapon, R. Bhat, D. M. Hwang and P. S. D. Lin: Appl. Phys. Lett., **57**, 914 (1990).

[4] J. Ishizaki, S. Goto, M. Kishida, T. Fukui and H. Hasegawa: Jpn. J. Appl. Phys., **33**, 721 (1994).

[5] J. Ishizaki, K. Ohkuri and T. Fukui: Jpn. J. Appl. Phys., **35**, 1280 (1996).

[6] J. Ishizaki, Y. Ishikawa, K. Ohkuri, M. Kawase and T. Fukui: Appl. Surf. Sci., **113/114**, 343 (1997).

[7] J. Ishizaki, Y. Ishikawa and T. Fukui: Mat. Res. Soc. Symp. Proc., **448**, 95 (1997).

Chapter V

Fabrication and Characterization of InGaAs Quantum Wires

5.1 Introduction

Lattice mismatched material systems with strain between two types of compound semiconductor materials with difference lattice constants are very promising to improve the characteristics of semiconductor lasers. For example, because of the increased energy splitting of heavy hole (HH) and light hole (LH) bands in the valence band of the strained QWL structures, the threshold current density of QWL lasers cane be reduced, and the difference between TE (transverse electric) and TM (transverse magnetic) mode gain can be increased. InAs/GaAs QDT lasers grown in Stranski-Krastanov mode have actually been fabricated, and their promising characteristics have also been demonstrated recently [1,2]. From the viewpoint of laser applications, the fabrication of semiconductor lasers operating in the infrared wavelength region has been more important; for example, the application to the excitation lasers, which have to be operated at around 980 nm, for an erbium (Er^{3+})-doped fiber amplifier for the light-wave communication systems [3].

Locally thick GaAs QWR structures have been fabricated at the edge of AlAs multiatomic steps in the previous chapter. However, even though thin AlAs layers had been used as a lower barrier layer of the QWRs instead of AlGaAs, the uniformity of multiatomic steps on a GaAs buffer layer would have been slightly degraded during the AlAs growth, as observed in the fine-area PL characterizations through the patterned mask. That is probably due to the shorter migration length of Al ad-atoms on the GaAs surfaces than that of Ga ones. To introduce InGaAs layers into the well layers on the GaAs multiatomic steps is beneficial to the fabrication of the QWRs because the coherent GaAs multiatomic steps can be directly used without slight disordering of the multiatomic step structures by Al-related alloy semiconductor

growth, and InGaAs/GaAs strained material systems become available even in the present QWR structures.

In this chapter, the formation and characterization of locally thick self-organized InGaAs strained QWR structures at the edge of coherent GaAs multiatomic steps grown by MOVPE on vicinal (001) GaAs substrates are demonstrated. To form much uniform QWR structures and apply them to semiconductor lasers operating in the infrared wavelength region, InGaAs layers are directly grown on coherent GaAs multiatomic steps. The growth mode transition of InGaAs layers from step flow growth mode to the mixture of step flow growth and three-dimensional nucleation mode as increasing the indium content is observed by AFM. Such growth mode transition can be controlled by adjusting the crystal growth conditions of InGaAs layers. Optical properties of InGaAs/GaAs QWRs are also examined, and one-dimensional nature of the QWRs will be investigated. Finally, the formation of coherent and straight InGaAs wire structures over more than thirty micrometer areas on patterned vicinal GaAs (001) substrates are briefly demonstrated.

5.2 Experimental procedure

Basic scheme for the sample preparation and the substrates used here were the same as the previous chapters. A typical sample structures of InGaAs QWRs are schematically shown in Fig. 5.1. Although there were two types of the QWR samples used here, no significant differences between them were observed. After the formation of GaAs multiatomic steps, the thin InGaAs layers were grown at 600 °C. Most of the samples were always grown at 600 °C unless otherwise specified, and the sample structures were as shown in Fig. 5.1 (a). AsH_3 partial pressure and the growth rate for the InGaAs layer growth were fixed at 6.7×10^{-5} atm and 0.050 nm/s, respectively. As mentioned before, the low AsH_3 partial pressure and the low growth rate are to enhance the surface migration of Ga and In atoms. Indium contents of InGaAs were 0.1, 0.15, 0.2 and 0.3, and their average thickness was always 3 nm.

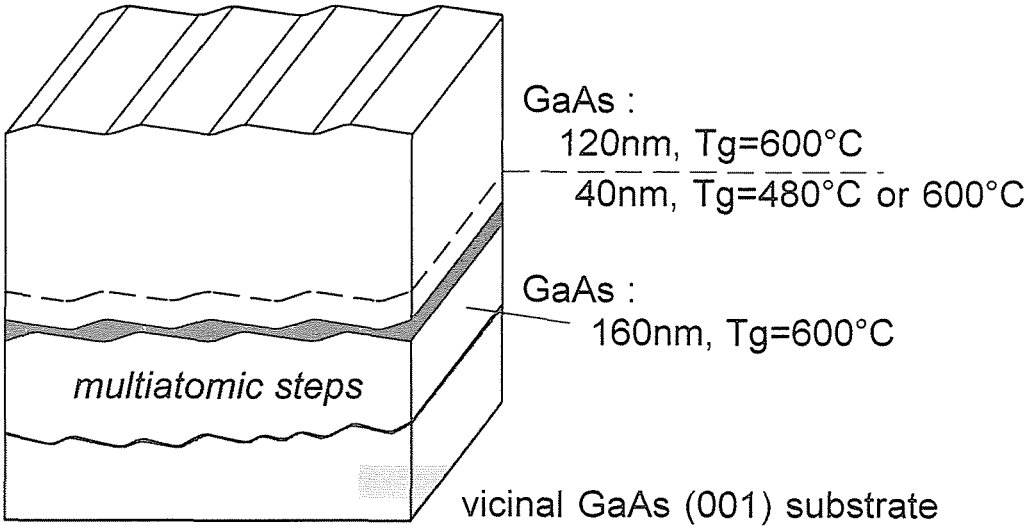

(a)

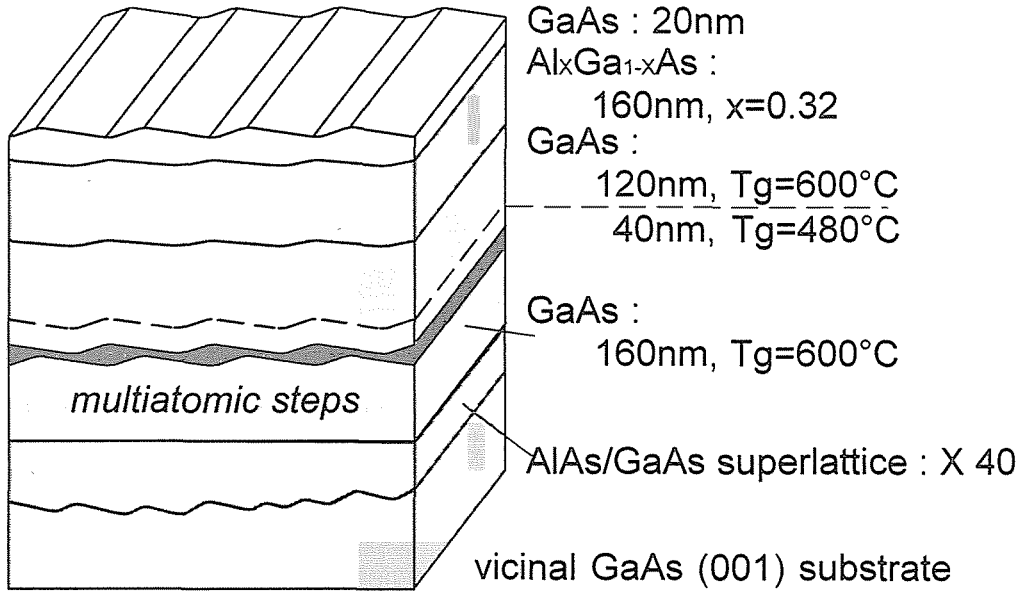

(b)

: InGaAs (Average thickness : 3nm)

Fig. 5.1 Schematic of InGaAs QWR structures on vicinal GaAs (001) substrates.

AFM was used for observations of GaAs and InGaAs surface morphology in air. Cross-sectional images of QWRs and QWL structures were characterized by TEM. These cross-sectional TEM images were taken with JEM-2010 at 200 kV. PL was measured at 77 K for the optical characterization of InGaAs/GaAs QWRs using an Ar^+ and Ti:S laser. PLE spectra were also measured to study the polarization anisotropy in InGaAs QWRs at 77 K. A continuously working Ti:S laser was used as an excitation source. With the measurement configuration showed in Fig. 2.1, it was confirmed that the polarization anisotropy in the present PLE system was almost negligible compared to that of the QWRs in the wavelength region measured in PLE. PL spectra of QWRs and QWL in magnetic fields were measured at 4.2 K in order to confirm the lateral confinement effect in QWRs. Ar^+ laser light of 514.5 nm was used for the excitation.

5.3 Growth Mode Transition of InGaAs on GaAs Multiatomic Steps

Figures 5.2(a) and (b) show AFM images of underlying GaAs layer surfaces prior to the growth of InGaAs layers on the 2.0°- and 5.0°-misoriented substrates, respectively. Coherent multiatomic steps were observed over several micrometer areas especially on 5.0°-misoriented substrates. Multiatomic steps on the 5.0°-misoriented surfaces were straighter than those on the 2.0°-misoriented ones. Moreover, the uniformity of the spacing of the multiatomic steps on the 5.0°-misoriented surface was much better than that on the 2.0°-misoriented one. Average heights and spacing of the multiatomic steps were 2.8 and 80 nm on the 2.0°-misoriented surface, and 6.1 and 70 nm on the 5.0°-misoriented surface, respectively. Figures 5.2 (c) and (d) show AFM images of thin $In_{0.1}Ga_{0.9}As$ layer surfaces on coherent GaAs multiatomic steps. Spacing of the InGaAs multiatomic steps was almost the same as that of the underlying GaAs ones, and the surfaces of terrace regions were oriented to the exact [001] direction. Three-dimensional growth mode was not observed in the InGaAs growth even on the singular GaAs (001) surface. These results suggest that

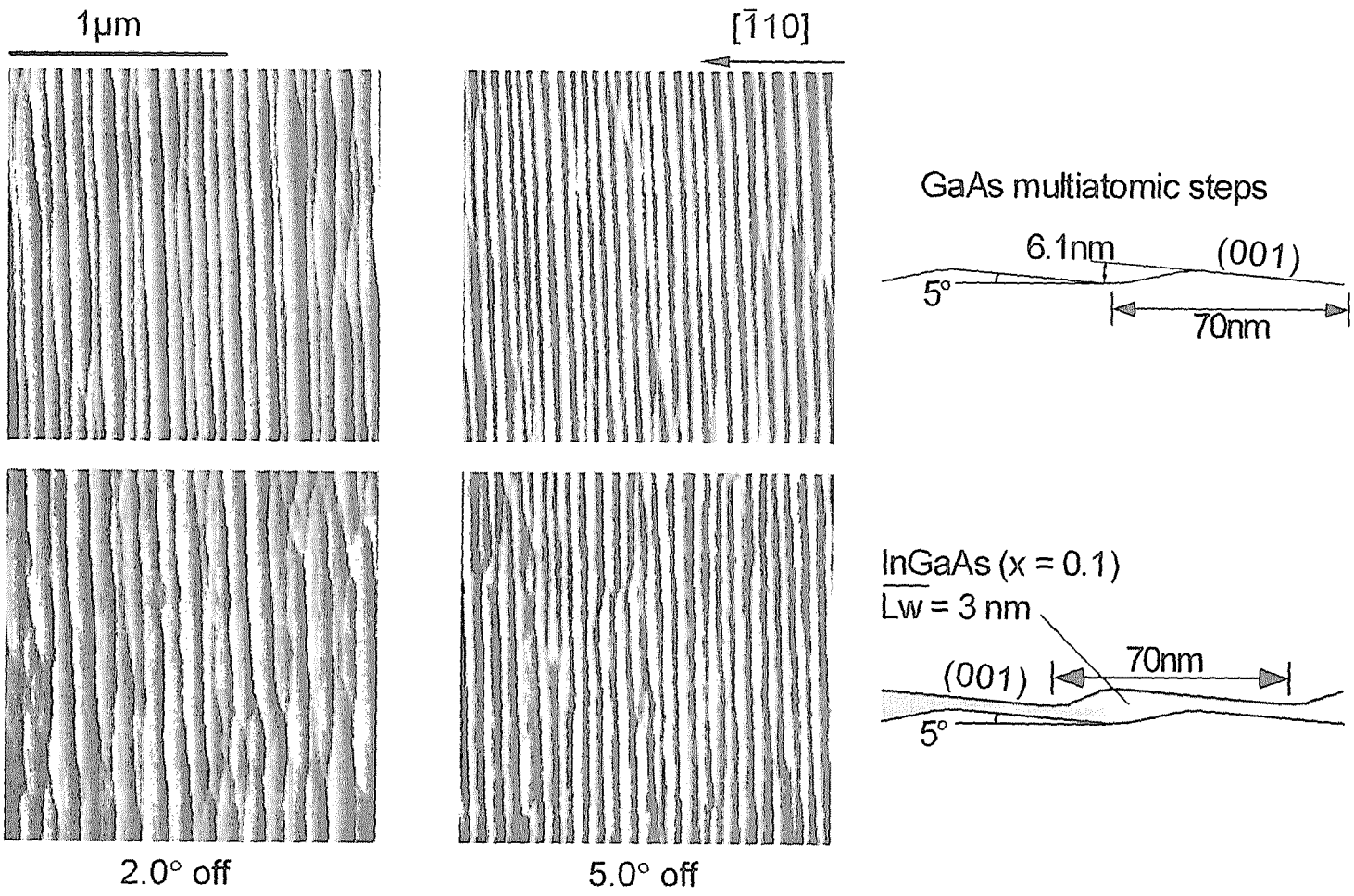

Fig. 5.2 Atomic force microscopy images of GaAs and InGaAs surfaces grown on vicinal GaAs (001) substrates.

$In_{0.1}Ga_{0.9}As$ layers were grown in "step flow growth mode", where this means the lateral growth from the step edges, rather than in Stranski-Krastanov growth mode, and locally thick QWR structures can be formed at the edge of GaAs multiatomic steps.

Next, the variation of surface morphologies on the thin InGaAs layers with indium contents between 0.1 and 0.3 is shown in Fig. 5.3. The substrate misorientation angles were 5.0°. When indium contents were smaller than 0.15, InGaAs layers were grown in step flow growth mode. For the $In_{0.2}Ga_{0.8}As$ growth, prominent undulations of multiatomic step front was partly observed due to the increase of the strain effect. The height of these undulation areas was about 10 nm. For the $In_{0.3}Ga_{0.7}As$ growth, many three-dimensional InGaAs island structures were formed at the edge of GaAs multiatomic steps in order to reduce the stress by the difference of lattice constants between InGaAs and GaAs. For the $In_{0.3}Ga_{0.7}As$ growth, it was also found that slight ordering of the island sizes and positions along the multiatomic steps. These island structures was always oval shaped, and it was confirmed by scanning both parallel and perpendicular to the multiatomic steps with AFM. Their size of the base was about 65 nm × 80 nm, and the height was about 210 nm. In the Stranski-Krastanov growth of InAs or InGaAs layers on the vicinal GaAs (001) surfaces grown by MOVPE, the ordering of three-dimensional islands at the step edges has been observed [4]. However, in order to control the size uniformity and the position of these three-dimensional InGaAs islands, further optimization of the growth condition is needed.

In order to clarify the growth mode of InGaAs layers at the edge of GaAs multiatomic steps, the average inclination angles of multiatomic step areas to the (001) terraces as a function of indium contents of InGaAs layers was measured. Figure 5.4 shows the average inclination angles measured from the line scanned profiles of AFM images. The inset shows the definition of the average inclination angle, and the error bars indicate standard deviations of the inclination angles. These data exclude the three-dimensional island like areas for $In_{0.2}Ga_{0.8}As$ and $In_{0.3}Ga_{0.7}As$ wafers. As increasing the indium content of the InGaAs layer, the average inclination

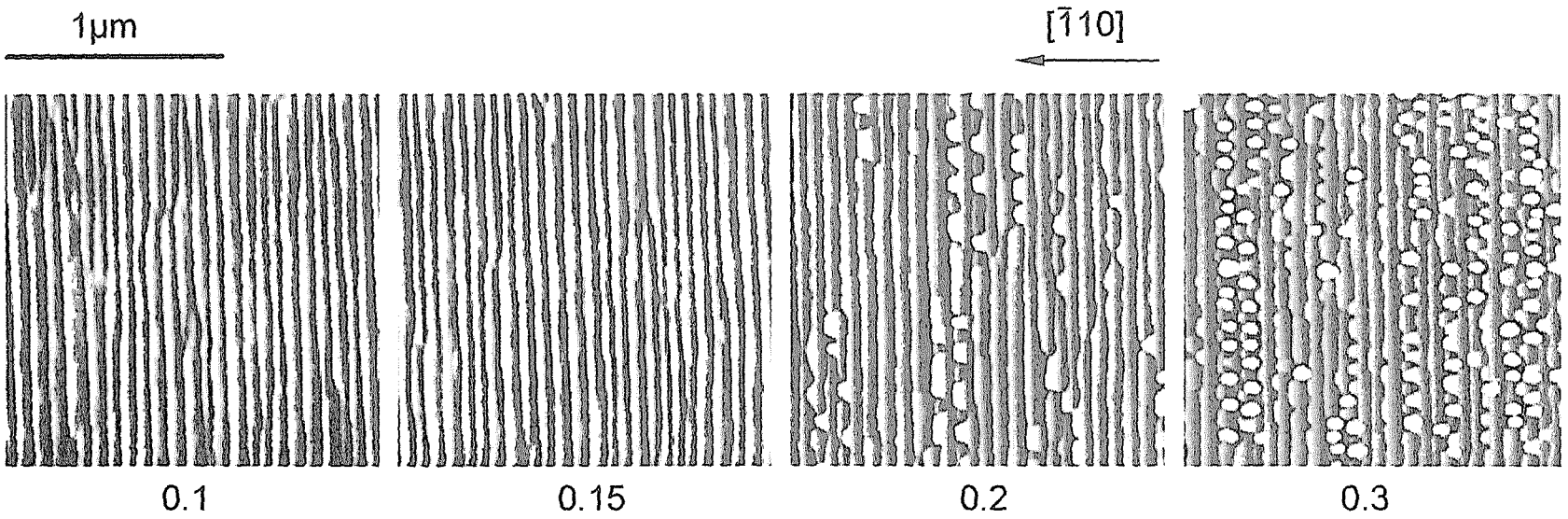

Fig. 5.3 Indium content dependence of InGaAs surface morphologies grown on vicinal GaAs (001) substrates.

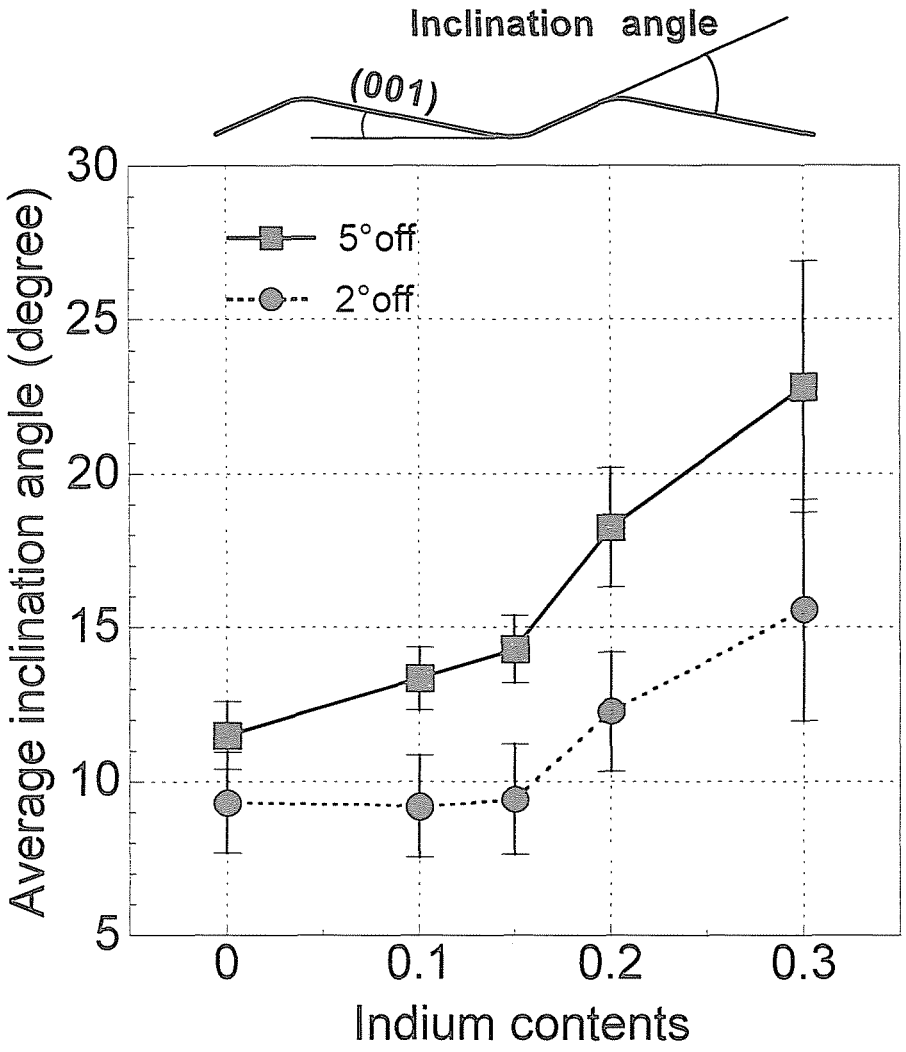

Fig. 5.4 Indium contents dependence of average inclination angle at the edge of InGaAs multiatomic step areas.

angle of the multiatomic step areas to the (001) terrace increases for both 2.0°- and 5.0°-misoriented substrates. Since the inclination angle for the GaAs multiatomic steps was always smaller than that for InGaAs ones, these results suggest that InGaAs QWR structures were successfully formed at the edge of GaAs multiatomic steps when the indium content was smaller than 0.15. For the indium contents larger than 0.2, three-dimensional island structures seemed to be connected with wire-like structures.

In the InGaAs layers with 0.3 indium contents, the density of the three-dimensional InGaAs islands formed at the edge of GaAs multiatomic steps increases as the substrate inclination angle getting larger. Figure 5.5 shows AFM surface images of thin $In_{0.3}Ga_{0.7}As$ layers on the singular (001), 2.0°- and 5.0°-misoriented (001) substrates. It was found that the density of the islands on the 5.0°-misoriented (001) substrates was about 10 times larger than on the 2.0°-misoriented ones. On the singular (001) substrates, which virtually incline by about 0.5° from the exact [001] direction, the step flow growth of InGaAs layers at the edge of GaAs *monoatomic* steps occurred and the stress originated from the lattice mismatch between InGaAs and GaAs was reduced uniformly, although two-dimensional growth nucleus could be formed. As increasing the misorientation angle, the multiatomic steps were formed and the step height and density also became larger. This means that the stress become larger and the growth rate of InGaAs increases at the edge of multiatomic steps as increasing the misorientation angle.

To avoid the three-dimensional island formation at the edge of GaAs multiatomic steps and the undulation of step fronts, the growth conditions for the optimization were discussed. Specifically, the growth mode transitions of the thin InGaAs layer on GaAs multiatomic steps due to changing AsH_3 partial pressures and growth temperatures were examined. Figure 5.6 shows surface morphologies of thin $In_{0.2}Ga_{0.8}As$ layers on the 2.0°- and 5.0°-misoriented (001) substrates grown under relatively high AsH_3 partial pressure (3.3×10^{-4} atm) compared with previous one, and Figure 5.7 shows those of $In_{0.3}Ga_{0.7}As$ layers. The growth temperature was 600 °C. In the case of InGaAs layers with 0.2 indium content, although no prominent undulations

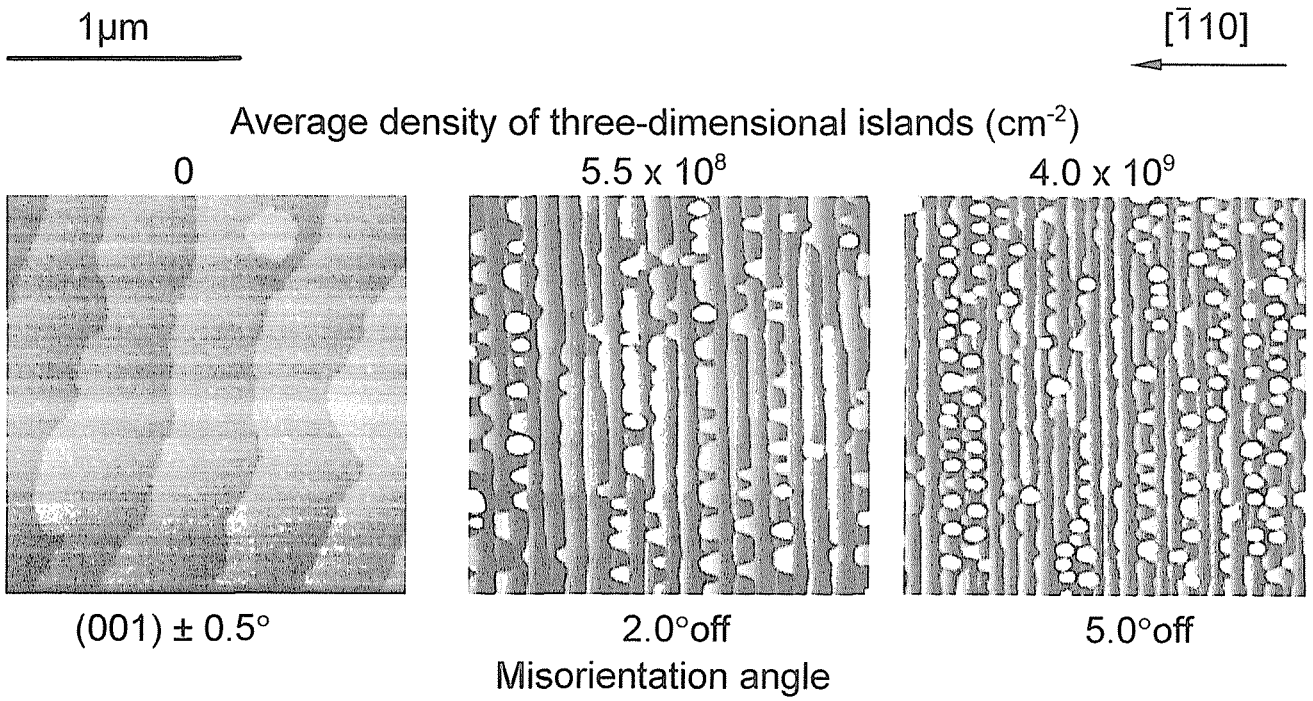

Fig. 5.5 Substrates' misorientation angle dependence of InGaAs surface morphologies grown on vicinal GaAs (001) substrates.

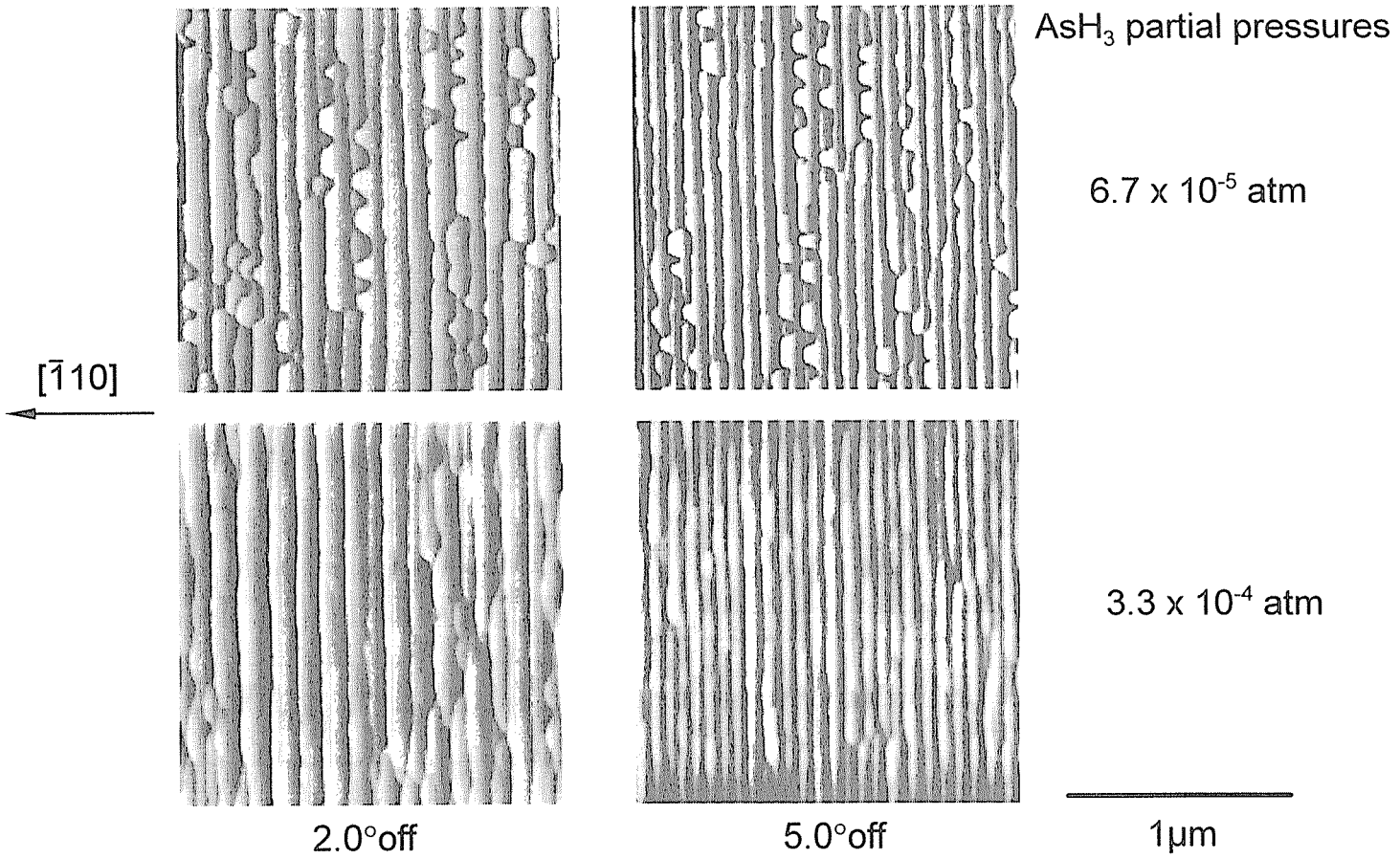

Fig. 5.6 Substrates' misorientation angle dependence of InGaAs surface morphologies grown on vicinal GaAs (001) substrates.

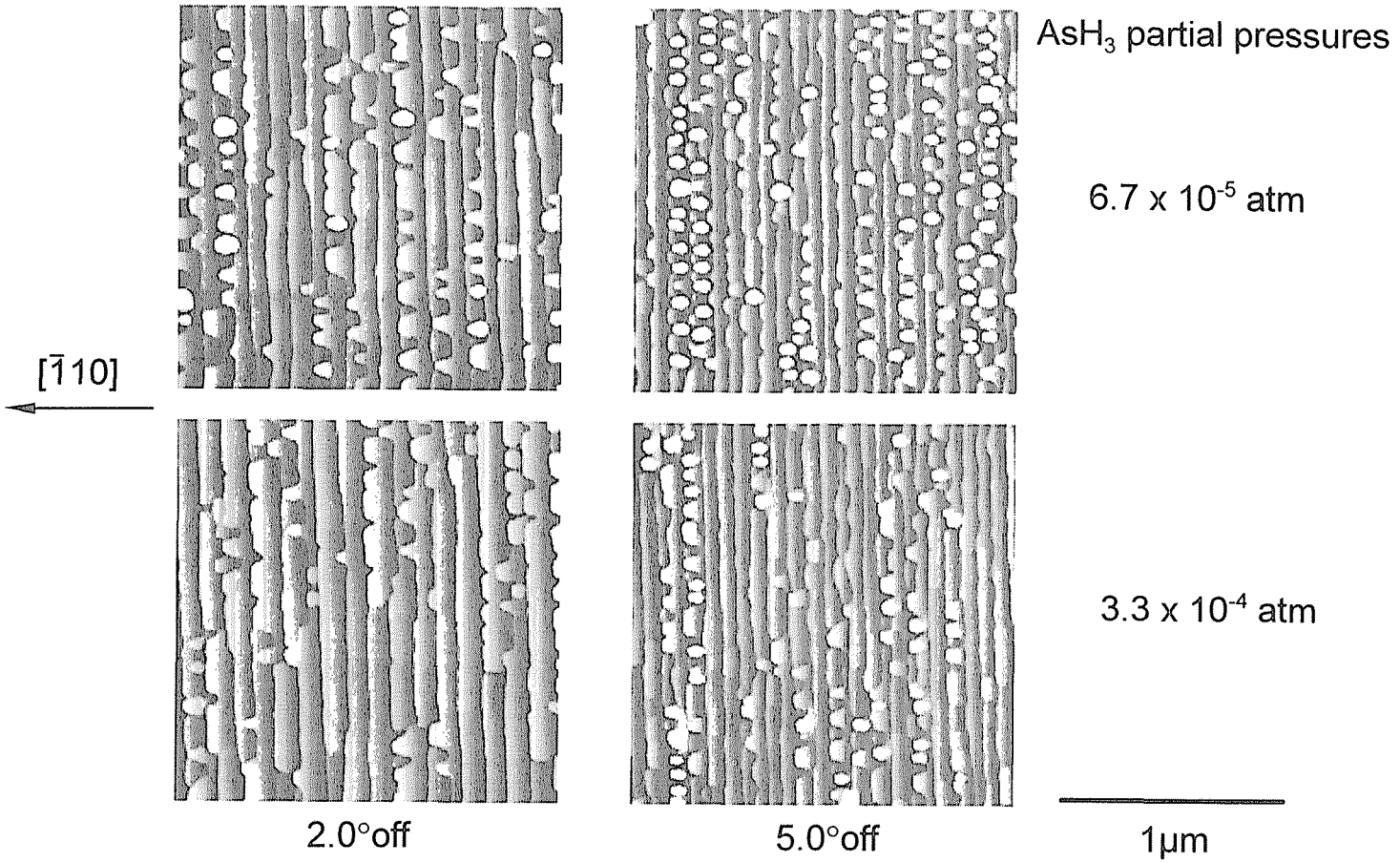

Fig. 5.7 Substrates' misorientation angle dependence of InGaAs surface morphologies grown on vicinal GaAs (001) substrates.

remained at the step fronts, their straightness were a little poor. On the surfaces of $In_{0.3}Ga_{0.7}As$ layers, there were still the three-dimensional islands, and their density was less than or comparable to that in the low AsH_3 partial pressure. Next, Figure 5.8 shows AFM images of the $In_{0.2}Ga_{0.8}As$ layers on the 2.0°- and 5.0°-misoriented (001) substrates grown at the relatively low temperatures, and Figure 5.9 is those for the $In_{0.3}Ga_{0.7}As$ wafers. The AsH_3 partial pressure was fixed in 6.7×10^{-5} atm. In both cases of $In_{0.2}Ga_{0.8}As$ and $In_{0.3}Ga_{0.7}As$ surfaces, the undulations and the three-dimensional islands at the step edges were clearly restrained, that is, "step flow growth" seemed to occur. At the growth temperature of 520 °C, especially on the 5.0°-misoriented surfaces, the straightness of the step edges was fairly high. However, it can be seen in Fig. 5.10 that the average inclination angle of the multiatomic step areas to the (001) terraces, for example, in the case of 0.3 indium content, was getting lower as decreasing the growth temperatures, although the angle was still a little larger than that of the GaAs ones. These facts is probably due to the decrease in the migration length of In and Ga atoms on the vicinal surfaces.

5.4 Fabrication of InGaAs Quantum Wire Structures Using Multiatomic Steps

Figure 5.11 shows a cross-sectional TEM image and a schematic illustration of InGaAs QWR structures, whose indium content was about 0.1, on the 5.0°-misoriented substrate. It was found that the thin InGaAs layer (dark area) was thicker at the edge of GaAs (bright areas) multiatomic steps than on the (001) terrace regions. However, the corrugation of the multiatomic steps on the InGaAs top surface seems to decrease compared to the underlying GaAs multiatomic steps' one, which is probably due to a slight segregation of indium atoms during the upper GaAs barrier layer growth at 600 °C. On the other hand, InGaAs/GaAs single QWL on the singular (001) substrate had flat heterointerfaces. From this TEM image, it was estimated that the lateral width and the vertical thickness of InGaAs QWR structures were about 25 and

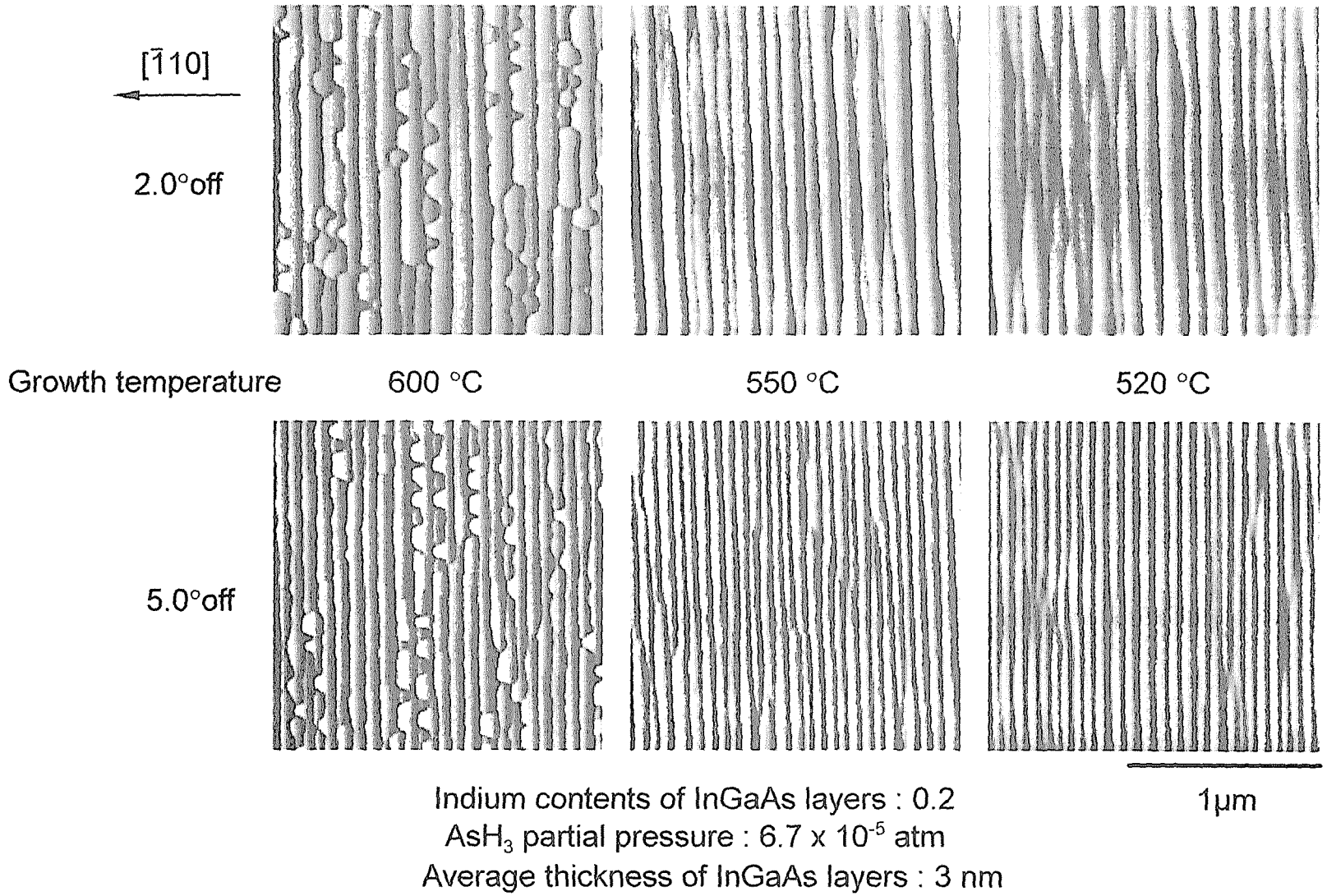

Fig. 5.8 Growth temperature dependence of InGaAs surface morphologies grown on vicinal GaAs (001) substrates.

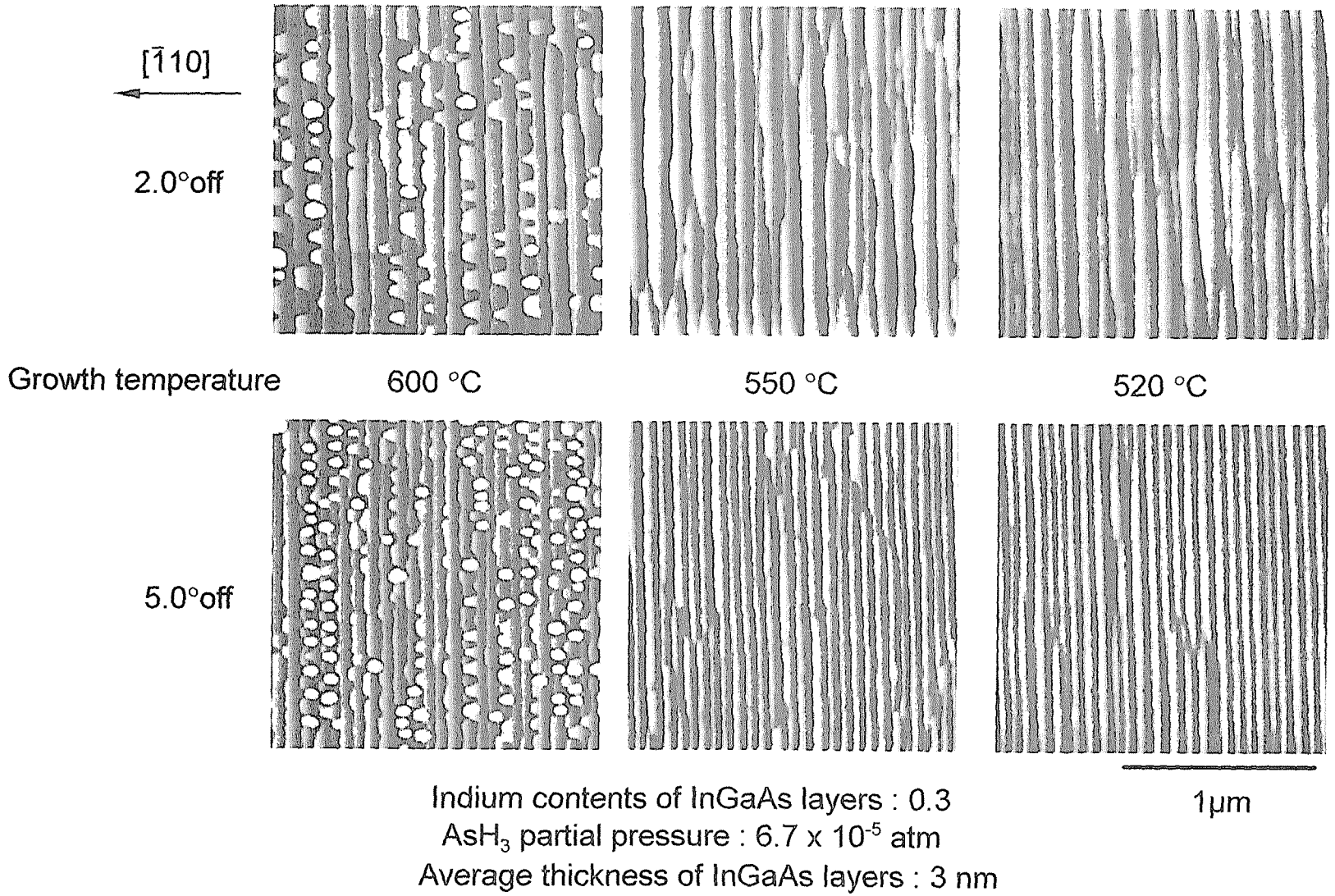

Fig. 5.9 Growth temperature dependence of InGaAs surface morphologies grown on vicinal GaAs (001) substrates.

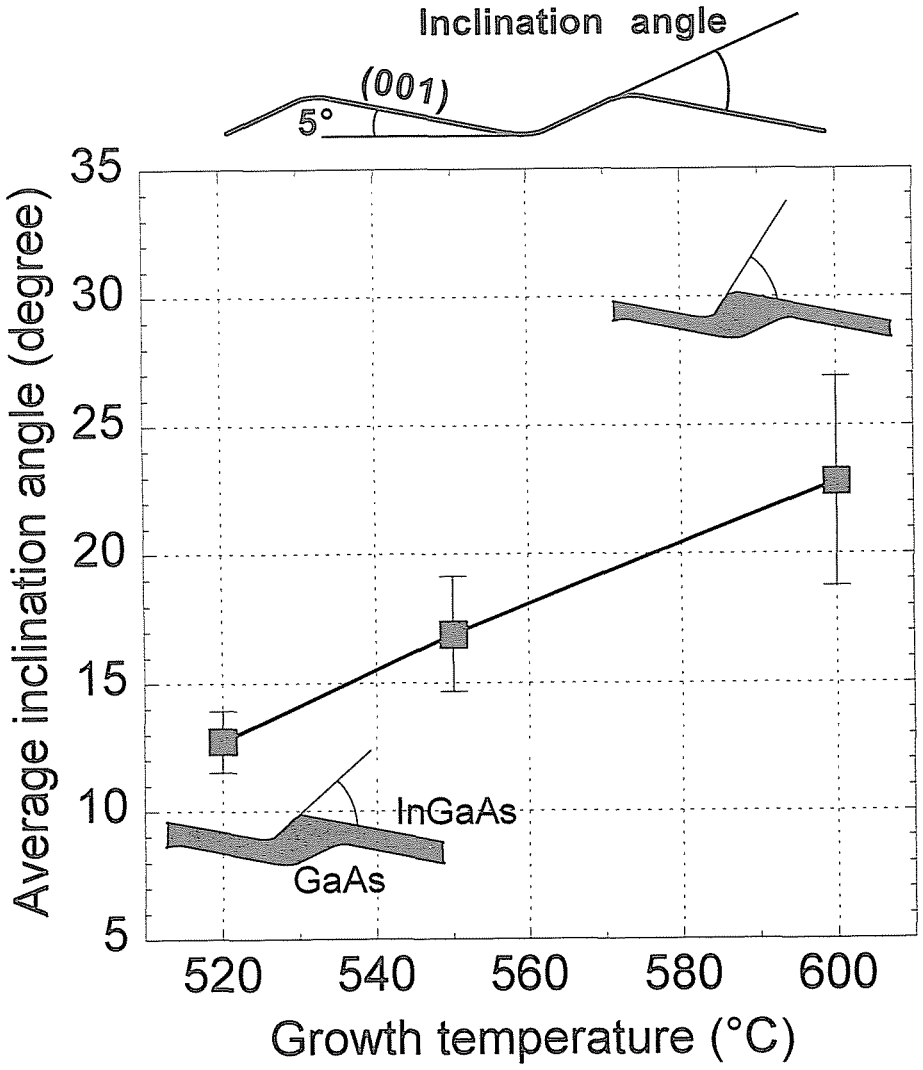

Fig. 5.10 Growth temperature dependence of average inclination angle at the edge of InGaAs multiatomic step areas.

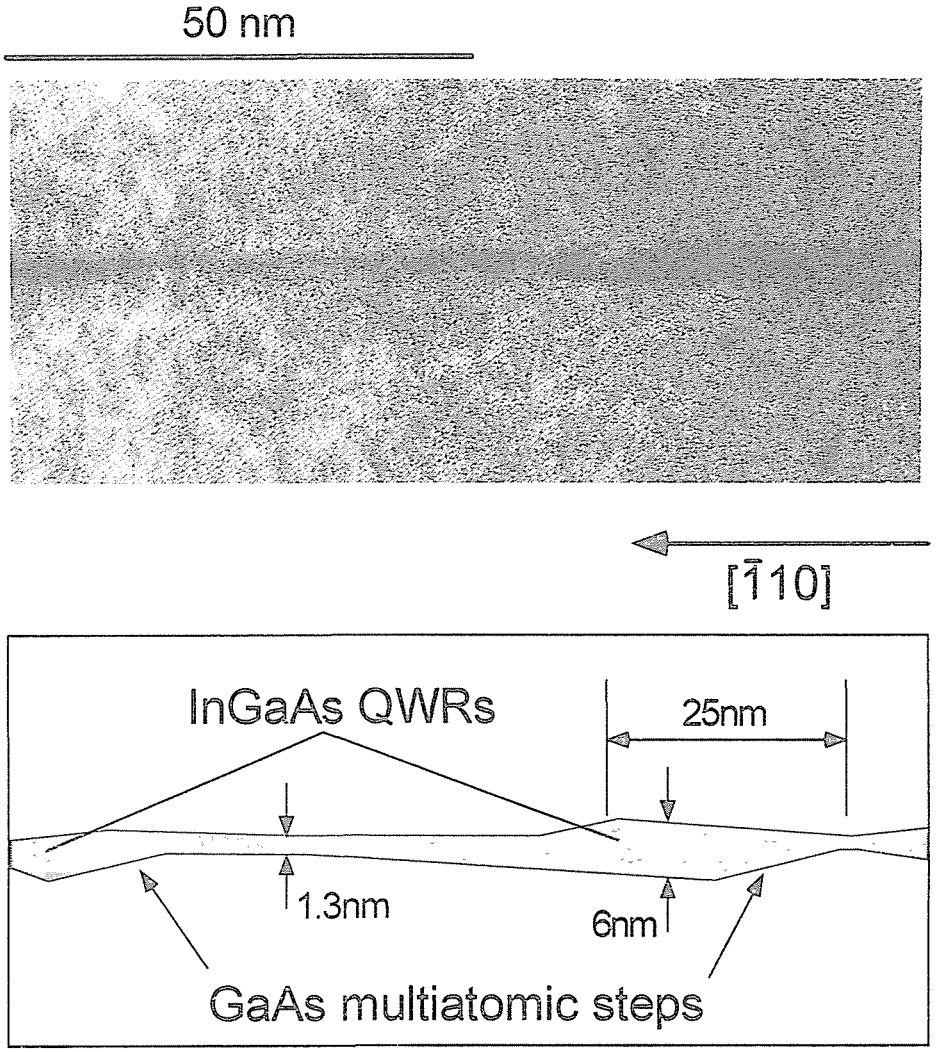

Fig. 5.11 Transmission electron microscopy images and its schematic of InGaAs QWR structures on 5.0°-misoriented GaAs (001) substrates. Average well layer thickness and indium content were about 3 nm and 0.1, respectively.

6 nm, respectively, and that the QWL thickness on the (001) terrace was about 1.3 nm.

5.5 Optical Characterization of InGaAs Quantum Wires

Photoluminescence Characterization

PL spectra of $In_{0.1}Ga_{0.9}As$ QWRs on the vicinal substrates and the reference QWL on the singular (001) substrate at 77 K are shown in Fig.5.12 (a). The PL peak position of the reference QWL was 1.406 eV, which corresponds to the emission from the $In_{0.1}Ga_{0.9}As$ strained QWL with a well thickness of about 3 nm. PL spectra of QWRs shift to a lower energy by 15 meV for the 2.0°-misoriented sample and 25 meV for the 5.0°-misoriented sample with respect to that of the QWL. Full width at half maximum (FWHM) of the PL spectra were about 29, 28 and 7 meV for 2.0°, 5.0°-misoriented and singular (001) samples, respectively. For the $In_{0.15}Ga_{0.85}As$ QWRs sample, these lower energy shifts (red-shift) and FWHM of the PL spectra were 23 and 27 meV for the 2.0°-misoriented sample, and 31 and 28 meV for the 5.0°-misoriented sample, respectively, as shown in Fig. 5.12 (b).

In the chapter 3, GaAs QWRs formed at the edge of the multiatomic steps on the 5.0°-misoriented substrate showed a lower energy shift (red-shift) by 23 meV with respect to that of the QWL, which agreed well with the numerical calculations for the QWR size obtained from the cross-sectional TEM images. Furthermore, it was reported that the average indium content of a MOVPE-grown InGaAs layer on a vicinal GaAs surface was smaller than that on a singular (001) surface, as investigated by an energy dispersive X-ray (EDX) analysis, and PL spectra of InGaAs/GaAs QWLs on the misoriented surfaces shifted to the higher energy side with respect to that on the singular (001) surface, that is, PL spectra showed blue-shift [5]. Therefore, in the current work, lower energy shifts (red-shift) for the misoriented samples with respect to the singular (001) samples are mainly caused by the locally thick InGaAs QWR formation at the edge of GaAs multiatomic steps, although the lateral variations of the indium contents could not be measured.

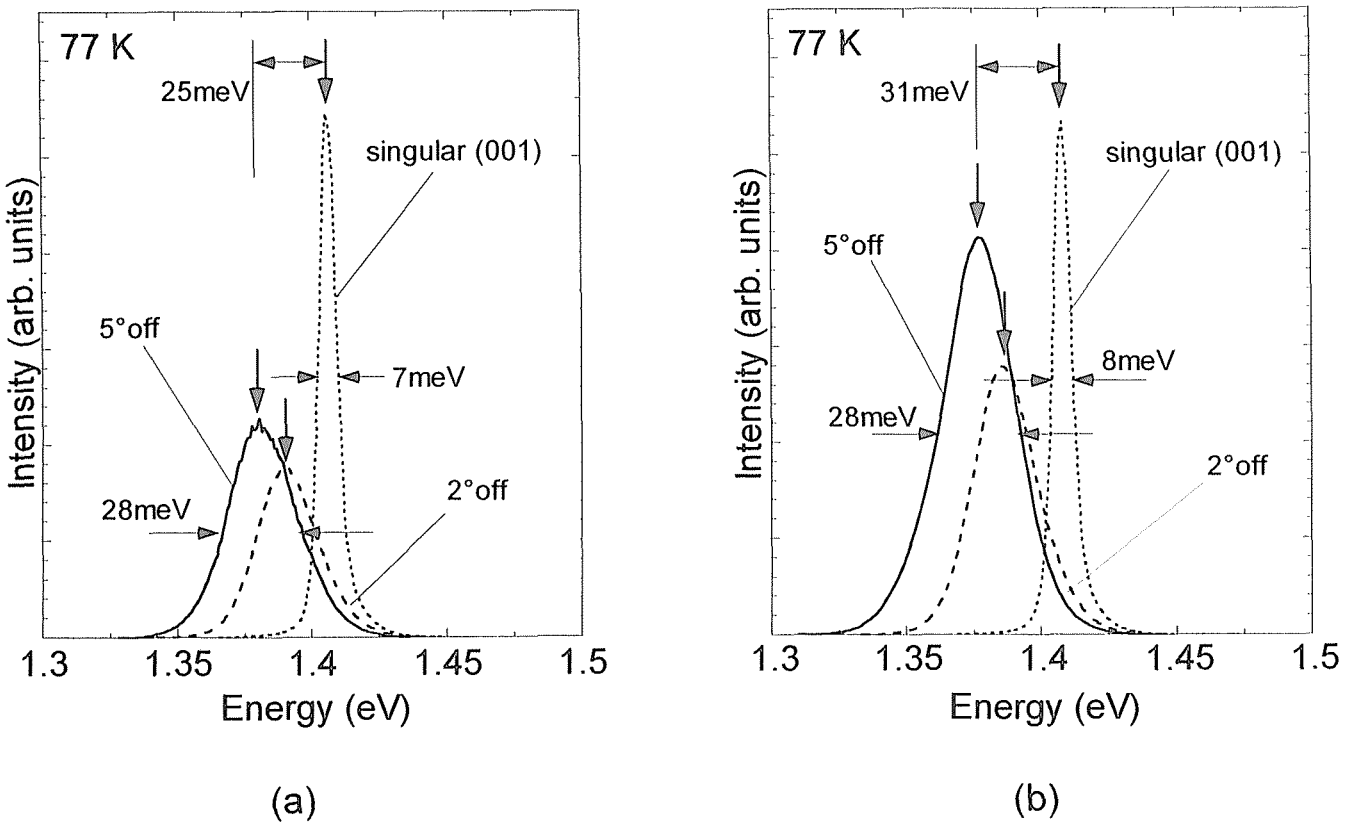

Fig. 5.12 Photoluminescence spectra of InGaAs QWR structures on 5.0°- misoriented substrate (solid line) and 2.0°- misoriented substrate (dashed line), and QWL on the singular (001) substrate (doted line). (a) $In_{0.1}Ga_{0.9}As/GaAs$ and (b) $In_{0.15}Ga_{0.85}As/GaAs$ samples.

As shown in Fig. 5.11, the top interfaces between InGaAs and GaAs tended to slightly flatten during the GaAs higher barrier layers growth probably because of slight segregation of indium atoms. To eliminate such flattening effect, a 40 nm-thick GaAs upper layer was grown at 480 °C after the growth of InGaAs layers, followed by GaAs layers grown at 600 °C. Figure 5.13 shows PL spectra of $In_{0.1}Ga_{0.9}As$ and $In_{0.15}Ga_{0.85}As$ QWRs fabricated by the scheme mentioned above, compared to the previous samples grown at 600 °C. The red-shift of $In_{0.15}Ga_{0.85}As$ QWR samples was about 45 meV. FWHMs of PL spectra from QWRs with the 40 nm-thick GaAs upper layers at 480 °C were 20 ~ 22 meV at 77 K, being 6 ~ 8 meV smaller than those of the previous results. On the other hand, in the QWL grown on the singular substrates, both the variations of PL peak positions and the reduction of FWHMs with respect to the previous results were only a few meV. This means that the re-evaporation of In atoms can be negligible during the growth at 600 °C. Therefore, these results indicate that the growth of 40 nm-thick GaAs upper layers at 480 °C made it possible to eliminate such flattening effects, and the size uniformity of InGaAs QWRs can be improved in such growth scheme.

In the section 5.3, it was found that, even on the 5.0°-misorieted $In_{0.3}Ga_{0.7}As$ surfaces, thin InGaAs layers could grow in "step flow growth mode", and QWR structures with the same period as that of underlying GaAs multiatomic steps could be formed. Figure 5.14 (a) and (b) show PL spectra of $In_{0.3}Ga_{0.7}As$/GaAs quantum structures grown on the 5.0°-misorieted substrates at (a) 600 °C and (b) 520 °C, respectively. Sample structures were shown in the schematic of Fig. 5.1 (b), and 40 nm-thick GaAs layers were grown at 480 °C after the InGaAs growth at 600 or 520 °C. In Fig. 5.14 (a), one can see two clear PL peaks at 1.305 and around 1.24 eV. Although a PL peak around 1.24 eV may be originated from three-dimensional island structures at the edge of multiatomic steps, it has not been clarified yet. On the other hand, a single PL peak can be seen at 1.270 eV in Fig. 5.14 (b). FWHMs of PL spectra of the 5.0°-misorieted and the singular (001) wafers were 27 and 22 meV, respectively, and PL spectrum of the 5.0°-misorieted wafers showed red-shift of 42 meV with respect to that of the singular ones. These results also support that InGaAs

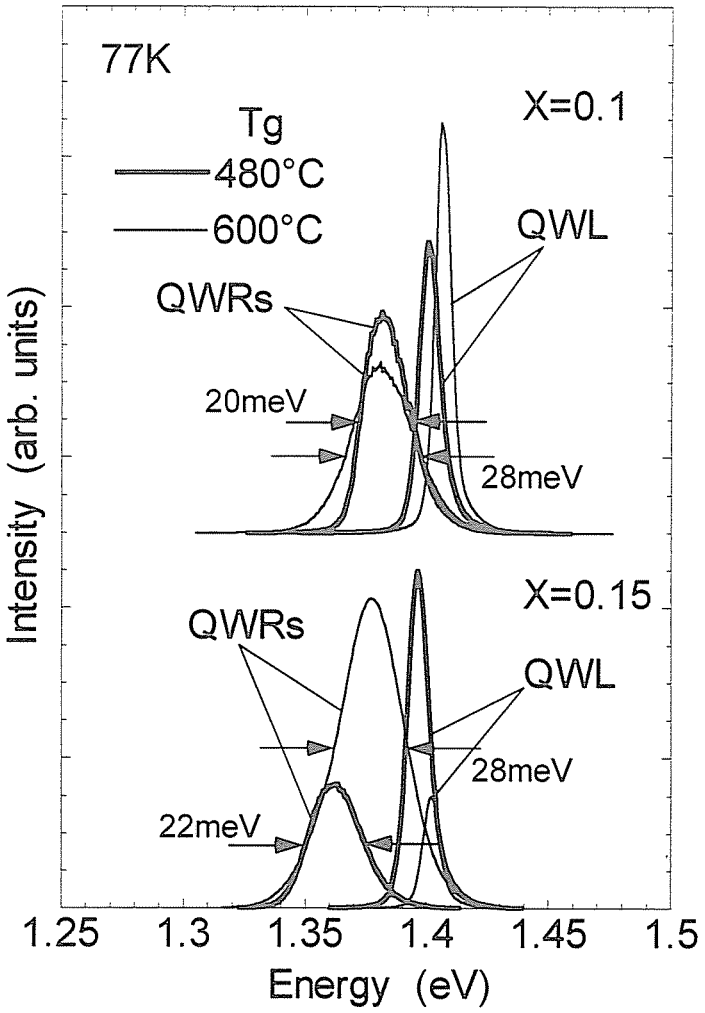

Fig. 5.13 Photoluminescence spectra (thick line) of $In_{0.1}Ga_{0.9}As$ (upper) and $In_{0.15}Ga_{0.85}As$ (lower) QWRs on 5.0°-misoriented substrates with 40 nm-thick GaAs upper layers grown at 480 °C, followed by GaAs layers grown at 600 °C, compared to the spectra (thin line) grown at 600 °C. QWL were also grown on singular (001) substrates for a reference.

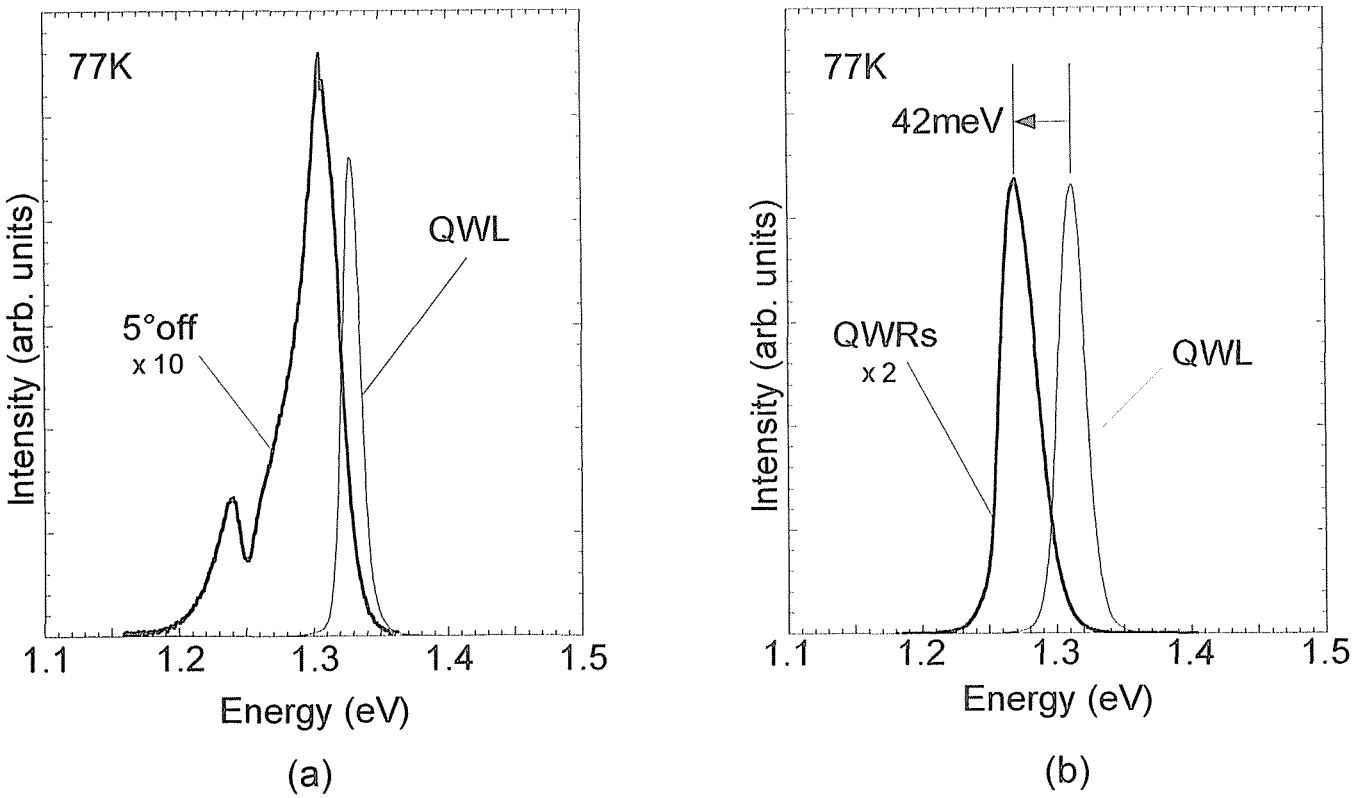

Fig. 5.14 Photoluminescence spectra of $In_{0.3}Ga_{0.7}As$ quantum structures (a) grown at 600 °C, compared with (b) QWR structures with 40 nm-thick GaAs upper layers grown at 480 °C, followed by GaAs layers grown at 600 °C on 5.0°-misoriented and singular (001) substrates.

QWR structures were formed at the edge of GaAs multiatomic steps even on the $In_{0.3}Ga_{0.7}As$ surfaces, as shown in Fig. 5.9. The energy difference of about 15 meV between PL peak positions of the QWL on the singular (001) substrates can be also seen. This fact implies that the surface segregation or the re-evaporation of In atoms occurs to some extent on the 600 °C-grown $In_{0.3}Ga_{0.7}As$ surfaces, and that it can be suppressed by the growth at 520 °C.

Polarization anisotropy in photoluminescence excitation spectra

The PL and PLE spectra of QWRs were taken at 77 K and the results are shown in Fig. 5.15. In the PLE measurements, the detection energy was 1.359 eV, which corresponded to the lower energy side of the PL spectrum of the QWRs as indicated by an arrow, and the electric field of the excitation is either parallel (thick line) or perpendicular (thin line) to the QWRs. Two peaks can be seen in PLE spectra at 1.408 eV and 1.455 eV in either cases of polarizations. It seems that the peak at 1.408 eV originates from heavy hole (HH)-electron excitons in the first subband in QWRs. On the other hand, the identification of the other peak is somewhat difficult because it is possible that it involves both the transition of light hole (LH)-electron excitons of the QWRs and that of the excitons in the excited states of the QWRs. The latter is more likely, because electroluminescence spectra at room temperature showed similar features in the energy difference between the ground and the excited states, as described in chapter 6. A large Stokes shift was also observed in the PLE spectra, and it can be estimated to be about 30 meV at 77 K. Although clear and detailed explanation for the origin of this Stokes shift cannot be given at present, it may arise from potential fluctuations along the wire axis, caused by size fluctuations and indium content variations of the InGaAs QWRs. Some fluctuations at the edge of InGaAs multiatomic steps, which can be shown in some AFM images in the section 5.3, also may imply the existence of indium content variations along the wire axis.

One can see polarization anisotropy in HH exciton transition. Its peak intensity for perpendicular polarization was about 85 % of that for parallel polarization. Although the quantitative argument is difficult because of the complicated valence

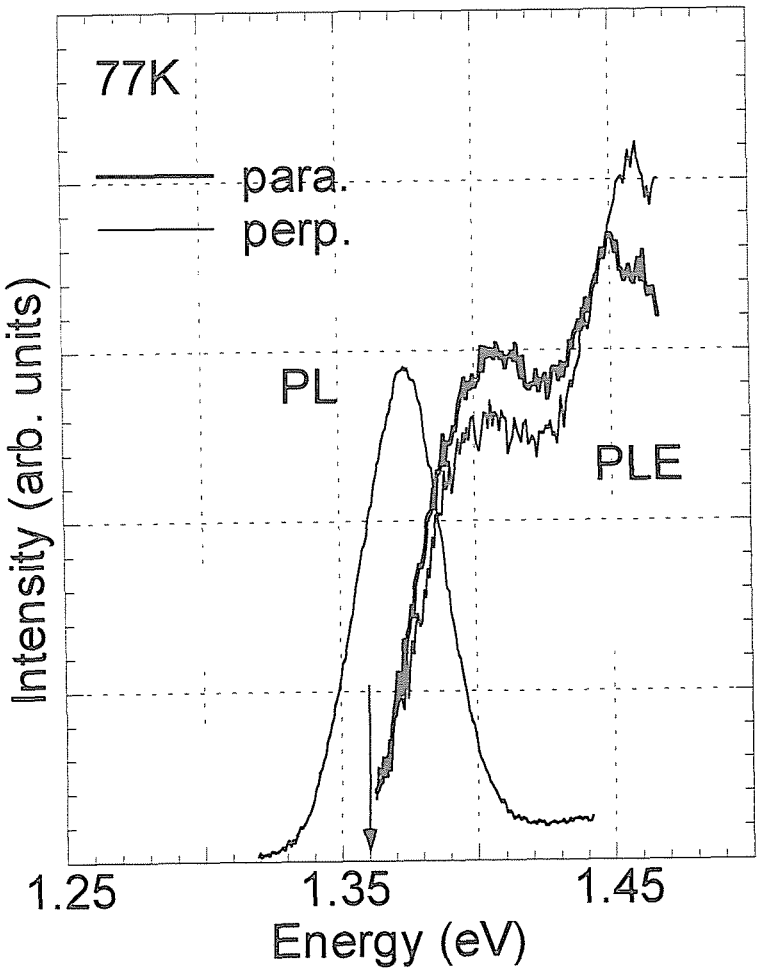

Fig. 5.15 PL and PLE spectra of $In_{0.15}Ga_{0.85}As$ QWRs on 5.0°- misoriented substrates at 77 K. An arrow shows detection energy (1.359 eV) in PLE measurements.

band mixing and the strain distribution with such cross-sectional shape of the sample as described in section 5.4, this polarization anisotropy in PLE spectra probably reflects the one dimensional nature of the QWRs.

Photoluminescence characterization in magnetic fields

Figure 5.16 (a) shows PL spectra of InGaAs QWRs on the 5.0°-misoriented substrate and QWL on the singular (001) substrate measured at 4.2 K in magnetic fields (B) up to 10 T. The direction of applied magnetic fields was parallel to the growth direction. The PL peak energies show clear blue shifts for both samples as the magnetic field increases. The amount of the shift at 10 T is 3.4 meV for the QWL sample, while it is 1.6 meV for the QWR sample, as shown in Fig. 5.16 (b), where the peak energies are plotted as a function of magnitude of magnetic fields (B). In addition, the peak shift, ΔE, is well fitted by the parabolic relation to B of diamagnetic shift of excitons, that is, $\Delta E = \beta B^2$, where β is the diamagnetic coefficient and is 16 $\mu eV/T^2$ for QWRs and 45 $\mu eV/T^2$ for QWL, respectively.

As shown in the cross-sectional TEM image of Fig 5.11, the InGaAs layer on multiatomic steps has in-plane thickness variation, and the thickest portion can be observed at the edge of GaAs multiatomic steps. Since its local thickness is larger than the width of InGaAs QWL on the singular substrate, the red shift of PL peak energy of the QWRs relative to the QWL is caused in the first order by such thickness difference. It is known, however, that the diamagnetic coefficient, β, decreases as the well thickness of the QWL becomes narrower [6]. In addition, the diamagnetic coefficient of unstrained InGaAs QWL is calculated to be 19 $\mu eV/T^2$ in the two dimensional limit (the reduced effective mass of excitons of $0.053m_0$ was used here [7], somewhat larger than the experimental value for QWRs). Therefore, these magneto-luminescence results clearly demonstrate the existence of lateral quantum confinement and one dimensional state in the strained InGaAs QWRs at the edge of multiatomic steps.

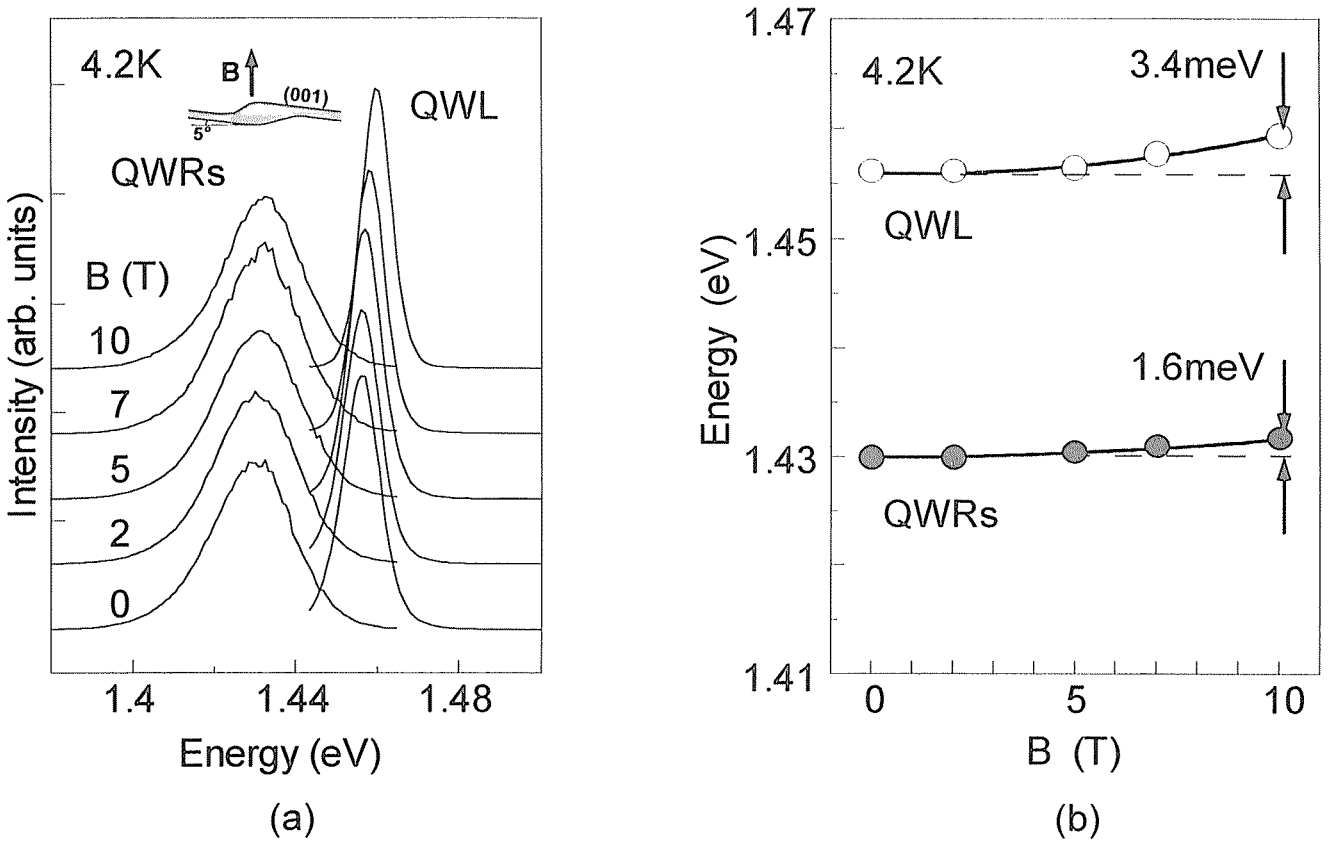

Fig. 5.16 (a) Photoluminescence spectra of QWRs on 5.0°- misoriented and QWL on singular (001) substrate at 4.2K in magnetic fields (B) up to 10 T. (b) Plot of peak energy positions as a function of the magnitude of magnetic fields (B), fitted by parabolic relation to B.

5.6 Fabrication of InGaAs Wire Structures on Patterned Vicinal Substrates

In chapter 4, as a control method for the uniformity of step period, the straightness and the continuity of multiatomic steps, GaAs multiatomic steps grown on patterned vicinal GaAs (001) substrates with a line and space pattern perpendicular to the misorientation direction of vicinal substrates were demonstrated. It found that the formation of GaAs multiatomic steps can be controlled by a line and space pattern on vicinal substrates, as reported on the AlGaAs multiatomic steps formed on the patterned vicinal surfaces misoriented to the [110] direction [8]. In this chapter, InGaAs wire structures grown on patterned vicinal substrates are also demonstrated and characterized.

Figure 5.17 shows the sample structure of InGaAs wire structures on patterned vicinal GaAs (001) substrates misoriented by 2.0° to the [-110] direction. Grooves with about 500 nm width were in the [110] direction, which was perpendicular to the misorientation direction, and their period was about 1 μm. In the first place, AlGaAs/GaAs multi-layers were grown in order to form coherent multiatomic steps. Then, InGaAs/GaAs QWR structures, whose average well layer thickness is about 3 nm, were fabricated at the edge of GaAs multiatomic steps. Indium content of thin InGaAs layers was always 0.15. In the case of the line and space pattern with 4 μm-period, the surface morphologies after the growth of InGaAs layers on GaAs multiatomic steps tended to become rough, although there was no three-dimensional island formation anywhere. Such tendency were fairly remarkable in the multiatomic steps areas at the step edges. On the terrace regions, some monoatomic steps can be observed. On the other hand, a typical AFM image of InGaAs wire structures formed on GaAs multiatomic steps with 1 μm-period is shown in Fig. 5.18. From the AFM characterizations, extremely straight InGaAs wire structures were formed with the same period with the substrate's one. Their continuity was also extremely high over thirty micrometer long. There were no three-dimensional island growth either at the edge of steps or on the terraces. The crystal orientation of terrace surfaces were the exact [001] direction, that is, no multiatomic steps were formed, and the step height

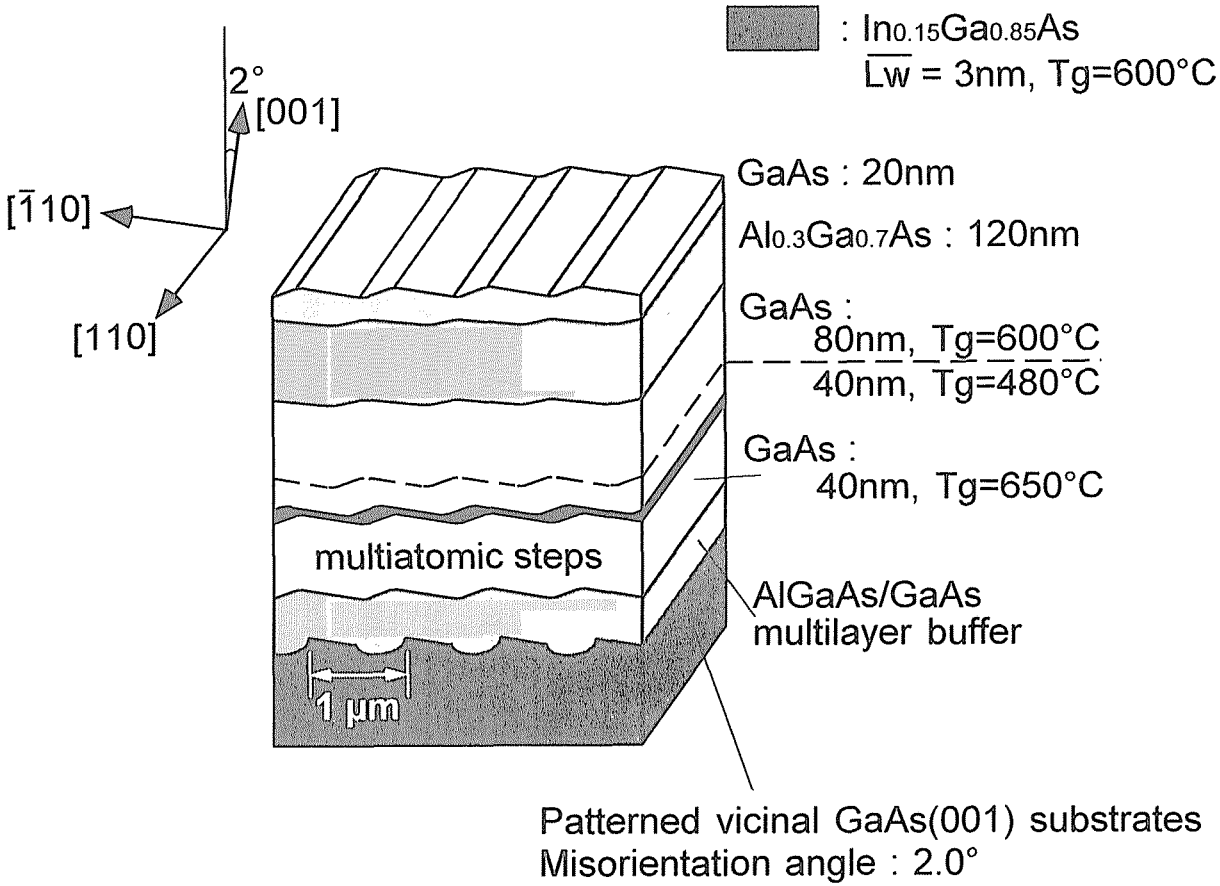

Fig. 5.17 Schematic of InGaAs wire structures on patterned vicianl substrates.

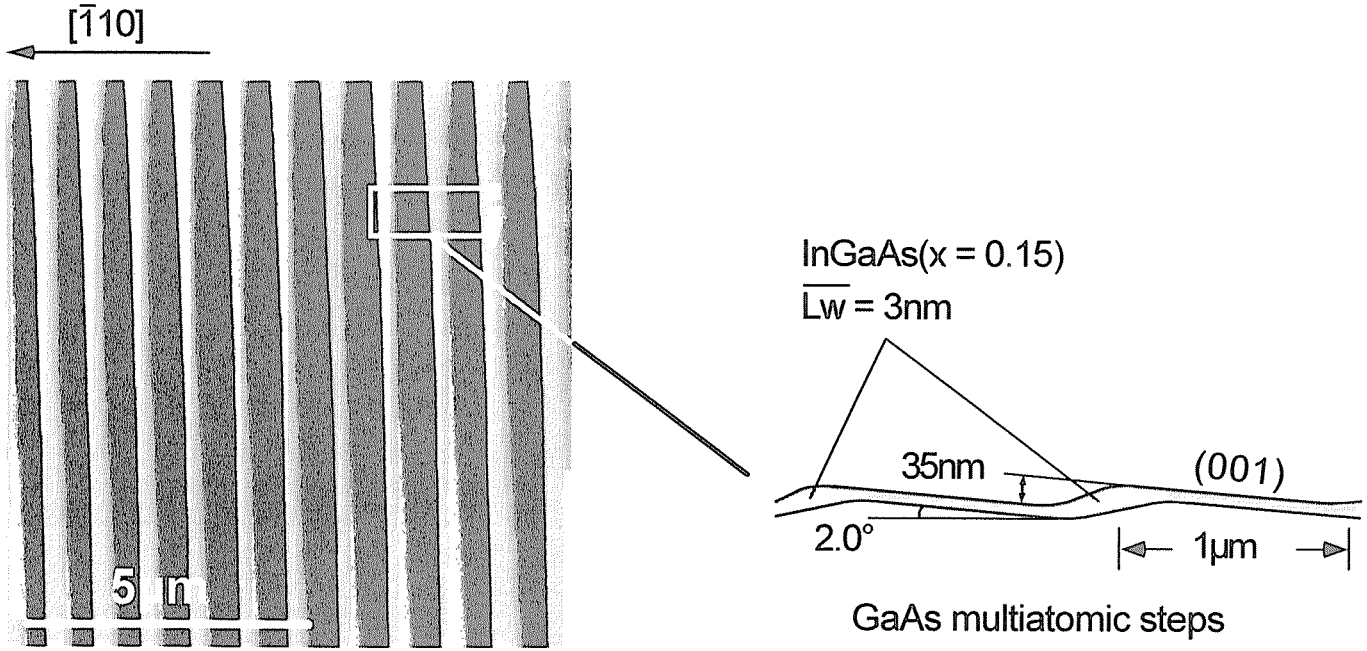

Fig. 5.18 Top view of atomic force microscopy image and its cross-sectional schematic of InGaAs wire structures on patterned vicianl substrates.

was estimated to be about 35 nm. Although further optimization of the growth conditions especially on the line and space patterns with the long period, these results indicate that the uniformity of step period, the straightness and the continuity of multiatomic steps can be controlled by using the patterned vicinal GaAs (001) substrates for the formation of GaAs multiatomic steps.

In Fig. 5.19, a cross-sectional SEM image and its schematic of InGaAs wire structures formed at the edge of GaAs multiatomic steps are shown. Growth rate of InGaAs layers at the edge of steps was larger than on the (001) terraces, resulting in the formation of locally thick wire-like structures. These structures were also characterized by CL at 4.2 K. Figure 5.20 shows the CL spectrum of InGaAs/GaAs single QWL structure grown on the 2.0°-misoriented substrate. Two distinctive peaks can be observed at about 849 and 871 nm. To clarify the origin of these two peaks, spatial resolved CL images were observed, as shown in Fig. 5.21. It was found that the CL peak at 849 nm was of InGaAs QWLs on the (001) terraces and that at 871 nm was of InGaAs wire structures at the edge of multiatomic steps. This clearly indicates that locally thick InGaAs well layers were formed at the edge of steps. Furthermore, uniform emissions were observed over thirty micrometer area, and, as shown in CL spectrum, the peak intensity of CL spectrum from InGaAs wire structures was almost the same as that from QWLs on the (001) terraces, nevertheless the area of wire structures was much smaller than that of QWLs on the terraces. These results indicate that extremely straight and coherent InGaAs QWRs can be fabricated by using the line and space patterned vicinal substrates, although further optimization of the growth conditions may be needed.

5.7 Summary

In this chapter, the growth mode transitions of strained InGaAs layers on multiatomic steps were investigated by AFM and were discussed. Moreover, the fabrication and the optical characterization of locally thick self-organized InGaAs

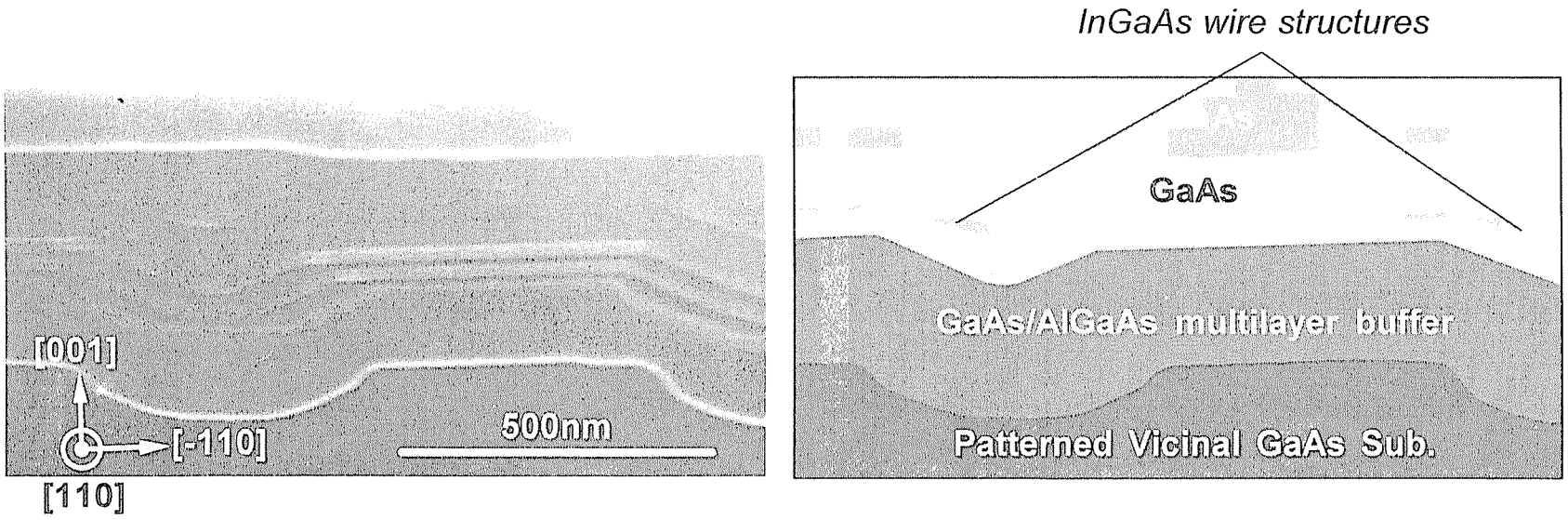

Fig. 5.19 Cross-sectional scanning electron microscopy image and its schematic of quantum structures on patterned vicianl substrates.

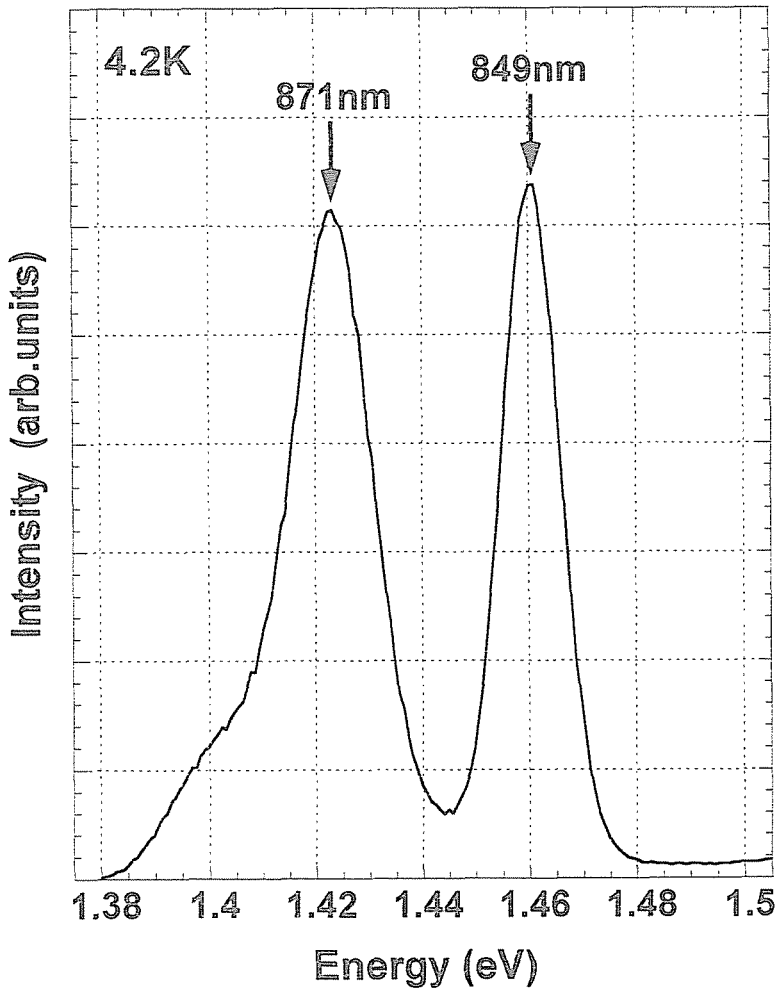

Fig. 5.20 Cathodoluminescence spectrum of quantum structures on patterned vicianl substrates misoriented by 2.0°.

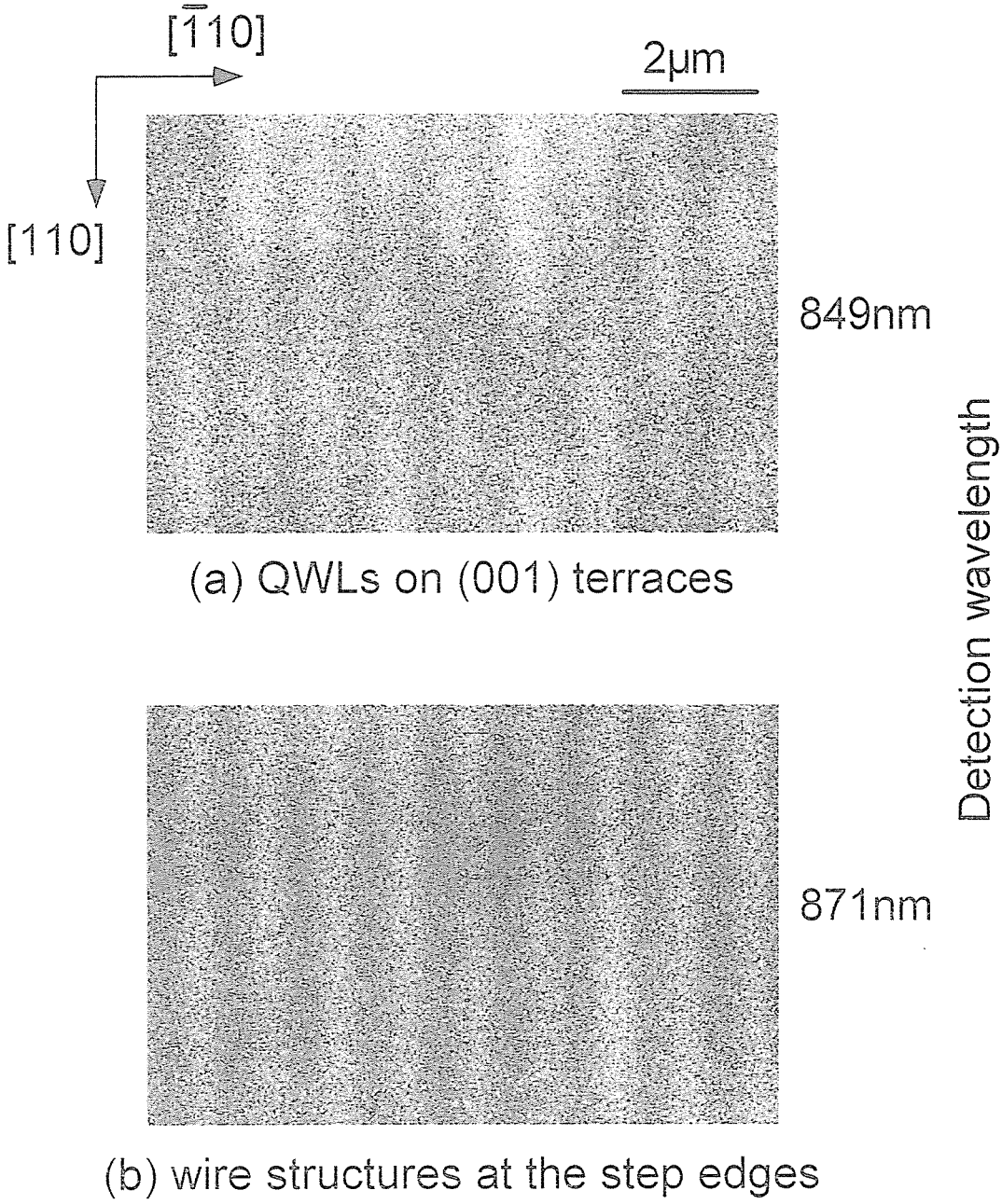

Fig. 5.21 Spatial resolved cathodoluminescence images taken at (a) 849nm and (b) 871nm.

strained QWR structures at the edge of coherent GaAs multiatomic steps grown by MOVPE on vicinal and patterned vicinal GaAs (001) substrates were demonstrated. The main results in this chapter are summarized below.

(1) According to the results of AFM observations, a thin InGaAs with less than 0.15 indium contents grew in "step flow growth mode" at the edge of the GaAs multiatomic steps, and coherent multiatomic steps could be formed, while that with more than 0.2 indium contents grew three dimensionally due to the increase of the stress at the edge of multiatomic steps. By the optimization of epitaxial growth conditions of InGaAs layers, wire-like structures could be formed even in the case of indium contents more than 0.2.

(2) InGaAs/GaAs strained QWR structures with less than 0.15 indium content were fabricated at the edge of coherent GaAs multiatomic steps. As a result of cross-sectional TEM observation, it was confirmed that the InGaAs layers at the edge of GaAs multiatomic steps was thicker than that on (001) terraces grown on 5.0°-misoriented substrates.

(3) PL spectra of InGaAs QWR samples showed the lower energy shift (red-shift) by 15 ~ 31 meV with respect to those of the QWL on the singular (001) substrate. These results indicate that the locally thick InGaAs strained QWRs were successfully formed at the edge of coherent GaAs multiatomic steps.

(4) Their polarization anisotropy in PLE spectra at 77 K was observed for the excitation light with electric fields being parallel or perpendicular to the QWRs. Two peaks in PLE spectra were observed at 1.408 and 1.455 eV. The peak at 1.408 eV is thought to originate from HH-electron excitons in the first subband in QWRs.

(5) PL properties in magnetic fields were also investigated at 4.2 K in order to examine the lateral confinement effect in the InGaAs QWRs. At the magnetic field of 10 T, PL peak position for QWRs shifted toward higher energy by 1.6 meV, while the amount of energy shifts for QWL on the singular (001) GaAs substrates was 3.4 meV. It was found that the diamagnetic coefficient was 16 $\mu eV/T^2$, which was much smaller than that of QWL on the singular (001) GaAs substrates (45 $\mu eV/T^2$). These results indicate that the effect of lateral confinement exists in the QWRs.

(6) InGaAs wire structures grown on patterned vicinal substrates had extremely high continuity and straightness over thirty micrometers. Uniform CL emissions were also observed more than thirty micrometer area, and the peak intensity of CL spectrum from InGaAs wire structures was almost the same as that from QWLs on the (001) terraces, nevertheless the area of wire structures was much smaller than that of QWLs on the terraces.

References

[1] N. Kirstaedter, N. N. Lecentsov, M.Grundmann, D. Bimberg, V. M. Ustinov, S. S. Ruvimov, M. V. Maximov, P. S. Kop'ev, Zh. I. Alferov, U. Richter, P. Werner, U. Gösele and J. Heydenreich: Electron. Lett., **30**, 1416 (1994).

[2] H. Shoji, K. Mukai, N. Ohtsuka, M. Sugawara, T. Uchida and H. Ishikawa: IEEE Photon. Technol. Lett., **12**, 1385 (1995).

[3] N. Chand, S. N. G. Chu, N. K. Dutta, J. Lopata, M. Geva, A. V. Syrbu, A. Z. Mereutza and V. P. Yakovlev: IEEE J. Quantum Electron., **30**, 424 (1994).

[4]M. Kitamura, M. Nishioka, J. Oshinowo and Y. Arakawa: Appl. Phys. Lett., **66**, 3663 (1995).

[5] K. Hiramoto, T. Tsuchiya, M. Sagawa and K. Uomi: J. Cryst. Growth, **145**, 133 (1994).

[6] S. Tarucha, H. Okamoto, Y. Iwasa and N. Miura: Solid State Commun., **52**, 815 (1984).

[7] D. J. Arent, K. Deneffe, C. Van Hoof, J. De Boeck and G. Borghs: J. Appl. Phys., **66**, 1739 (1989).

[8] E. Colas, E. Kapon, S. Simhony, H. M. Cox, R. Bhat, K. Kash and P. S. D. Lin: Appl. Phys. Lett., **55**, 867 (1989).

Chapter VI

InGaAs Quantum Wire Lasers

6.1 Introduction

In the previous chapter, the fabrication and optical properties of strained InGaAs/GaAs QWRs formed at the edge of GaAs multiatomic steps by MOVPE were demonstrated. So far, there have been only a few reports on the application of these kinds of QWR structures or multiatomic steps to electronic devices such as "electron wave interference transistors" [1,2]. Application of QWR structures using monoatomic steps on vicinal substrates to semiconductor lasers has been reported [3,4], as well as other self-organized quantum structures. Actual applications to the semiconductor lasers operating in the infrared wavelength region have been intensively demonstrated in the investigations of zero-dimensional QDT structures formed during the epitaxial growth of lattice-mismatched materials system [5-7].

Although most of semiconductor lasers with low-dimensional quantum confinement structures were a standard Fabry-Pérot type diode laser with two sets of mirrors utilizing the cleaved facets, other types of semiconductor lasers can be fabricated by using *in situ* self-organized techniques in the epitaxial growth, especially in MOVPE. For example, vertical micro-cavity lasers with two sets of AlAs/AlGaAs multi-layer distributed Bragg reflectors (DBR) were demonstrated by using the triangular shaped InGaAs QWRs grown by selective area MOVPE [8] and self-assembled InGaAs QDTs grown by Stranski-Krastanov growth mode [9]. In this type of lasers, it is possible to produce extremely high reflectivity, 99.9 %, only by using the multi-layers simultaneously formed during the epitaxial growth. As the other novel semiconductor lasers fabricated by using self-organized techniques, a hexagonal facet GaAs/AlGaAs lasers has been demonstrated by selective area MOVPE growth on GaAs (111)B substrates [10]. Although this type of lasers has basically the Fabry-Pérot cavities, it is possible to form the {110} facet mirrors during the MOVPE

growth and various kinds of rectangular optical waveguides at the same time with the formation of laser structures [11].

In this chapter, the first successful laser operation of InGaAs/GaAs QWRs on GaAs multiatomic steps by current injections are demonstrated. Following the section 6.2, which describes the sample preparation procedures of laser chips, EL characterization results and actual lasing characteristics of InGaAs QWRs diode laser are summarized.

6.2 Sample Preparation Procedure

A vicinal n-GaAs (001) substrate, whose carrier concentration was more than 1.0 $\times 10^{18}$ cm^{-3}, misoriented by 5.0° to the [-110] direction and a singular n-GaAs (001) substrate were used. Indium content of InGaAs layers was either 0.15 or 0.30. Growth temperature was 600 °C for $In_{0.15}Ga_{0.85}As$ layers and 520 °C for $In_{0.3}Ga_{0.7}As$ layers. In order to fabricate laser diode with InGaAs QWRs in its active layer, the separate confinement heterostructure (SCH) was grown, as shown in Fig. 6.1. SiH_4 gas was used as n-type dopant for the growth of n-AlGaAs cladding layers, whereas p-type doping of p-AlGaAs cladding layers was achieved by an intentional incorporation of carbon (C) impurities under the growth condition of low V / III ratio (V / III = 29, using TMGa, TMAl and AsH_3). Carrier concentrations of n- and p- type AlGaAs cladding layers were between 2.0 $\times 10^{17}$ cm^{-3} and 8.0 $\times 10^{17}$ cm^{-3}, and aluminum contents of AlGaAs layers were 0.32. After the growth of a thick AlGaAs layer, its surface morphology tends to be rough, that is, it is difficult to form coherent and straight AlGaAs multiatomic steps. Therefore, before the growth of non-doped GaAs layers in order to form the multiatomic steps, $(GaAs)_2$ / $(AlAs)_1$ superlattice buffer layers were grown to form the surfaces with monoatomic steps. It was confirmed by AFM observations that GaAs multiatomic steps and InGaAs wire-like structures can be formed after the thick Si-doped AlGaAs cladding layers, followed by the growth of

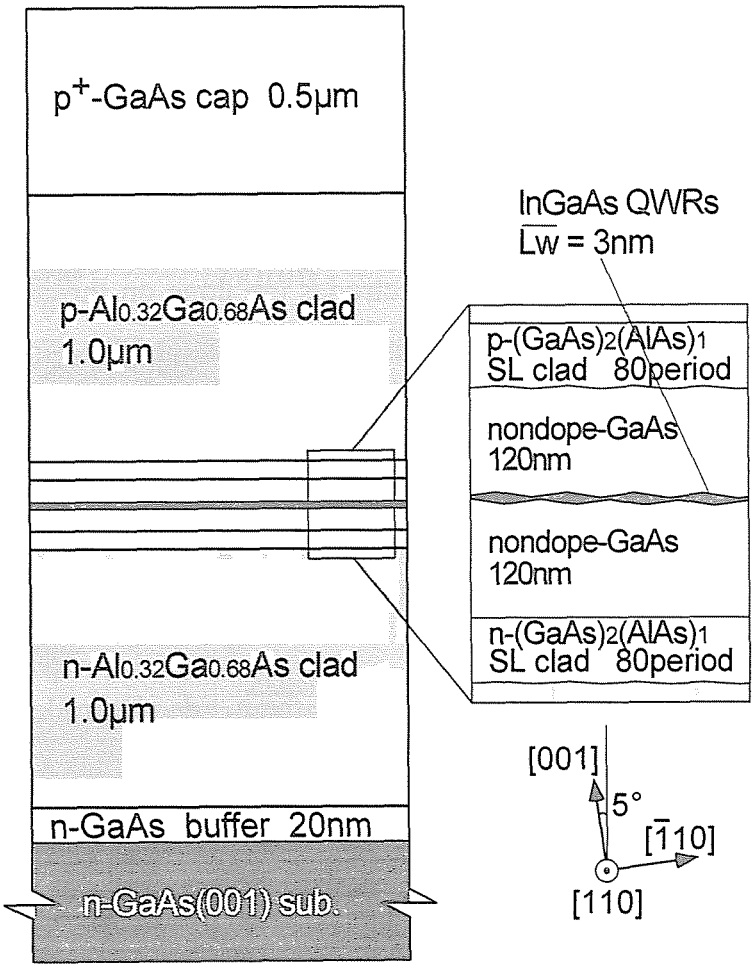

Fig. 6.1 Sample structure of separate confinement heterostructure lasers.

Si-doped $(GaAs)_2$ / $(AlAs)_1$ superlattice buffer layers. Furthermore, in order to eliminate the "flattening" of InGaAs layers on multiatomic steps, which was discussed in section 5.5, a 40 nm-thick non-doped GaAs upper layer was grown at 480 °C on InGaAs QWR layer, followed by a GaAs layers grown at 600 °C. Other growth conditions were the same as those described in chapter 5.

After the MOVPE growth of a SCH structure, a standard Fabry-Pérot type laser diode (LD) with as-cleaved {110} facet mirrors was fabricated. Figure 6.2 shows the flowchart of the sample preparation procedures. An alloy of gold (Au) - zinc (Zn) and that of Au - germanium (Ge) - nickel (Ni) were used as p- and n- type ohmic electrodes, respectively. Preparation procedures of laser chips are introduced in detail as follows:

(1) The processes for the fabrication of electrodes are done on the p-type surfaces in the first place. After the conventional photo-lithography processes, Au-Zn electrode materials are evaporated on the surfaces.

(2) 300 μm-wide areas of Au-Zn layers, which have a 320 μm-period, are remained by the lift off processes with a organic solvent. After that, to form the ohmic contact with p^+-GaAs cap layers, samples are annealed at 430 °C for 3 min, and Au-Zn are alloyed.

(3) After the photo-lithography processes to cover the p-side electrodes with a positive photo-resist, 10 μm-deep and 20 μm-wide grooves, which are to divide samples into laser chips, are formed by etching. H_3PO_4 : H_2O_2 : H_2O (= 1 : 3 1) chemical etching solution was used at room temperature. After the etching, the photo-resists are removed.

(4) Before the processes for the formation of n-type electrodes, n-type GaAs substrates, that is, the back of the samples, are thinned down until the thickness of about 150 ~ 180 μm.

(5) After the thinning and polishing processes, Ge-Au-Ni electrode materials are evaporated on the back of samples, and are alloyed by annealing at 400 °C for 2 min 30 sec to form the ohmic contact.

(6) In order to divide samples into the arrays of laser chips, they are cleaved

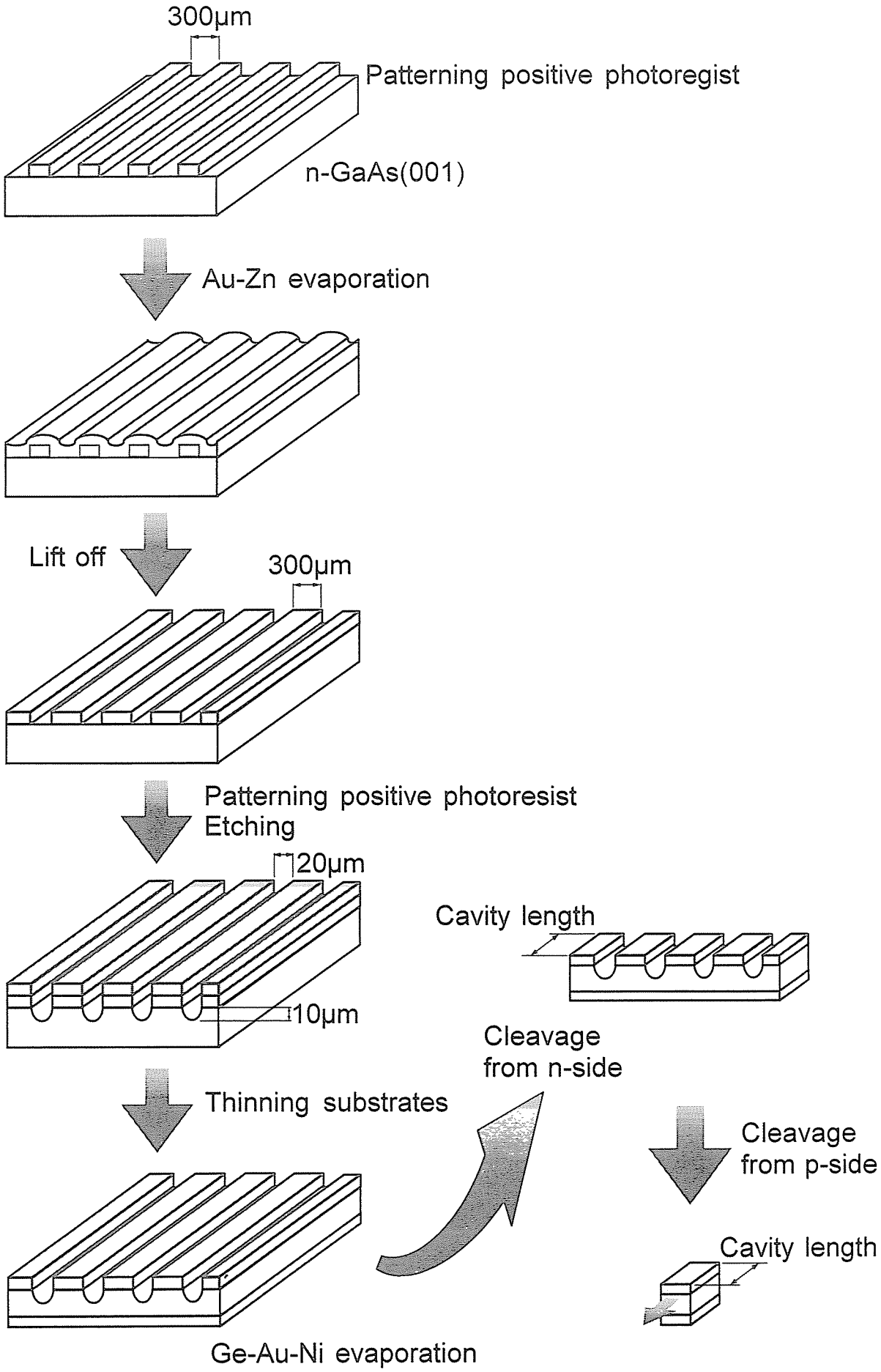

Fig. 6.2 Preparation procedures for laser diode chips.

perpendicular to the etched grooves between 300 μm-wide Au-Zn electrodes. These cleavage processes are the most important because as-cleaved {110} facet mirrors for the cavity are formed by the cleavages. Therefore, the cleavages are done from the back of samples carefully.

(7) Finally, each laser chips is obtained by the cleavages using the etched grooves of the sample surfaces. These laser chips are fixed by indium (In) metal and wax dissolved by acetone on the sample holders made of copper (Cu) as the p-side surfaces of the samples are down, and gold wires are bonded to the n-side electrodes.

Cavity length was about 600 μm and its direction was in either the [110] or the [-110] direction, where the [110] direction is parallel to the QWRs and multiatomic steps and the [-110] direction is parallel to the misorientation direction of the vicinal substrates, that is, perpendicular to the QWRs. Width of electrodes was about 300 μm. Electroluminescence (EL) and lasing operation were investigated by current injections under the pulsed bias conditions at room temperature and 77 K. Unless otherwise specified, the pulsed conditions were as follows: repetition rate of 12 kHz and pulse width of 1.0 μs.

6.3 Characterization of Laser Diode

First, figure 6.3 shows EL spectra of QWL on the singular (001) substrate by pulsed currents injection at room temperature. Peak positions of EL spectra were 1.350 eV, and the weak side peaks at around 1.385 eV could be observed. Figure 6.4 also shows EL spectra of QWR-LD structure and their dependence on injection currents measured at room temperature plotted in logarithmic scale. In the sample, cavity direction was equal to the QWRs' one, that is, the [110] direction. The EL spectra have a peak at 1.312 eV and are also asymmetric even at the smallest injection current investigated here. This asymmetry is also caused by the feature around 1.36

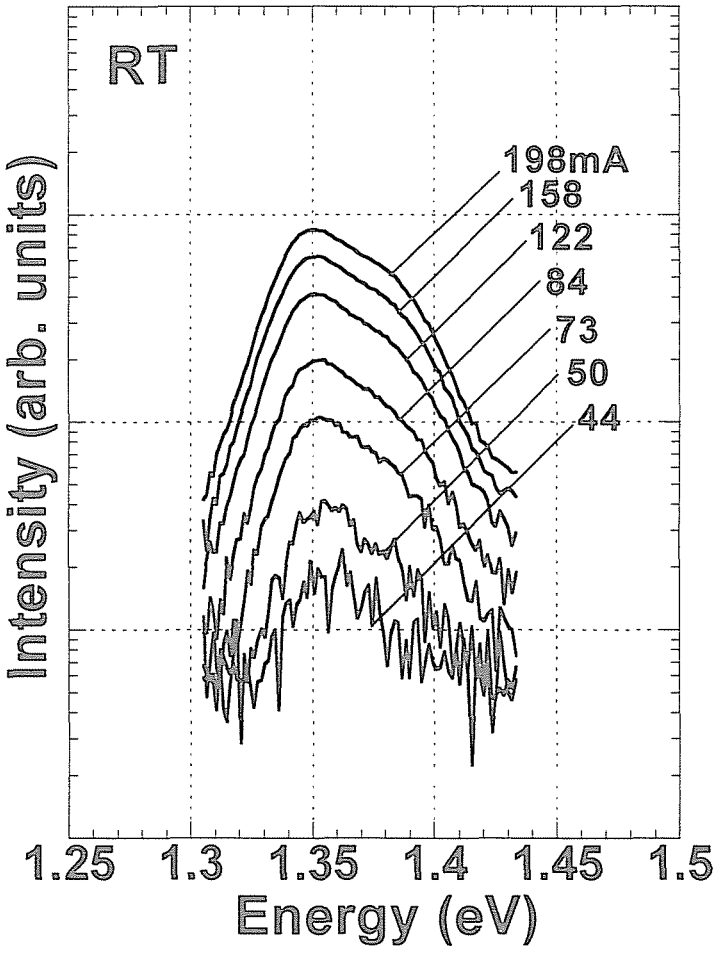

Fig. 6.3 Electroluminescence spectra of QWL on singular GaAs (001) substrates and its dependence on pulsed injection currents at room temperature in logarithmic scale.

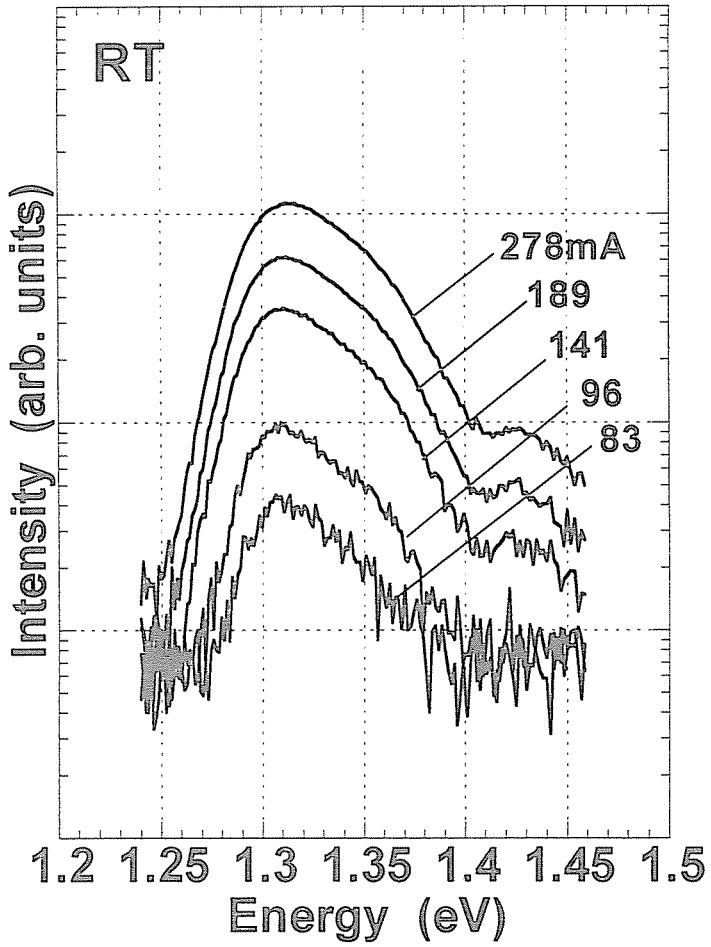

Fig. 6.4 Electroluminescence spectra of QWRs on 5.0°-misoriented GaAs (001) substrates and its dependence on pulsed injection currents at room temperature in logarithmic scale.

eV, and it becomes more prominent at higher injection currents. The asymmetry is probably due to the thermal distribution in the ground subband of QWRs and to the population in the excited states, because the energy difference between 1.312 eV and around 1.36 eV is comparable to that between two peaks in PLE spectra shown in chapter 5. The weak feature at 1.422 eV can be ascribed to the EL from GaAs. At 77 K, this SCH diode showed clear lasing operation by pulsed current injections. Figure 6.5 shows EL and lasing spectra at 77 K. The spectra are fairly symmetric and become sharper and stronger as the current increases. FWHM of the lasing spectra was less than 3 meV, and the wavelength at lasing operation was around 896 nm (1.384 eV), which was almost the same as the peak position of PL spectra at 77 K as described in chapter 5. Figure 6.6 shows current – light output (I – L) characteristics at 77 K under the pulsed bias conditions. It was roughly estimated the threshold current to be 212 mA, which corresponds to the threshold current density of 118 A/cm^2. These results are the first demonstration of a laser diode using self-organized InGaAs QWRs on GaAs multiatomic steps in its active layer. Next, the behavior of InGaAs QWR-LDs emitting in the two directions, which mean that cavity directions are in the [110] and the [-110] direction, and the comparison of them with the behavior of QWL-LD were investigated at 77 K under the pulsed bias conditions. Figure 6.7 shows the emissions of $In_{0.15}Ga_{0.85}As$ QWRs- and QWL-LDs below and above threshold at 77 K. The wavelength at lasing operation of the QWL-LD was around 864 nm, which corresponded to the emission energy of 1.435 eV. Emission peak energy of the QWR-LDs was always about 40 meV lower than that of the QWL-LD. This result is consistent with the results obtained in the PL measurements at 77 K, and the amount of these red-shifts is comparable to that in the PL spectra. The small energy difference between the two QWR-LD samples with the cavity in the direction parallel to QWRs array direction and perpendicular to it can probably be attributed to the growth thickness difference from wafer to wafer. Figure 6.8 also shows I – L characteristics of these LDs at 77 K. Threshold current (I_{th}) of QWL-LD was estimated to be 150 mA, and that of QWR-LDs with cavity parallel and perpendicular to the QWRs array direction was 212 and 105 mA, respectively, which correspond to the threshold

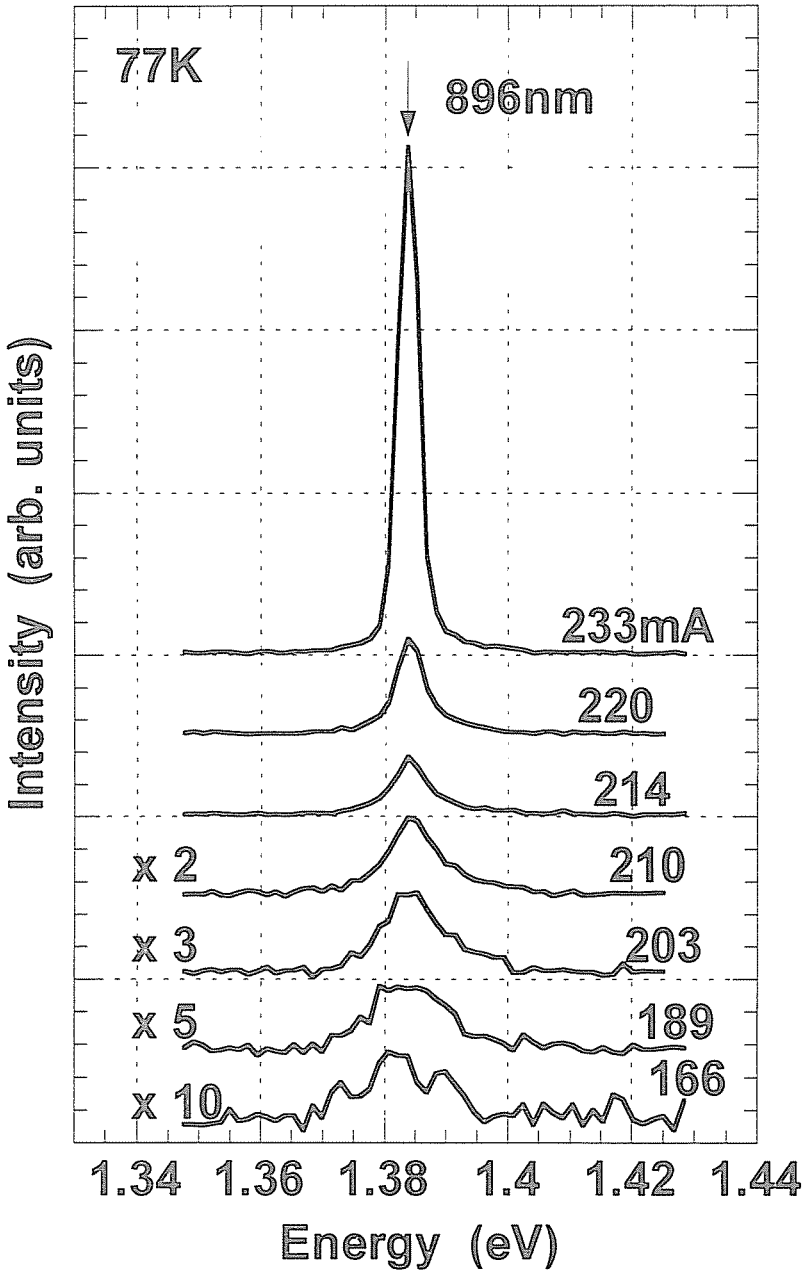

Fig. 6.5 Electroluminescence and lasing spectra of QWRs on 5.0°-misoriented GaAs (001) substrates by pulsed current injections at 77 K. Wavelength at pulsed laser operation was 896 nm being the same as the PL peak position at 77 K. Indium content is 0.15.

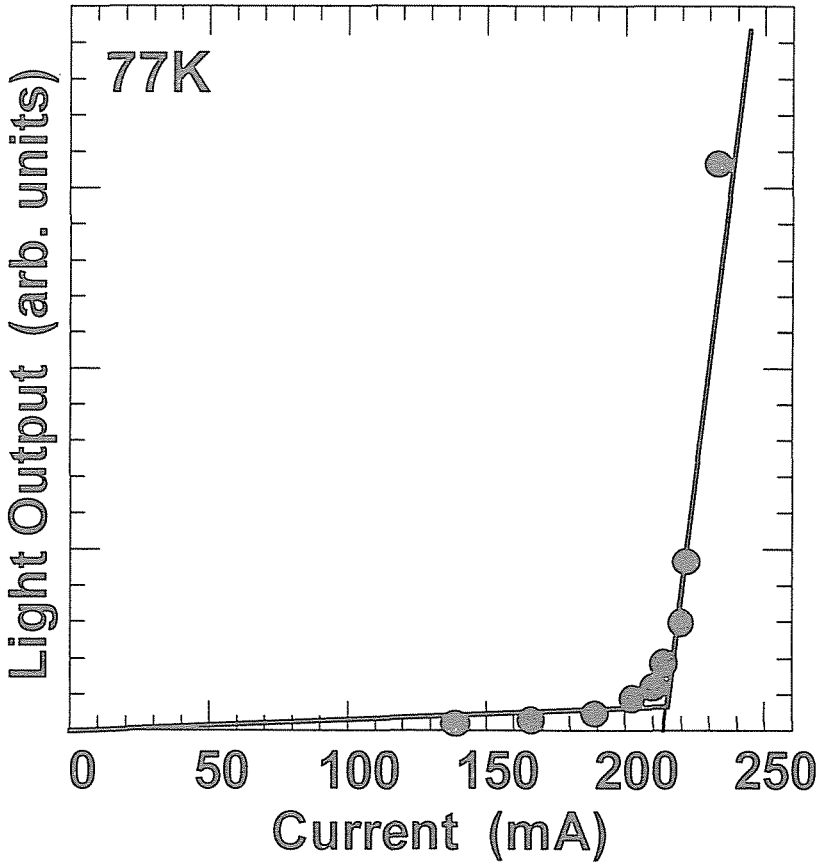

Fig. 6.6 Current – light output (I – L) characteristics of QWRs on 5.0°-misoriented substrates at 77 K.

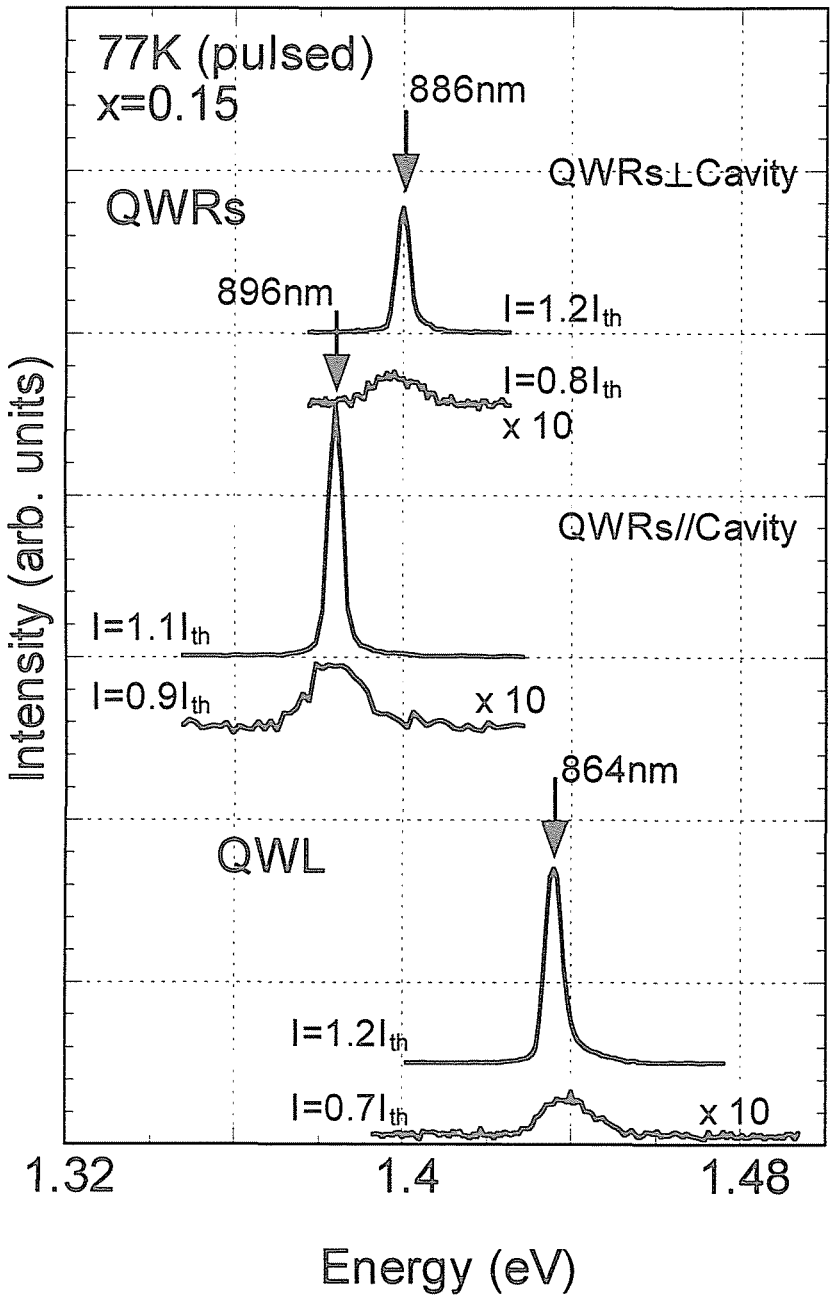

Fig. 6.7 Electroluminescence and lasing spectra of QWRs and QWL by pulsed current injections at 77 K. Peak energy at pulsed laser operation of QWRs laser was lower than that of QWL.

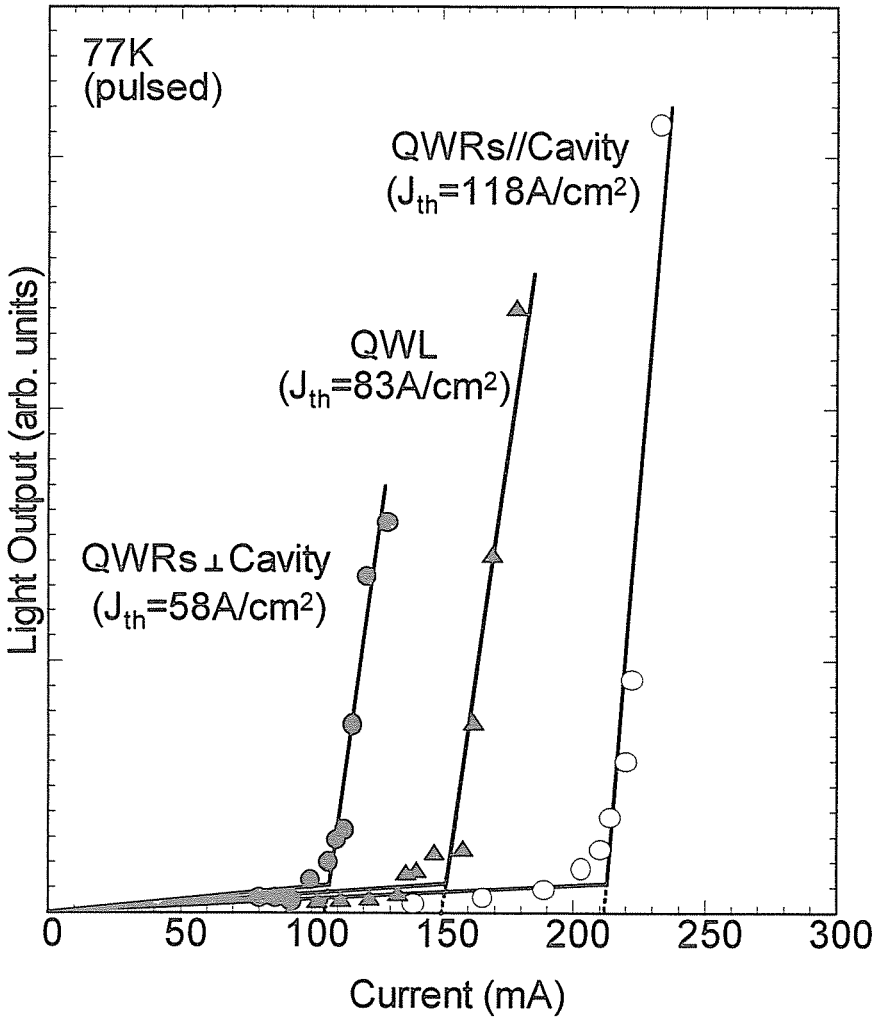

Fig. 6.8 I – L characteristics of QWRs and QWL at 77 K. When cavity direction was perpendicular to QWRs' direction, threshold current density of QWRs laser was lower than that of QWL.

current density (J_{th}) of 83, 118 and 58 A/cm^2. In QWRs lasers, the effect of anisotropy of the electronic dipole moment, which leads to the dependence of gain on the direction of QWRs against the light propagation, has been theoretically discussed, and it has been well known that maximum gain can be obtained for QWRs perpendicular to light propagation, that is, when electric field vector (E) of the light propagation becomes parallel to the direction of QWRs array [12]. Such phenomenon has also been experimentally confirmed, for example, as described in Refs. 3, 4 and 13. Figure 6.9 shows schematic of the relationship between the QWRs array and the cavity direction, that is, the direction of the light propagation for the QWR-LDs investigated here. In the present work, when the cavity direction was perpendicular to the QWRs array direction, threshold current density of the QWR-LD was lower than that of the QWL-LD, as shown in Fig. 6.8. This result shows the first successful demonstration of self-organized InGaAs QWRs laser formed on GaAs multiatomic steps because the result obtained here may be attributed to one-dimensional characteristics of InGaAs QWRs.

In the section 5.3, it was found that, even on the 5.0°-misoriented $In_{0.3}Ga_{0.7}As$ surfaces, InGaAs QWR structures could be fabricated. Next, EL and lasing characteristics of SCH-LDs with $In_{0.3}Ga_{0.7}As$ QWRs in their active layers are also investigated. Figures 6.10 and 6.11 show EL spectra at room temperature of QWR-LDs with cavity parallel and perpendicular to QWRs array direction, respectively. In Fig. 6.10, peak position of EL spectra shifted to higher energy side as higher currents were injected. Additional peaks around 1.26 eV, which are ascribed to the population in the excited states, can also be observed under higher injection currents condition. In the current study, although the details of reasons could not be revealed, broadening of the line width in the main peaks of EL spectra can be probably due to the size distribution of the QWR structures or the carrier population in the excited states. These QWRs were also characterized at 77 K. Figures 6.12 and 6.13 show EL and lasing spectra at 77 K of these QWR-LDs. In both cases, clear lasing spectra can be observed at around 1.0 μm. Especially in Fig. 6.12, higher energy shifts of the peak position with increasing injection currents were also seen, as shown in EL spectra at

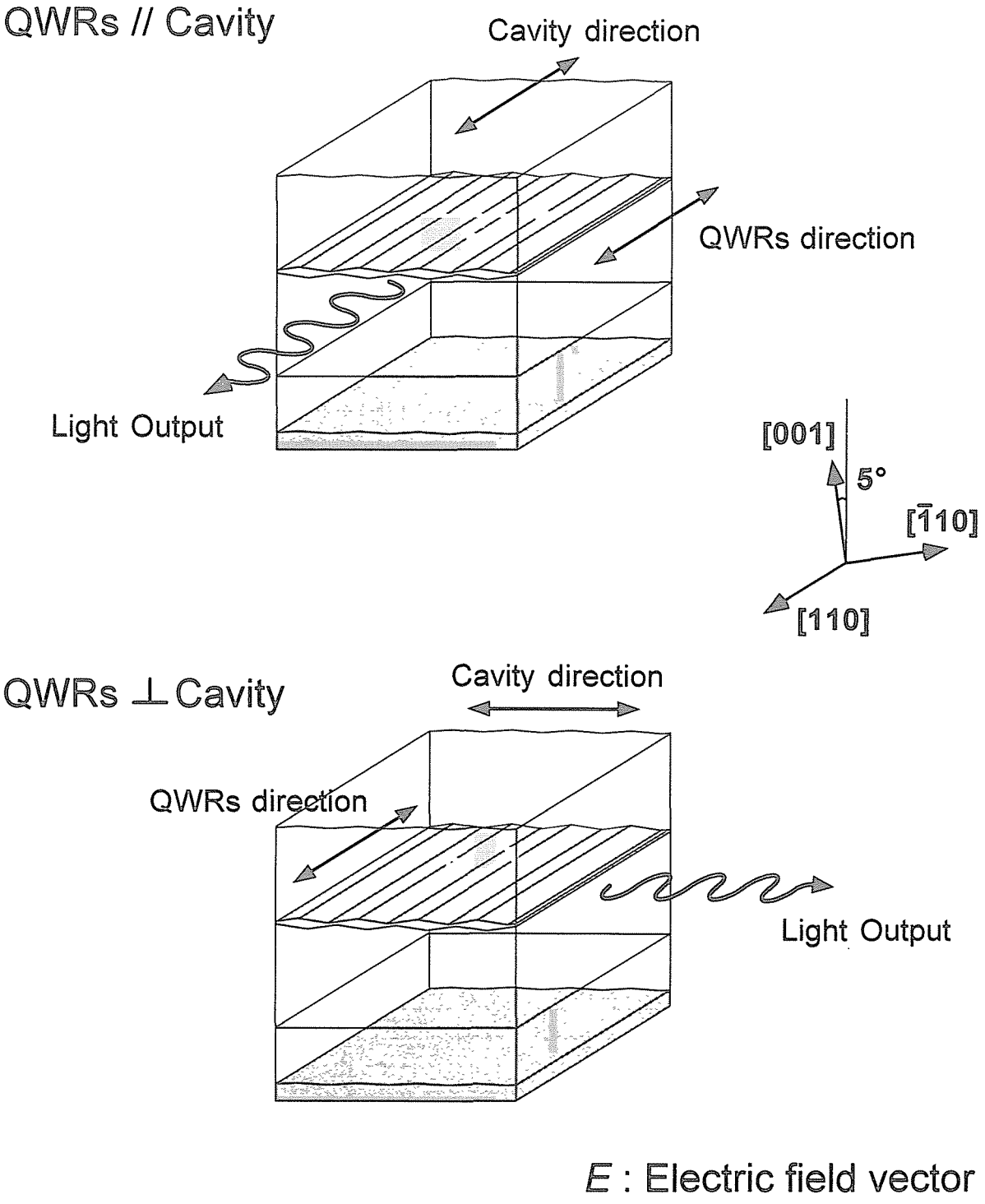

Fig. 6.9 Schematic of relationship between QWRs and cavity directin of QWRs laser samples. When cavity direction is perpendicular to QWRs' one, electric field vector (E) of light is parallel to QWRs.

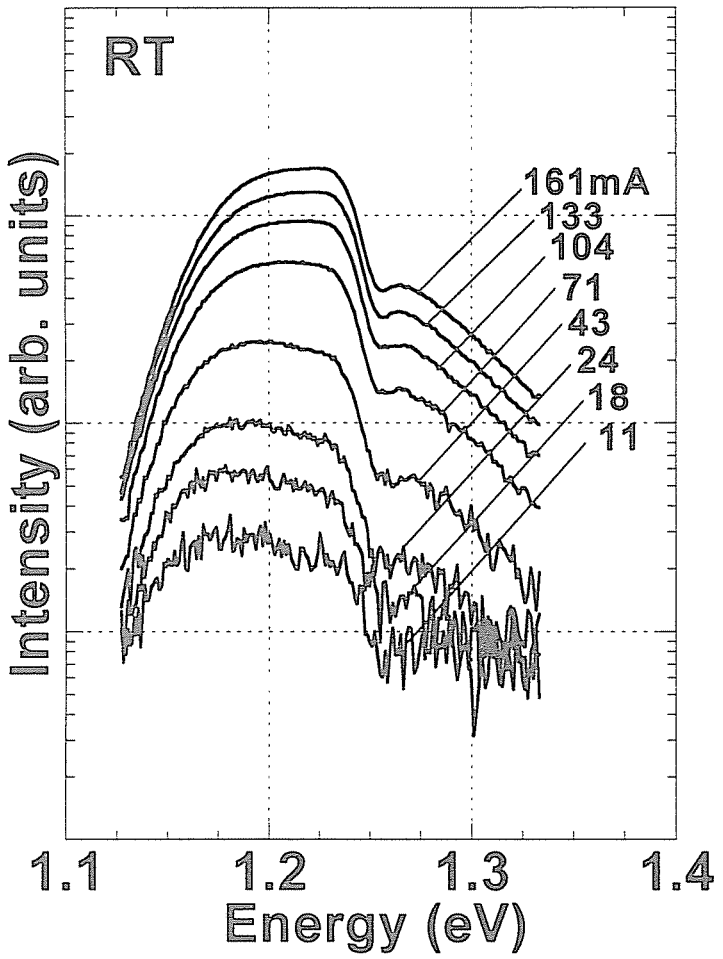

Fig. 6.10 Electroluminescence spectra of QWRs on 5.0°-misoriented GaAs (001) substrates and its dependence on pulsed injection currents at room temperature in logarithmic scale. Indium content is 0.3 and cavity direction is parallel to QWRs.

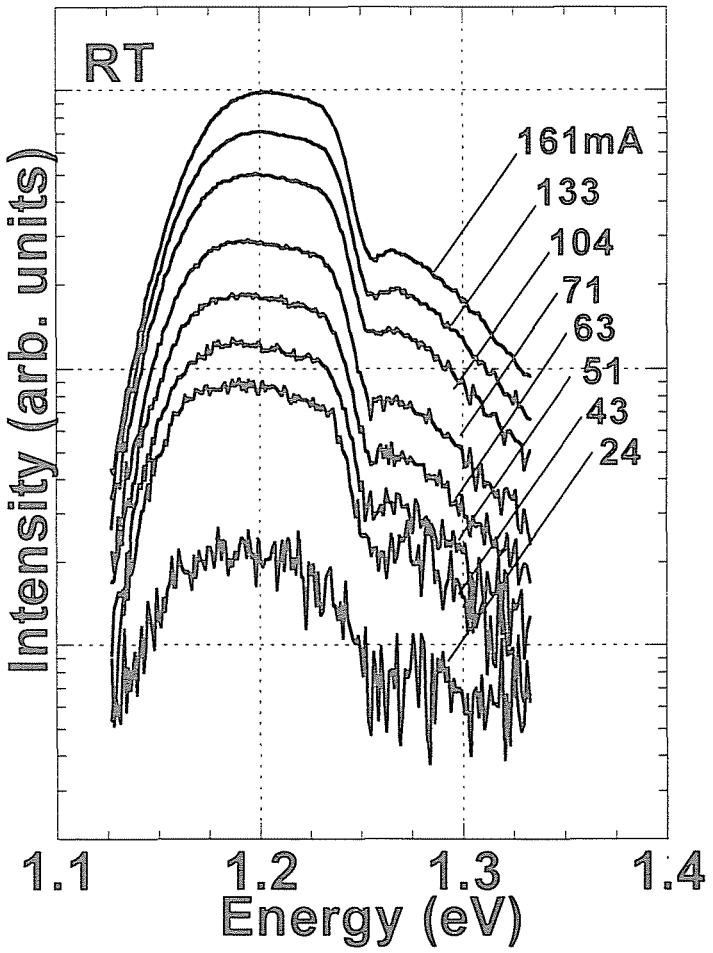

Fig. 6.11 Electroluminescence spectra of QWRs on 5.0°-misoriented GaAs (001) substrates and its dependence on pulsed injection currents at room temperature in logarithmic scale. Indium content is 0.3 and cavity direction is perpendicular to QWRs.

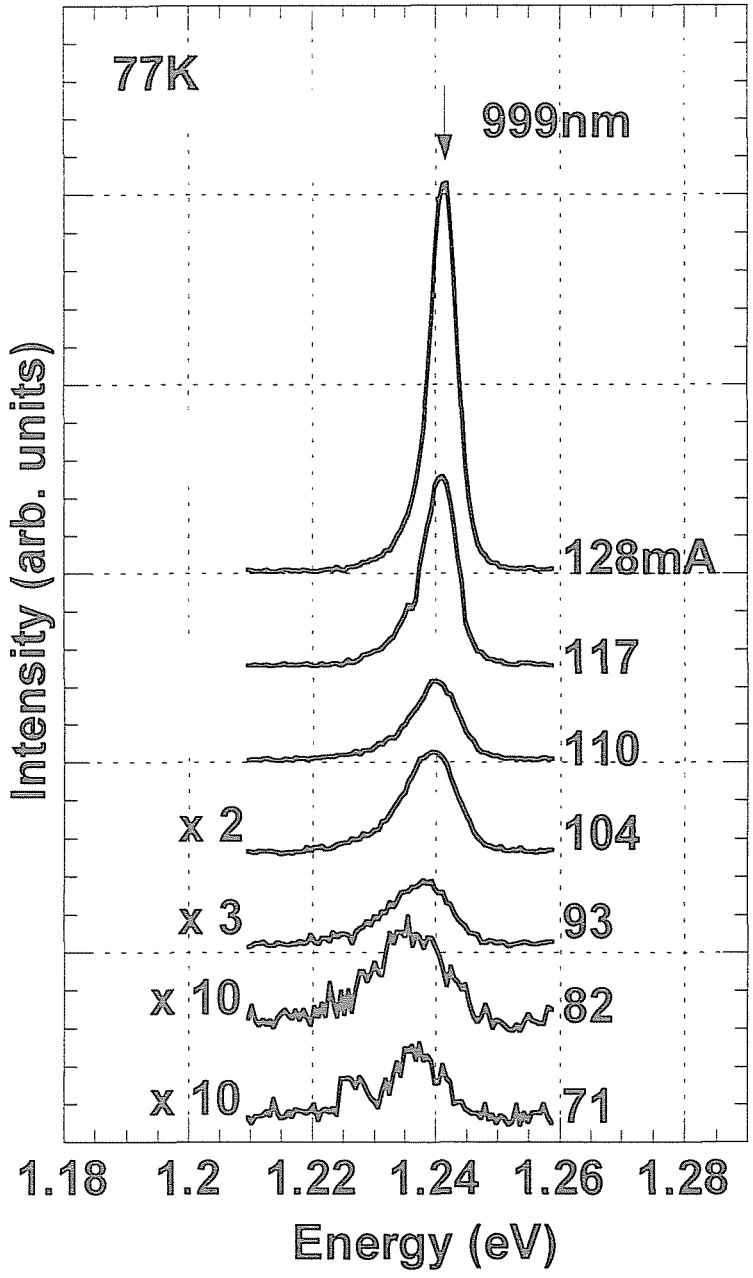

Fig. 6.12 Electroluminescence and lasing spectra of QWRs on 5.0°-misoriented GaAs (001) substrates by pulsed current injections at 77 K. Indium content is 0.3 and cavity direction is parallel to QWRs.

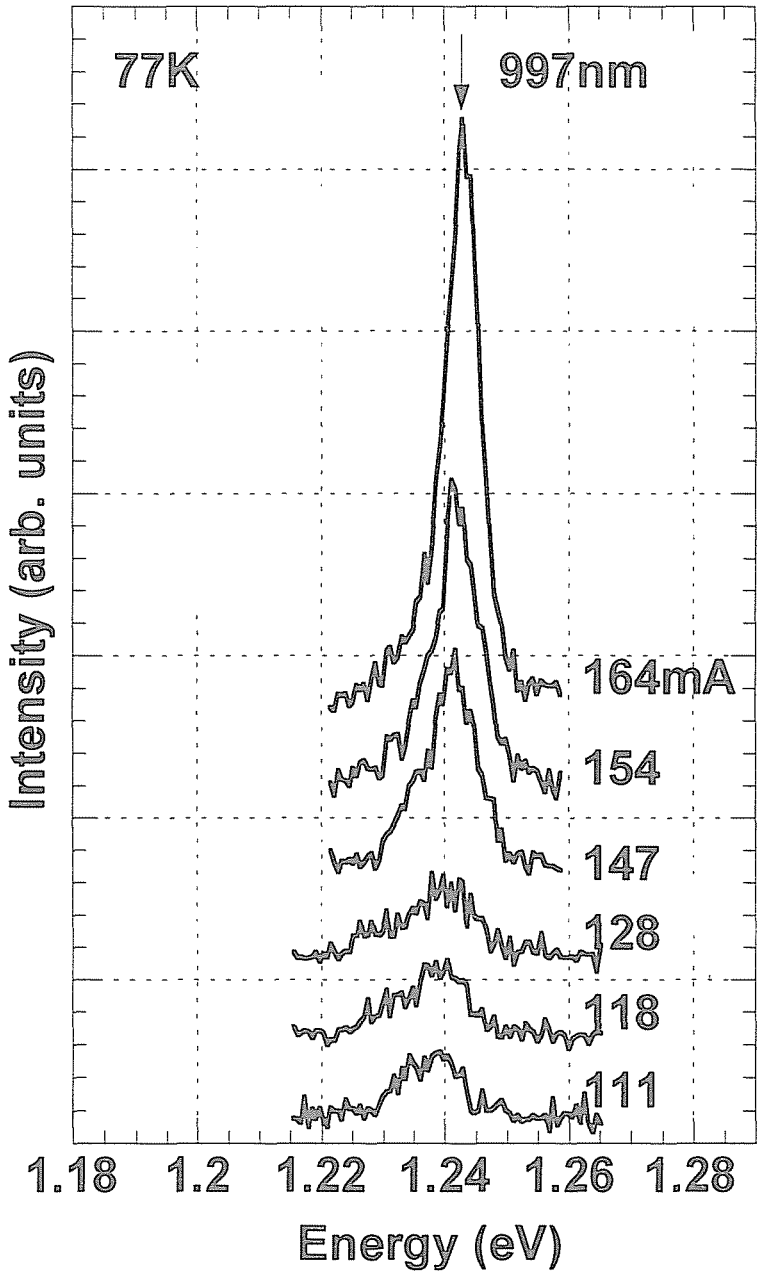

Fig. 6.13 Electroluminescence and lasing spectra of QWRs on 5.0°-misoriented GaAs (001) substrates by pulsed current injections at 77 K. Indium content is 0.3 and cavity direction is perpendicular to QWRs.

room temperature in Fig. 6.10. I – L characteristics of $In_{0.3}Ga_{0.7}As$ QWR-LDs at 77 K are summarized in Fig. 6.14. Threshold currents of the sample with parallel and perpendicular to the QWRs array direction were about 103 and 135 mA, respectively. These figures correspond to the threshold current density of 57 and 75 A/cm^2. There was only a slight difference between the threshold current densities of such two samples, being different from the result of $In_{0.15}Ga_{0.85}As$ QWR-LDs in Fig. 6.8. In the QWR-LDs used here, thin $In_{0.3}Ga_{0.7}As$ layers were grown on GaAs multiatomic steps at 520 °C. As described in chapter 5.3, the average inclination angle at the edge of $In_{0.3}Ga_{0.7}As$ multiatomic step areas becomes lower, as the thin InGaAs layers are grown at lower growth temperature. Therefore, in-plane thickness variations of $In_{0.3}Ga_{0.7}As$ layers between at the edge of multiatomic steps and on the (001) terraces seems to be smaller than those of $In_{0.15}Ga_{0.85}As$ layers. This result means that lateral confinement effect of the $In_{0.3}Ga_{0.7}As$ QWRs at the edge of multiatomic steps becomes smaller than that of the $In_{0.15}Ga_{0.85}As$ QWRs because the thickness differences of $In_{0.3}Ga_{0.7}As$ layers between at the edge of GaAs multiatomic steps and on the (001) terraces tend to become smaller. It may lead to the small difference of the threshold current densities in the $In_{0.3}Ga_{0.7}As$ QWR-LDs. In the $In_{0.3}Ga_{0.7}As$ QWR-LD whose cavity direction is parallel to the QWRs' direction, EL spectra were also characterized at room temperature under the higher current injection conditions. Pulsed bias condition was different from the measurements in Fig. 6.10, that is, the repetition rate was 12 kHz and duty ratio was 90 %. As shown in Fig. 6.15, weak peaks, which had about 10 meV-energy separations each other, appeared in the main peak of EL spectra, and the highest energy peak of around 1.26 eV became clear and sharper, with increasing the injection currents. These results may indicate that the maximum gain can be obtained in the higher energy states of the InGaAs QWRs, and then, lasing of InGaAs QWR-LDs can operate even at room temperature.

The self-organized InGaAs QWRs used here might be have the fluctuation of their size uniformity of about ± 13 %, and their continuity is not perfect, because the patterned vicinal substrates was not used. Since any attempts to reduce the threshold current density were not performed, of course, the values of the threshold current

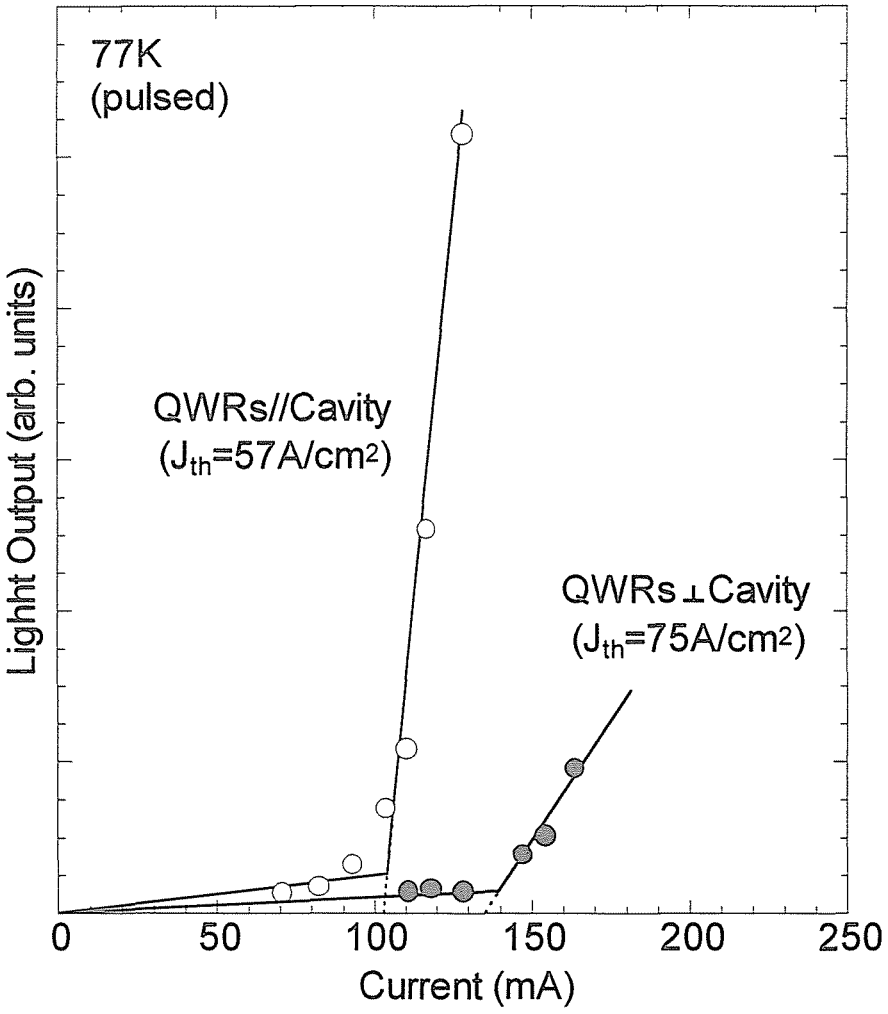

Fig. 6.14 I – L characteristics of QWRs at 77 K. Indium content is 0.3.

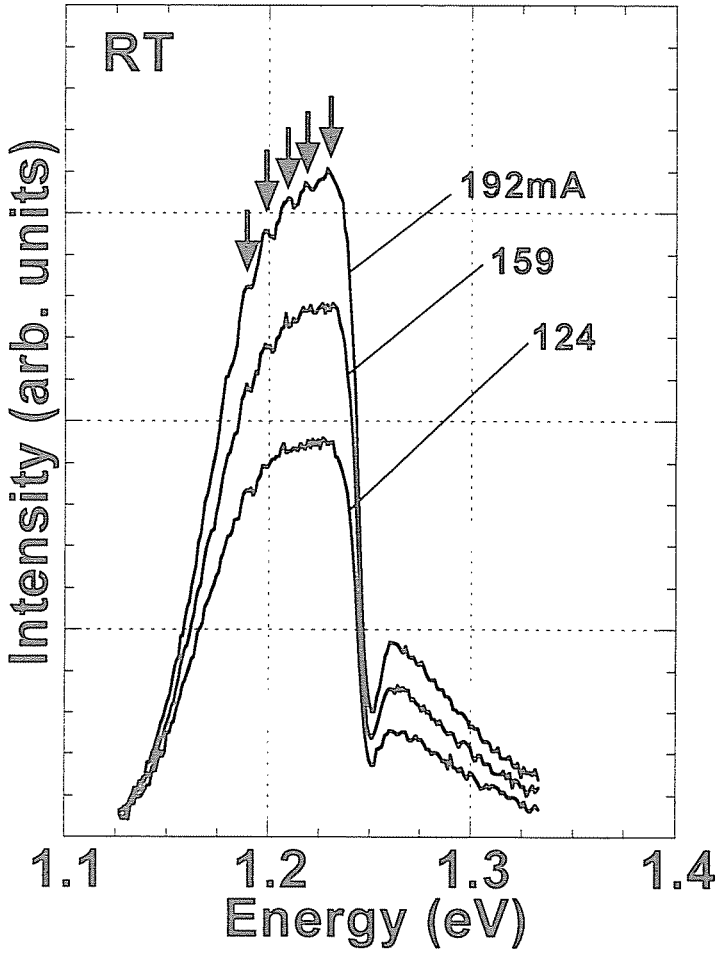

Fig. 6.15 Electroluminescence spectra of QWRs with 0.3 indium content at room temperature. Repetition rate is 12 kHz and duty ratio is 90 %. Cavity direction is parallel to QWRs.

density obtained here is not the smallest ones. In the current InGaAs QWR-LDs, however, it is also possible to reduce its threshold current density by introducing the current blocking layers and high reflection (HR) coated {110} facet mirrors. Further improvement of lasing characteristics will be also expected by the optimization of epitaxial growth conditions, doping conditions of cladding layers, ohmic contact of p- or n- type electrodes, and so on.

6.4 Summary

In this chapter, EL properties of the InGaAs QWRs were investigated at room temperatures, and the first attempts to form SCH-LDs with the InGaAs QWRs in its active layers and to characterize them were demonstrated. The main results are summarized below.

(1) EL spectra of the QWR-LDs at room temperature had the asymmetric shape probably because of the thermal distribution in the ground subband of the QWRs and to the population in the excited states.

(2) For the first time, the pulsed laser operation of the SCH-LDs using InGaAs QWRs in its active layers at 77 K by current injection was successfully demonstrated. Wavelength at the pulsed lasing operation was around 896 nm at 77 K, which was almost the same as the peak position of PL spectra and longer wavelength than that of the QWL-LD, 864 nm, at 77 K. It was roughly estimated the threshold current density to be 118 A/cm^2.

(3) In lasing operation of $In_{0.15}Ga_{0.85}As$ QWR-LDs, when the direction of cavity was perpendicular to the QWRs array direction, the threshold current density of QWR-LD was lower than that of QWL-LD. It was roughly estimated to be 58 A/cm^2 under the pulsed bias conditions at 77 K.

(4) $In_{0.3}Ga_{0.7}As$ QWR-LDs were also fabricated by the growth of thin InGaAs layers at 520 °C on GaAs multiatomic steps. Emission wavelength of the QWR-LDs was around 1.0 μm at 77 K. By changing indium contents of InGaAs QWRs on GaAs

multiatomic steps, emission wavelength at lasing operation can be controlled from around 0.9 μm to 1.0 μm at 77 K.

References

[1] J. Motohisa, M. Akabori, S. Hara, J. Ishizaki, K. Ohkuri and T. Fukui: Physica B, 227, 295 (1996).

[2] M. Akabori, J. Motohisa, T. Irisawa, S. Hara, J. Ishizaki and T. Fukui: Jpn. J. Appl. Phys., 36, 1966 (1997).

[3] H. Saito, K. Uwai and N. Kobayashi: Jpn. J. Appl. Phys., 32, 4440 (1993).

[4] J. Yoshida, A. Kikuchi, I. Nomura and K. Kishino: Proc. 7th Int. Conf. IPRM (IEEE Catalog #95CH35720), 29 (1995).

[5] N. Kirstaedter, N. N. Lecentsov, M.Grundmann, D. Bimberg, V. M. Ustinov, S. S. Ruvimov, M. V. Maximov, P. S. Kop'ev, Zh. I. Alferov, U. Richter, P. Werner, U. Gösele and J. Heydenreich: Electron. Lett., 30, 1416 (1994).

[6] H. Shoji, K. Mukai, N. Ohtsuka, M. Sugawara, T. Uchida and H. Ishikawa: IEEE Photon. Technol. Lett., 12, 1385 (1995).

[7] J. Temmyo, E. Kuramochi, M. Sugo, T. Nishiya, R. Nötzel and T. Tamamura: Electron. Lett., 31, 209 (1995).

[8] T. Arakawa, M. Nishioka, Y. Nagamune and Y. Arakawa: Appl. Phys. Lett., 64, 2200 (1994).

[9] Y. Arakawa, M. Nishioka, H. Nakayama and M. Kitamura: IEICE Trans. Electron., E79-C, 1487 (1996).

[10] S. Ando, N. Kobayashi and H. Ando: Jpn. J. Appl. Phys., 32, L1293 (1993).

[11] S. Ando, N. Kobayashi and H. Ando: Jpn. J. Appl. Phys., 34, L4 (1995).

[12] M. Asada, Y. Miyamoto and Y. Suematsu: Jpn. J. Appl. Phys., 24, L95 (1985).

[13] P. J. Pearah, A. C. Chen, A. M. Moy, K. –C. Hsieh and K. –Y. Cheng: IEEE J. Quantum Electron., QE-30, 608 (1994).

Chapter VII

Summary and Conclusions

In the current work, self-organized GaAs and InGaAs QWRs have been fabricated on GaAs multiatomic steps grown by MOVPE, and their optical properties have been characterized. Furthermore, the fabrication and their characteristics of the laser diode using InGaAs QWRs in its active layers was demonstrated for the first time. In this chapter, the main results in the present work are summarized.

In chapter 3, the self-organizing fabrication of GaAs/AlGaAs QWRs utilizing coherent GaAs multiatomic steps, which can be naturally formed during the MOVPE growth, were demonstrated. As results of the cross-sectional TEM observations, it was confirmed that GaAs layers at the edge of multiatomic steps on the 5.0°- misoriented surfaces, whose average height, average spacing and distribution of inter-step spacing were 7.0 nm, 80 nm and within ± 13 %, respectively, was thicker than that on the (001) terraces. In PL spectra of such locally thick GaAs wire structures on the 5.0°-misoriented substrates, PL peak energy showed the energy shift of 23 meV to the lower energy side (red-shift) with respect to that of QWL on the singular GaAs (001) substrate. The result of PL energy shift in GaAs wire structures was also compared with a simple numerical calculation. It was shown that the PL peak energy shift of the 5.0°- misoriented wafer was in good agreement with the calculation results. This means that GaAs QWRs were formed by the lateral growth of GaAs layers at the edge of multiatomic steps.

In chapter 4, as the improvement methods for size uniformity of QWR structures, the use of thin AlAs layers on coherent GaAs multiatomic steps as a lower barrier layers of QWR structures and GaAs multiatomic steps on patterned vicinal (001) substrates were demonstrated. According to the AFM observations, on the AlAs multiatomic steps, the average height, average spacing and the distribution of the step

spacing were 5.7 nm, 66 nm, and within ± 14 %, respectively, although AlGaAs surfaces tend to be disordered easily. Therefore, the underlying coherent GaAs multiatomic steps can be well traced by AlAs rather than AlGaAs. PL spectra of GaAs QWRs using AlAs also showed the red-shift, and their FWHM was about 16 meV smaller than those using AlGaAs. It was confirmed that the reduction in FWHM originated from the much improvement of the size uniformity in QWR structures by using AlAs as a lower barrier layer. Polarization anisotropy in PL spectra, which was about 0.12, also supported the successful formation of the QWRs.

GaAs layers grown on patterned vicinal GaAs (001) substrates by MOVPE formed extremely straight and coherent multiatomic steps. SEM observations revealed that such multiatomic steps can be formed in the same period with the underlying vicinal substrates' one. Cross-sectional SEM images showed that GaAs well layer thickness at the edges of multiatomic steps was about 2 times thicker than that on the terraces for the wafers with the 1 μm-period line and space pattern. From cross-sectional CL image observations, two emission peaks in CL spectrum at 4.2 K were from QWL at the edges and on the (001) terraces of multiatomic steps. The thickness of GaAs well layers estimated from CL emission peak energy was consistent with that from SEM images. Top view of CL images, which showed uniform emissions both from the edge and the (001) terrace areas of multiatomic steps over a wide area more than thirty micrometers, also supported that it is possible to control the straightness and continuity of QWRs.

In chapter 5, to form much uniform QWR structures directly at the edge of coherent GaAs multiatomic steps on vicinal GaAs (001) substrates, the formation of locally thick self-organized InGaAs wire structures was demonstrated. According to the results of AFM observations, a thin InGaAs layers with less than 0.15 indium contents can be grown in step flow growth mode at the edge of the GaAs multiatomic steps, and coherent multiatomic steps with almost the same period as underlying GaAs ones were formed. On the other hand, although InGaAs layers with more than 0.2 indium contents grew three-dimensionally because of the increase of the strain

effect at the edge of multiatomic steps, by adjusting the epitaxial growth conditions of InGaAs layers, wire-like structures can be formed even in the case of indium contents more than 0.2. Cross-sectional TEM observations revealed that $In_{0.1}Ga_{0.9}As$ layers at the edge of GaAs multiatomic steps was thicker than that on the (001) terraces grown on 5.0°-misoriented substrates.

PL spectra of InGaAs QWR samples also showed lower energy shifts by 15 ~ 31 meV with respect to those of QWL on a singular (001) substrate. FWHM of PL spectrum from the QWRs was 28 meV at 77 K. Although the top interfaces between InGaAs and GaAs tended to slightly flatten during the GaAs higher barrier layers growth probably because of slight segregation of indium atoms, the growth of 40 nm-thick GaAs upper layers at 480 °C made it possible to eliminate such flattening effects. The improvement of size uniformity can be seen in the reduction of FWHM of PL spectra, and the FWHMs were 20 ~ 22 meV at 77 K, being 6 ~ 8 meV smaller than those of the previous results. The polarization anisotropy in PLE spectra and PL properties in magnetic fields supported that the effect of lateral confinement exists in the QWRs.

InGaAs wire structures were also demonstrated using coherent GaAs multiatomic steps on patterned vicinal substrates. Such wire structures showed uniform emissions over more than thirty micrometers, nevertheless their areas were much smaller than those of QWL on the (001) terraces and peak shifts to the lower energy side with respect to the QWLs.

In chapter 6, the SCH-LD with InGaAs QWRs in its active layers was fabricated for the first time, and the pulsed laser operation at 77 K by current injections was successfully demonstrated. Wavelength at pulsed lasing operation was around 896 nm, which was almost the same as the peak position of PL spectra at 77 K, indicating the lasing spectrum was from the InGaAs QWRs. It was roughly estimated the threshold current density to be 118 A/cm^2. Lasing wavelength of the QWR-LDs was longer than that of the QWL-LD, 864 nm. In lasing operation of $In_{0.15}Ga_{0.85}As$ QWR-LDs, when the direction of cavity was perpendicular to the QWRs array direction, the threshold

current density of QWR-LD was lower than that of QWL-LD. These results may be ascribed to the one-dimensional characteristics InGaAs QWRs on GaAs multiatomic steps.

$In_{0.3}Ga_{0.7}As$ QWR-LDs were also fabricated by the growth of thin InGaAs layers at 520 °C on GaAs multiatomic steps. Emission wavelength of the QWR-LDs was around 1.0 μm at 77 K. It means that, by changing indium contents of InGaAs QWRs on GaAs multiatomic steps, emission wavelength at lasing operation can be controlled from around 0.9 μm to 1.0 μm at 77 K.

Publication List

I. Publication related to this thesis

(1) Shinjiroh Hara, Jun-ya Ishizaki, Junichi Motohisa, Takashi Fukui and Hideki Hasegawa: "Formation and Photoluminescence Characterization of Quantum Well Wires using Multiatomic Steps Grown by Metalorganic Vapor Phase Epitaxy", J. Cryst. Growth, Vol.145, Nos. 1-4, pp.692-697 (1994).

(2) Takashi Fukui, Jun-ya Ishizaki, Shinjiroh Hara, Junichi Motohisa and Hideki Hasegawa: "Multiatomic Step Formation Mechanism of MOVPE Grown GaAs Vicinal Surface and Its Application to Quantum Well Wires", J. Cryst. Growth, Vol.146, Nos. 1-4, pp.183-187 (1995).

(3) Shinjiroh Hara, Junichi Motohisa, Takashi Fukui and Hideki Hasegawa: "Quantum Well Wire Fabrication Method Using Self-Organized Multiatomic Steps on Vicinal (001) GaAs Surfaces by Metalorganic Vapor Phase Epitaxy", Jpn. J. Appl. Phys., Vol. 34, Part 1, No. 8B, pp.4401-4404 (1995).

(4) Kazunobu Ohkuri, Jun-ya Ishizaki, Shinjiroh Hara and Takashi Fukui: "Multiatomic Step Formation on GaAs (001) Vicinal Surfaces During Thermal Treatment", J. Cryst. Growth, Vol. 160, Nos. 3/4, pp.235-240 (1996).

(5) Takashi Fukui, Shinjiroh Hara, Jun-ya Ishizaki, Kazunobu Ohkuri and Junichi Motohisa: "Coherent Multiatomic Step Formation on GaAs (001) Vicinal Surfaces by MOVPE and Its Application to Quantum Well Wires", Inst. Phys. Conf. Ser., No. 145, Chapter 7, pp.919-924 (1996).

(6) Shinjiroh Hara, Junichi Motohisa and Takashi Fukui: "Formation and Characterization of InGaAs Strained Quantum Wires on GaAs Multiatomic Steps Grown by Metalorganic Vapor Phase Epitaxy", J. Cryst. Growth, Vol. 170, Nos. 1-4, pp.579-584 (1997).

(7) Shinjiroh Hara, Junichi Motohisa and Takashi Fukui: "Optical Characterization and Laser Operation of InGaAs Quantum Wires on GaAs Multiatomic Steps", Solid State Electron., to be published (1998).

(8) Shinjiroh Hara, Junichi Motohisa and Takashi Fukui: "Self-Organized InGaAs Quantum Wire Lasers on GaAs Multiatomic Steps", Electron. Lett., to be published (1998).

II. Publication related to other works

(9) Junichi Motohisa, Masashi Akabori, Shinjiroh Hara, Jun-ya Ishizaki, Kazunobu Ohkuri and Takashi Fukui: "Theoretical and Experimental Investigation of An Electron Interference Device Using Multiatomic Steps on Vicinal GaAs Surfaces", Physica B, Vol.227, pp.295-298 (1996).

(10) Masashi Akabori, Junichi Motohisa, Tomoki Irisawa, Shinjiroh Hara, Jun-ya Ishizaki and Takashi Fukui: "A Novel Electron Wave Interference Device Using Multiatomic Steps on Vicinal GaAs Surfaces Grown by Metalorganic Vapor Phase Epitaxy: Investigation of Transport Properties", Jpn. J. Appl. Phys., Vol. 36, Part 1, No. 3B, pp. 1966-1971 (1997).

III. Presentation in international conferences related to this thesis

(1) Shinjiroh Hara, Jun-ya Ishizaki, Junichi Motohisa, Takashi Fukui and Hideki Hasegawa: "Formation and Photoluminescence Characterization of Quantum Well Wires using Multiatomic Steps Grown by Metalorganic Vapor Phase Epitaxy", presented at the 7th International Conference on Metalorganic Vaper Phase Epitaxy, Yokohama, Japan, May 31-June 3, 1994.

(2) Jun-ya Ishizaki, Kazunobu Ohkuri, Shinjiroh Hara, Junichi Motohisa, Takashi Fukui and Hideki Hasegawa: "Behavior of the Multilayer Step of MOVPE Grown GaAs on Vicinal (001) GaAs Substrate Investigated by Atomic Force Microscopy", presented at the 13th Symposium on Alloy Semiconductor Physics and Electronics, Izu-Nagaoka, Japan, July 20-22, 1994.

(3) Takashi Fukui, Jun-ya Ishizaki, Shinjiroh Hara, Junichi Motohisa and Hideki Hasegawa: "New Fabrication Processes of GaAs Quantum Well Wires on Vicinal Substrate by MOVPE",

presented at the 7th International MicroProcess Conference, Hsinchu, Taiwan, July 11-14, 1994.

(4) Takashi Fukui, Jun-ya Ishizaki, Shinjiroh Hara, Junichi Motohisa and Hideki Hasegawa: "Multiatomic Step Formation Mechanism of MOVPE Grown GaAs Vicinal Surface and Its Application to Quantum Well Wires", presented at the 8th International Conference on Vaper Growth and Epitaxy, Freiburg, Germany, July 24-29, 1994.

(5) Shinjiroh Hara, Junichi Motohisa, Takashi Fukui and Hideki Hasegawa: "Novel Quantum Well Wire Fabrication Method Using Self-organized Multiatomic Steps on GaAs (001) Vicinal Surfaces by MOVPE", presented at the International Workshop on Mesoscopic Physics and Electronics (MPE'95), Tokyo, Japan, March 6-8, 1995.

(6) Kazunobu Ohkuri, Jun-ya Ishizaki, Shinjiroh Hara and Takashi Fukui: "Coherent Multiatomic Step Formation on GaAs (001) Vicinal Surfaces by Thermal Treatment in AsH_3/H_2 Atmosphere", presented at the 8th International MicroProcess Conference, Sendai, Japan, July 17-20, 1995.

(7) Takashi Fukui, Shinjiroh Hara, Jun-ya Ishizaki, Kazunobu Ohkuri and Junichi Motohisa: "Coherent Multiatomic Step Formation on GaAs (001) Vicinal Surfaces by MOVPE and Its Application to Quantum Well Wires", presented at the 22th International Symposium on Compound Semiconductors, Cheju Island, Korea, August 28 - September 2, 1995.

(8) Takashi Fukui, Jun-ya Ishizaki, Kazunobu Ohkuri, Shinjiroh Hara and Junichi Motohisa: "Investigation and Application of Multiatomic Steps on (001) GaAs Vicinal Surfaces Grown by Metalorganic Chemical Vapor Deposition", presented at the 4th China-Japan Symposium of Thin Films, Zhejiang Province, China, October 24-28, 1995.

(9) Shinjiroh Hara, Junichi Motohisa and Takashi Fukui: "Optical Characterization of InGaAs Strianed Quantum Wires Formed on GaAs Multiatomic Steps", presented at the 3rd Warkshop on Optical Properties of Mesoscopic Semiconductor Structures, Snowbird, Utah, USA, May 7-10, 1996.

(10) Shinjiroh Hara, Junichi Motohisa and Takashi Fukui: "Formation and Characterization of InGaAs Strained Quantum Wires on GaAs Multiatomic Steps Grown by Metalorganic Vapor Phase Epitaxy", presented at the 8th International Conference on Metalorganic Vaper Phase Epitaxy, Cardiff, Wales, UK, June 9-13, 1996.

(11) Takashi Fukui, Jun-ya Ishizaki, Shinjiroh Hara, Kazuhide Kumakura and Junichi Motohisa: "Fabrication of High Density GaAs/AlGaAs Quantum Wire and Quantum Dot Structures by MOVPE", presented at the 1996 International Symposium on Formation ,Physics and Device Application of Quantum Dot Structures (QDS'96), Sapporo, Japan, November 4-7, 1996.

(12) Yasuhiro Oda, Shinjiroh Hara and Takashi Fukui: "Fabrication and characterization of self-organized quantum wire structures grown by MOVPE on patterned vicinal substrates", presented at the 1997 International Microprocesses and Nanotechnology Conference, Nagoya, Japan, July 7-10, 1997.

(13) Takashi Fukui, Shinjiroh Hara, Kazuhide Kumakura and Junichi Motohisa: "Self-Organized Techniques for Quantum Nanostructures", presented at the 1997 International Microprocesses and Nanotechnology Conference, Nagoya, Japan, July 7-10, 1997.

(14) Yasuhiro Oda, Shinjiroh Hara and Takashi Fukui: "Cathodoluminescence characterization of self-organized quantum wire structures on patterned vicinal substrates", presented at the 16th Electronic Materials Symposium, Minoh, Osaka, Japan, July 9-11, 1997.

(15) Shinjiroh Hara, Junichi Motohisa, Yasuhiro Oda and Takashi Fukui: "Natural Formation and Optical Characterization InGaAs Quantum Wires Using GaAs Multiatomic Steps on Vicinal Substrates", presented at the International Workshop on Nano-Physics and Electronics (NPE'97), Tokyo, Japan, September 18-20, 1997.

(16) Junichi Motohisa, Shinjiroh Hara, M. Akabori, T. Irisawa and Takashi Fukui: "Application of Self-Organized Multiatomic Steps on Vicinal GaAs Surfaces for Quantum Structures and Devices", presented at the 1997 Japan-China Workshop on Thin Films, Tokyo, Japan, October 16-17, 1997.

(17) Shinjiroh Hara, Junichi Motohisa and Takashi Fukui: "OPTICAL PROPERTIES OF SELF-

ORGANIZED InGaAs QUANTUM WIRES ON GaAs MULTIATOMIC STEPS BY MOVPE", presented at the 1997 Fall Meeting of the Material Research Society, Boston, MA, USA, December 1-5, 1997.

IV. Presentation in international conferences related to other works

(18) Junichi Motohisa, Masashi Akabori, Shinjiroh Hara, Jun-ya Ishizaki, Kazunobu Ohkuri and Takashi Fukui: "Theoretical and Experimental Investigation of an Electron Interference Devices Using Multiatomic Steps on Vicinal GaAs Surfaces", presented at the 3rd International Symposium on New Phenomena in Mesoscopic Structures, Hawaii, U.S.A., December 4-8, 1995.

(19) Masashi Akabori, Junichi Motohisa, Shinjiroh Hara, Jun-ya Ishizaki, Kazunobu Ohkuri and Takashi Fukui: "Electron Transport in a Novel Electron Wave Interference Device using Multiatomic Steps on Vicinal GaAs Surfaces", presented at the 15th Electronic Materials Symposium, Izu-Nagaoka, Japan, July 10-12, 1996.

(20) Masashi Akabori, Junichi Motohisa, Tomoki Irisawa, Shinjiroh Hara, Jun-ya Ishizaki, Kazunobu Ohkuri and Takashi Fukui: "A Novel Electron Wave Interference Device Using Multiatomic Steps on Vicinal GaAs Surfaces Grown by MOVPE: Investigation of Transport Properties", presented at the 1996 International Conference on Solid State Devices and Materials, Yokohama, Japan, August 26-29, 1996.

(21) Junichi Motohisa, Masashi Akabori, Tomoki Irisawa, Shinjiroh Hara, Jun-ya Ishizaki and Takashi Fukui: "A Novel Coupled Quantum Dot Structure Utilizing Multiatomic Steps on GaAs Vicinal Surfaces", presented at the 1996 International Symposium on Formation ,Physics and Device Application of Quantum Dot Structures (QDS'96), Sapporo, Japan, November 4-7, 1996.

V. Presentation in domestic conferences related to this thesis (in Japanese)

(1) Jun-ya Ishizaki, Shinjiroh Hara, Shu Goto, Motoya Kishida, Horotatsu Ishii, Takashi Fukui and Hideki Hasegawa: "Atomic Force Microscopy Characterization of GaAs Surfaces Grown on Vicinal Substrates by MOCVD (2)", presented at the 40th Spring Meeting, 1993; The Japan Society of Applied Physics and Related Societies, Tokyo, March, 1993.

(2) Shinjiroh Hara, Jun-ya Ishizaki, Motoya Kishida, Junichi Motohisa, Takashi Fukui and Hideki Hasegawa: "Analysis of GaAs Lateral Growth Rate on Vicinal Substrates by MOCVD", presented at the 54th Autumn Meeting, 1993; The Japan Society of Applied Physics, Sapporo, September, 1993.

(3) Jun-ya Ishizaki, Shinjiroh Hara, Shu Goto, Motoya Kishida, Junichi Motohisa, Takashi Fukui and Hideki Hasegawa: "Atomic Force Microscopy Characterization of GaAs Surfaces Grown on Vicinal Substrates by MOCVD (3)", presented at the 54th Autumn Meeting, 1993; The Japan Society of Applied Physics, Sapporo, September, 1993.

(4) Shinjiroh Hara, Jun-ya Ishizaki, Motoya Kishida, Junichi Motohisa, Takashi Fukui and Hideki Hasegawa: "Optical Properties of Quantum Well by MOCVD Growth on Vicinal Substrates", presented at the 1993 Joint Convention; The Hokkaido Chapters of the Institutes of Electrical and Information Engineers, Sapporo, October, 1993.

(5) Jun-ya Ishizaki, Shinjiroh Hara, Shu Goto, Motoya Kishida, Takashi Fukui and Hideki Hasegawa: "Atomic Force Microscopy Characterization of GaAs Surfaces Grown by MOCVD on Vicinal Substrates (2)", presented at the 1993 Joint Convention; The Hokkaido Chapters of the Institutes of Electrical and Information Engineers, Sapporo, October, 1993.

(6) Shinjiroh Hara, Jun-ya Ishizaki, Megumi Usami, Junichi Motohisa, Takashi Fukui and Hideki Hasegawa: "Formation and Optical Characterization of Quantum Well Wires Using Multiatomic Steps", presented at the 41st Spring Meeting, 1994; The Japan Society of Applied Physics and Related Societies, Kawasaki, March, 1994.

(7) Takashi Fukui, Jun-ya Ishizaki, Shinjiroh Hara and Hideki Hasegawa: "Impurity Effect on Step Bunching of GaAs Surface by MOCVD", presented at the 41st Spring Meeting, 1994; The Japan Society of Applied Physics and Related Societies, Kawasaki, March, 1994.

(8) Shinjiroh Hara, Jun-ya Ishizaki, Junichi Motohisa, Rechard Nötzel, Takashi Fukui and Hideki Hasegawa: "Improvement of Size Uniformity of Quantum Well Wires Using Multiatomic Steps", presented at the 55th Autumn Meeting, 1994; The Japan Society of Applied Physics, Nagoya, September, 1994.

(9) Kazunobu Ohkuri, Jun-ya Ishizaki, Shinjiroh Hara Takashi Fukui and Hideki Hasegawa: "Study on Morphology of GaAs Vicinal Surface after Thermal Treatment", presented at the 55th Autumn Meeting, 1994; The Japan Society of Applied Physics, Nagoya, September, 1994.

(10) Shinjiroh Hara, Jun-ya Ishizaki, Junichi Motohisa, Takashi Fukui and Hideki Hasegawa: "Fabrication of Quantum Well Wire Structures Utilizing Multiatomic Steps on Vicinal Substrates", presented at the 1994 Joint Convention; The Hokkaido Chapters of The Institutes of Electrical and Information Engineers, Muroran, October, 1994.

(11) Kazunobu Ohkuri, Jun-ya Ishizaki, Shinjiroh Hara, Takashi Fukui and Hideki Hasegawa: "Step Bunching by Thermal Treatment on GaAs Vicinal Surfaces", presented at the 1994 Joint Meeting; The Hokkaido Chapters of The Japan Society of Applied Physics, Kushiro, November, 1994.

(12) Shinjiroh Hara, Junichi Motohisa and Takashi Fukui: "Study of Size Uniformity of Quantum Well Wires Using Multiatomic Steps", presented at the 56th Autumn Meeting, 1995; The Japan Society of Applied Physics, Kanazawa, August, 1995.

(13) Shinjiroh Hara, Junichi Motohisa and Takashi Fukui: "Fabrication and Study of Size Uniformity of Quantum Well Wires on Vicinal GaAs Surfaces", presented at the 1995 Joint Meeting; The Hokkaido Chapters of The Japan Society of Applied Physics, Otaru, January, 1996.

(14) Shinjiroh Hara, Junichi Motohisa and Takashi Fukui: "Formation and Characterization of InGaAs Strained Quantum Wires Using Multiatomic Steps", presented at the 43rd Spring Meeting, 1996; The Japan Society of Applied Physics and Related Societies, Asaka, March, 1996.

(15) Shinjiroh Hara, Junichi Motohisa and Takashi Fukui: "Optical Characterization of InGaAs Strained Quantum Wires Using Multiatomic Steps", presented at the 57th Autumn Meeting, 1996; The Japan Society of Applied Physics, Fukuoka, September, 1996.

(16) Takashi Fukui, Jun-ya Ishizaki, Shinjiroh Hara, Kazuhide Kumakura and Junichi Motohisa: "AFM Observation of Quantum Wire and Quantum Dot Structures", presented at the 1996 Autumn Meeting; The Japan Society of Physics, Yamaguchi, October, 1996.

(17) Yasuhiro Oda, Shinjiroh Hara, Junichi Motohisa and Takashi Fukui: "Observation of Multiatomic Steps Grown by MOVPE on Vicinal Patterned Substrates", presented at the 1996 Joint Meeting; The Hokkaido Chapters of The Japan Society of Applied Physics, Kitami, November, 1996.

(18) Shinjiroh Hara, Junichi Motohisa and Takashi Fukui: "Observation of Growth Mode of InGaAs Layers on Multiatomic Steps and Fabrication of InGaAs Strained Quantum Wires", presented at the 44th Spring Meeting, 1997; The Japan Society of Applied Physics and Related Societies, Funabashi, March, 1997.

(19) Takashi Fukui, Jun-ya Ishizaki and Shinjiroh Hara: "Formation of Multilayer Step and Fabrication of Nano-Scale Structure on Vicinal (001) GaAs Surfaces by MOVPE", presented at the 44th Spring Meeting, 1997; The Japan Society of Applied Physics and Related Societies, Funabashi, March, 1997.

(20) Yasuhiro Oda, Shinjiroh Hara, Junichi Motohisa and Takashi Fukui: "Fabrication and Characterization of Multiatomic Steps Grown by MOVPE on Vicinal Patterned Substrates", presented at the 44th Spring Meeting, 1997; The Japan Society of Applied Physics and Related Societies, Funabashi, March, 1997.

(21) Takashi Fukui, Jun-ya Ishizaki, Shinjiroh Hara, Kazuhide Kumakura and Junichi Motohisa: "Self-organized Semiconductor Nano-Structures", presented at the 28th National Conference on Crystal Growth, Sapporo, July, 1997.

(22) Shinjiroh Hara, Yasuhiro Oda and Takashi Fukui: "Formation of InGaAs Quantum Wires Using Multiatomic Steps on Vicinal and Patterned Vicinal Substrates", presented at the 58th Autumn Meeting, 1997; The Japan Society of Applied Physics, Akita, October, 1997.

(23) Yasuhiro Oda, Shinjiroh Hara and Takashi Fukui: " Fabrication and Characterization of

Multiatomic Steps Grown by MOVPE on Vicinal Patterned Substrates (2)", presented at the 58th Autumn Meeting, 1997; The Japan Society of Applied Physics, Akita, October, 1997.

(24) Junichi Motohisa, Shinjiroh Hara, Tetsuo Umeda, Kazuhide Kumakura and Takashi Fukui: "Fabrication and Characterization of Self-Organized In(Ga)As Quantum Nanostructures by MOVPE", presented at the 58th Autumn Meeting, 1997; The Japan Society of Applied Physics, Akita, October, 1997.

(25) Shinjiroh Hara, Junichi Motohisa and Takashi Fukui: "Fabrication of InGaAs Quantum Wire Lasers Using GaAs Multiatomic Steps", presented at the 45th Spring Meeting, 1998; The Japan Society of Applied Physics and Related Societies, Tokyo, March, 1998.

VI. Presentation in domestic conferences related to other works (in Japanese)

(26) Jun-ya Ishizaki, Kazunobu Ohkuri, Shinjiroh Hara, Shu Goto, Takashi Fukui and Hideki Hasegawa: "Atomic Force Microscopy Characterization of GaAs Surfaces Grown on Vicinal Substrates by MOCVD (4)", presented at the 41st Spring Meeting, 1994; The Japan Society of Applied Physics and Related Societies, Kawasaki, March, 1994.

(27) Jun-ya Ishizaki, Kazunobu Ohkuri, Shinjiroh Hara, Takashi Fukui and Hideki Hasegawa: "Bunching Process of Atomic Step on GaAs Vicinal Surfaces Observed by Atomic Force Microscope", presented at the 55th Autumn Meeting, 1994; The Japan Society of Applied Physics, Nagoya, September, 1994.

(28) Jun-ya Ishizaki, Kazunobu Ohkuri, Shinjiroh Hara, Takashi Fukui and Hideki Hasegawa: "Atomic Force Microscopy Characterization Multilayer Step on GaAs Vicinal Surfaces", presented at the 1994 Joint Meeting; The Hokkaido Chapters of The Japan Society of Applied Physics, Kushiro, November, 1994.

(29) Jun-ya Ishizaki, Kazunobu Ohkuri, Shinjiroh Hara and Takashi Fukui: "Temperature Dependence of Atomic Step Formation on Vicinal GaAs Surfaces", presented at the 42nd Spring Meeting, 1995; The Japan Society of Applied Physics and Related Societies, Hiratsuka, March, 1995.

(30) Junichi Motohisa, Shinjiroh Hara and Takashi Fukui: "Electron Interference Device Using Multi-atomic Steps on Vicinal Surfaces: Effect of Potential Fluctuation", presented at the 56th Autumn Meeting, 1995; The Japan Society of Applied Physics, Kanazawa, August, 1995.

(31) Kazunobu Ohkuri, Jun-ya Ishizaki, Shinjiroh Hara and Takashi Fukui: "Step Bunching on GaAs Vicinal Surface after Thermal Treatment (III)", presented at the 56th Autumn Meeting, 1995; The Japan Society of Applied Physics, Kanazawa, August, 1995.

(32) Masashi Akabori, Shinjiroh Hara, Jun-ya ishizaki, Junichi Motohisa and Takashi Fukui: "Fabrication of Electron Wave Interference Device Using Multi-atomic Steps", presented at the 1995 Joint Convention; The Hokkaido Chapters of the Institutes of Electrical and Information Engineers, Sapporo, October, 1995.

(33) Kazunobu Ohkuri, Jun-ya Ishizaki, Shinjiroh Hara, and Takashi Fukui: "Step Bunching on GaAs (001) Vicinal Surface During MOVPE and Thermal Treatment", presented at the 1995 Joint Meeting; The Hokkaido Chapters of The Japan Society of Applied Physics, Otaru, January, 1996.

(34) Masashi Akabori, Junichi Motohisa, Shinjiroh Hara, Jun-ya ishizaki, Kazunobu Ohkuri and Takashi Fukui: "Fabrication and Characterization of Electron Wave Interference Device Utilizing Multiatomic Steps", presented at the 1995 Joint Meeting; The Hokkaido Chapters of The Japan Society of Applied Physics, Otaru, January, 1996.

(35) Kazunobu Ohkuri, Jun-ya Ishizaki, Shinjiroh Hara, and Takashi Fukui: "The Mode Transition of The Multiatomic Step Formation on Vicinal GaAs Surfaces", presented at the 43rd Spring Meeting, 1996; The Japan Society of Applied Physics and Related Societies, Asaka, March, 1996.

(36) Masashi Akabori, Junichi Motohisa, Shinjiroh Hara, Jun-ya ishizaki, Kazunobu Ohkuri and Takashi Fukui: "Electron Interference Device Using Multiatomic Steps on Vicinal Surfaces: Fabrication and Characterization", presented at the 43rd Spring Meeting, 1996; The Japan Society of Applied Physics and Related Societies, Asaka, March, 1996.

(37) Masashi Akabori, Junichi Motohisa, Tomoki Irisawa, Shinjiroh Hara, Jun-ya ishizaki and Takashi

Fukui: "Electron Interference Device Using Multiatomic Steps on Vicinal Surfaces: Electron Transport Properties", presented at the 57th Autumn Meeting, 1996; The Japan Society of Applied Physics, Fukuoka, September, 1996.

(３８) Masashi Akabori, Junichi Motohisa, Tomoki Irisawa, Shinjiroh Hara, Jun-ya ishizaki and Takashi Fukui: "Electron Wave Interference Device Using Multiatomic Steps", Technical Report of The Institute of Electronics, Information and Communication Engineers, Vol. 96, No. 352, pp.53-58, November 8, 1996.